

University of Windsor

Scholarship at UWindor

Electronic Theses and Dissertations

Theses, Dissertations, and Major Papers

2019

Effects of gamma irradiation treatment of oil sands process material on zooplankton accrual and early community development in field based mesocosms

Chantal For Dings-Avery
University of Windsor

Follow this and additional works at: <https://scholar.uwindsor.ca/etd>

Recommended Citation

Dings-Avery, Chantal For, "Effects of gamma irradiation treatment of oil sands process material on zooplankton accrual and early community development in field based mesocosms" (2019). *Electronic Theses and Dissertations*. 7697.

<https://scholar.uwindsor.ca/etd/7697>

This online database contains the full-text of PhD dissertations and Masters' theses of University of Windsor students from 1954 forward. These documents are made available for personal study and research purposes only, in accordance with the Canadian Copyright Act and the Creative Commons license—CC BY-NC-ND (Attribution, Non-Commercial, No Derivative Works). Under this license, works must always be attributed to the copyright holder (original author), cannot be used for any commercial purposes, and may not be altered. Any other use would require the permission of the copyright holder. Students may inquire about withdrawing their dissertation and/or thesis from this database. For additional inquiries, please contact the repository administrator via email (scholarship@uwindsor.ca) or by telephone at 519-253-3000ext. 3208.

EFFECTS OF GAMMA IRRADIATION TREATMENT OF OIL SANDS PROCESS
MATERIAL ON ZOOPLANKTON ACCRUAL AND EARLY COMMUNITY
DEVELOPMENT IN FIELD BASED MESOCOSMS

by

Chantal V. Dings-Avery

A Thesis
Submitted to the Faculty of Graduate Studies
Through the Department of Biological Sciences
In Partial Fulfilment of the Requirements for
The Degree of Master of Science at the
University of Windsor

Windsor, Ontario, Canada

2019

© 2019 Chantal V. Dings-Avery

EFFECTS OF GAMMA IRRADIATION TREATMENT OF OIL SANDS PROCESS
MATERIAL ON ZOOPLANKTON ACCRUAL AND EARLY COMMUNITY
DEVELOPMENT IN FIELD BASED MESOCOSMS

by

Chantal V. Dings-Avery

APPROVED BY:

J. Martin

Suncor Energy, Inc.

A. Fisk

Great Lakes Institute for Environmental Research

T. Pitcher

Department of Biological Sciences

C. Weisener, Co-Advisor

Great Lakes Institute for Environmental Research

J. J. H. Ciborowski, Advisor

Department of Biological Sciences

August 27, 2018

Declaration of Originality

I hereby certify that I am the sole author of this thesis and that no part of this thesis has been published or submitted for publication.

I certify that, to the best of my knowledge, my thesis does not infringe upon anyone's copyright nor violate any proprietary rights and that any ideas, techniques, quotations, or any other material from the work of other people included in my thesis, published or otherwise, are fully acknowledged in accordance with the standard referencing practices. Furthermore, to the extent that I have included copyrighted material that surpasses the bounds of fair dealing within the meaning of the Canada Copyright Act, I certify that I have obtained a written permission from the copyright owner(s) to include such material(s) in my thesis and have included copies of such copyright clearances to my appendix.

I declare that this is a true copy of my thesis, including any final revisions, as approved by my thesis committee and the Graduate Studies office, and that this thesis has not been submitted for a higher degree to any other University or Institution.

Abstract

Oil sands mining and extraction produce wastewater and tailings enriched in salts and naphthenic acid fraction compounds (NAFCs), which persist and are toxic to biota. I determined if gamma irradiation (GI) of oil sands process materials (OSPM), which breaks down NAFCs in fluid fine tailings (FFT) and water (OSPW), can stimulate development of biological communities and ecosystem processes by reducing NAFC concentrations and toxicity. In a 33-month field study, I tracked zooplankton community accrual and patterns of diel dissolved oxygen to determine the potential for carbon accumulation in a suite of 68-L outdoor mesocosms constructed from untreated and GI treated OSPM that were reinoculated with indigenous microbial communities and compared them to freshwater and hyposaline wetland reference mesocosms. GI reduced NAFC concentrations by 54 – 98% in OSPW and 0 – 62% in FFT. Zooplankton biomass, species richness and density were stimulated in GI treated OSPM mesocosms compared to the untreated OSPM mesocosms. After 1.5 years, zooplankton species richness and biomass in GI treated OSPM mesocosms were numerically equivalent to values in reference mesocosms, but density was still marginally impaired. Primary production in both untreated and GI treated mesocosms remained low compared to reference wetlands. The colonization of macrophytes was inhibited by untreated OSPM. Considerably fewer, and smaller emergent macrophyte stems developed in GI treated OSPM than in reference mesocosms. Submerged aquatic vegetation was sparse and only occurred in one GI treated OSPM replicate. Primary production and respiration rates of OSPM mesocosms were 20 – 30% of those observed in reference mesocosms. Lower biological activity of OSPM mesocosms was attributed to a lack of macrophyte colonization in tailings pond mesocosms, likely related to persistent turbidity and unsuitable sediment characteristics.

*To all of my friends and family
for their unconditional support.*

Acknowledgments

First and foremost, I would like to thank my parents; without them I would not exist to write this thesis. Secondly, I would like to thank my supervisor Dr. Jan J.H. Ciborowski and my co-supervisor Dr. Chris Weisener, because without them, this thesis would not exist. Thank you Jan, for your kind words, your never ending support, gentle reminders, and endless patience, and always asking just the right question(s) to help guide me on my way. Thank you Chris; without your biogeochemical expertise and commitment this project would have never been conceived. Thank you for your countless trips to Fort Mac to help sample the mesocosms, and for bouncing ideas with me during beers at the end of the day. Next, I would like to thank Josh Martin both my industrial mentor and our liaison who contributed greatly to the logistics of providing access to the site, and environmental clearances. I would also like to recognize my committee members Dr. Aaron Fisk, and Dr. Trevor Pitcher for challenging me to think critically and for always welcoming my random knocks on their doors.

A special thank you to all of the many industrial liaisons who helped me keep this project running as smoothly as could be expected – the entire crew at Syncrude’s Reclamation and Closure Department; Jessica Piercey and Lori Cyprien for always keeping the freezer stocked with ice cream, and for saving us from ever having to fill out a work permit, to Chris Beierling and Mohamed Salem for always lending a helping hand, for searching the warehouse for field equipment, and helping us obtain our preservatives. To all of the field leads who came to make sure we were doing our work safely, and for listening to me talk endlessly about my project. Many thanks to Correen Luchka at Suncor who worked

incredibly hard at coordinating all of our odd requests; and the numerous field leads and crew members from Geotechnical Services for babysitting my experiment over the winters.

I would like to thank the numerous undergraduate and graduate students who helped me collect data, and whom I had the pleasure of collaborating with. Every one of you lent me a piece of your perspective and a fresh pair of eyes to look at a wetland with. Your passion and love of wetlands inspires me, and always provided the parties with perfect conversations to be had over drinks.

To all of those in my department; To Nancy Barkley for always taking care of me and finding a paper trail or two when needed, and for helping me meet all of my deadlines (especially when they were last minute, which most of them were). To my fellow colleagues Kellie Menard, Marlena McCabe, Danielle Gunsch, Alyssa Frazao who have offered me endless support, wisdom, laughter, and offers of beer. To all of the field crew members in the Ciborowski and Weisener labs who have helped me collect data, organize samples, and who have made the countless drives across country: Hannah Bagnall, Hannah Wiseman, Crystal Kelly, Amalia Despenic, Katrina Lukianchuk, Danielle VanMensel, Thomas Reid, Rachel Boutette, Hearthly Mayordo and especially Pablos banditas and our Fort McMurray Thursday night jam crew.

A very special thank you to my best friends Maya and Jensine, my family, especially my Mom, and my girlfriend Mel for taking care of me, feeding me and supporting me endlessly. And to my dance sister Sandra, and my dance family for always helping me dance it out and always sharing your kind words. And lastly to my Fort McMurray partner in crime Kellie, who was with me for every field season; the last year (and then

some) without you has been so lonely (have you finished your cross stitch yet or did I win?).

Lastly, to my sources of funding: This project truly was a collaborative project and it wouldn't have been possible without each and every person and agency. This research was funded in part by an NSERC Collaborative Research and Development grant cosponsored by Suncor Energy Inc., Syncrude Ltd, Shell Canada Energy, Canadian Natural Resources Ltd., Imperial Oil Resources and Total E&P Canada to Dr. Christopher Weisener and Dr. Jan Ciborowski. I gratefully acknowledge the receipt of an NSERC-Industrial Postgraduate Scholarship cofunded by NSERC and Suncor Energy, Inc. and additional graduate and research assistantships from the University of Windsor.

Table of Contents

Declaration of Originality	iii
Abstract	iv
Dedication	v
Acknowledgments.....	vi
List of Tables	xi
List of Figures	xiii
List of Abbreviations	xv
Chapter 1 - Introduction	1
Project Summary and Objectives	1
Wetland ecosystems	3
Boreal forest wetlands	4
Athabasca Oil Sands	5
Tailings toxicity.....	7
Implications for reclamation.....	9
Degradation of NAFCs	11
Research scope and objectives	14
Chapter 2 - The Effects of Untreated and Gamma Irradiated Oil Sands Process Materials on Zooplankton Community Accrual in Field Based Mesocosms.....	18
Introduction	18
Zooplankton in the western boreal forest zone.....	20
Wetlands in the Athabasca Oil Sands region.....	21
Toxicity of OSPW to zooplankton	22
Objectives	24
Methods	26
Results	41
Discussion.....	59
Chapter 3 – The Effects of Untreated and Gamma Irradiated Oil Sands Process Materials on Ecosystem Metabolism in Field-Based Mesocosms	67
Introduction	67
Patterns of dissolved oxygen and production in shallow ponds	71

Objectives	72
Methods and Materials	74
Results	82
Discussion.....	98
Synopsis.....	105
Chapter 4 - Synopsis, Implications of Findings, and Recommendations for Future Research	107
Significance	107
Major findings	108
Recommendations for future studies	111
References.....	113
Appendix 1 – Summary of wetlands and tailings ponds used in the construction of mesocosms	129
Appendix 2 – Proportion of relative abundance of all zooplankton taxa including rotifers identified in all mesocosm for all sampling dates and total crustacean zooplankton biomass	131
Appendix 3 – Macrophyte percent cover and biomass.....	144
Appendix 4 – Supplementary information for Chapter 3	147
Vita Auctoris.....	153

List of Tables

Table 2.1: Concentration of naphthenic acid fraction compounds (mg/L) in the water of OSPM mesocosms.	45
Table 2.2: Concentration of naphthenic acid fraction compounds (mg/L) in the fluid fine tailings (FFT) of OSPM mesocosms.	46
Table 2.3: Total suspended solids and turbidity by GI treatment and relative salinity.	46
Table 2.4: Mixed model results for the fixed effects of GI treatment and relative salinity for crustacean zooplankton richness, biomass, mean weighted length and density.	54
Table 3.1: Total number of sonde days logged for each GI treatment and relative salinity by year.	81
Table 3.2: Results of mixed model analysis for the fixed effects of GI and relative salinity on production, respiration and net ecosystem production.	90
Table 3.3: Mean and 95% CI estimates of gross primary production, respiration and net ecosystem production by GI treatment, relative salinity, and sampling year.	91
Table 3.4: Mean±SE of the percent of sampled days that mesocosms were net autotrophic.	92
Table A1-1: Selected characteristics of wetland materials collected for the construction of reference mesocosms.	129
Table A1-2: Select characteristics of tailings pond materials collected for the construction of OSPM mesocosms.	130
Table A2-1: Proportion of crustacean zooplankton and rotifer relative abundance, and total crustacean zooplankton biomass identified in G- and G+ mesocosms for all sampling dates.	131
Table A2-2: Proportion of crustacean zooplankton and rotifer relative abundance, and total crustacean zooplankton biomass identified in Blank mesocosms for all sampling dates.	142

Table A3-1: Estimated percent cover of submerged aquatic vegetation (SAV) for untreated mesocosms.	144
Table A3-2: Estimated percent cover of submerged aquatic vegetation (SAV) for gamma irradiated mesocosms.	142
Table A3-3: Dry weight (g) of various macrophyte compartments and biofilm collected from destructive sampling of mesocosms on the final day of the study.	146
Table A4-1: Mean volume and standard error of the volume of distilled water added to maintain mesocosm water levels for each sampling season.	152

List of Figures

Fig. 2.1: Google Earth image of Alberta showing Fort McMurray and the study area.	38
Fig. 2.2: Google Earth image of the reference sites, tailings ponds, and experimental trenches.	39
Fig. 2.3: Photo of the mesocosm set up at the Experimental trenches.	40
Fig. 2.4: Mean \pm SE crustacean zooplankton species richness by GI treatment, relative salinity, and sample date.	55
Fig. 2.5: Mean \pm SE crustacean zooplankton biomass octaves ($\mu\text{g/L}$) by GI treatment, relative salinity, and sample date.	56
Fig. 2.6: Mean \pm SE mean weighted length (mm) of crustacean zooplankton by GI treatment, relative salinity, and sample date.	57
Fig. 2.7: Mean \pm SE density octaves (individuals/L) of crustacean zooplankton by GI treatment, relative salinity, and sample date.	58
Fig. 3.1: Photo of the dissolved oxygen logger and light logger deployed in a mesocosm.	79
Fig. 3.2: Gross primary production ($\text{O}_2 \mu\text{mol /L/day}$) by GI treatment, relative salinity, and sample date.	93
Fig. 3.3: Difference in estimates of gross primary production ($\text{O}_2 \mu\text{mol /L/day}$) between pairs of G+/G- wetland replicates for 2016 and 2017.	94
Fig. 3.4: Estimates of respiration ($\text{O}_2 \mu\text{mol /L/day}$) by GI treatment, relative salinity, and sample date.	95
Fig. 3.5: Difference in estimates of respiration ($\text{O}_2 \mu\text{mol /L/day}$) between pairs of G+/G- wetland replicates for 2016 and 2017.	96
Fig. 3.6: Estimates of net ecosystem production ($\text{O}_2 \mu\text{mol /L/day}$) by GI treatment, relative salinity, and sample date.	97
Fig. A4-1: Schematic diagram of the setup of the mesocosms at the experimental trenches.	147

Fig. A4-2: Continuous temperature record of mean water temperatures from October 3, 2015 to June 23, 2017.	148
Fig. A4-3: Mean mesocosm water temperature from May 1 to September 7, 2015 recorded every 15 minutes.	149
Fig. A4-4: Mean mesocosm water temperature from May 1 to September 7, 2016 recorded every 15 minutes.	149
Fig. A4-5: Mean mesocosm water temperature from April 1 to June 16, 2017 recorded every 15 minutes.	150
Fig. A4 - 6: Mean difference of minimum, maximum and maximum daily change in DO concentration by GI treatment, relative salinity, and date.	151

List of Abbreviations

AOS – Athabasca oil sands

COD – Chemical oxygen demand, rate of oxygen consumed by chemical oxidation in the sediment

FFT – fluid fine tailings

FW mesocosms – Freshwater mesocosms constructed from freshwater reference wetland materials with a conductivity of less than 500 μS

G-: material that has not been exposed to gamma irradiation and that was inoculated with an inoculum composed of equal parts of untreated wetland and tailings material from all 9 initial sources (6 wetlands and 3 tailings ponds)

G+: material that has been exposed to gamma irradiation and reinoculated with a 10% by volume inoculum composed of equal parts untreated wetland and tailings material from all 9 initial sources (6 wetlands and 3 tailings ponds)

GI – Gamma irradiation

GPP – Gross primary production, the rate at which oxygen is produced

HSW mesocosms – Hyposaline water mesocosms constructed from hyposaline water wetland materials with a conductivity between 700 – 1500 μS

OSPM – Oil sands process-affected materials

OSPW – Oil sands process-affected water

OSPM mesocosms – Mesocosms constructed with oil sands process material from tailings ponds with a conductivity between 1700 – 2700 μS

NAFCs – Naphthenic acid fraction compounds

NEP – Net ecosystem production, the balance between production and respiration.
Positive values are indicative of carbon accrual, and negative values are indicative of carbon loss

NPP – Net primary production, the rate at which oxygen is produced after accounting for oxygen lost to respiration

R – Respiration, the rate at which oxygen is respired

TSS – Total suspended solids

Chapter 1 - Introduction

Project Summary and Objectives

The Athabasca Oil Sands (AOS) are the third largest oil reserve in the world with an estimated 2.7 billion cubic meters of recoverable bitumen (Brown and Ulrich 2015). Due to the solid nature of bitumen, conventional pumping methods cannot be used to extract the bitumen. Approximately 20% of the AOS is close enough to the surface to be mined, which has resulted in large scale disturbances to approximately 600 km² of boreal forest in northern Alberta, all of which will need to be reclaimed (Kasperski and Mikula 2011). Mining companies are required to reclaim the landscape to an “equivalent land capability” but not necessarily the same landscape that was there before (Alberta Government 2015). Reclamation of the oil sands will involve safely incorporating large quantities of mine tailings into the environment to build sustainable, productive and diverse boreal ecosystem landscapes (Allen 2008, Alberta Government 2015). To achieve equivalent productivity, the reclaimed landscape will have to support a mosaic of upland forests and wetland types, contain a comparable number of native boreal species, boreal ecosystem biodiversity, and support similar ecosystem services, such as nutrient cycling, carbon accumulation, and water supply (Vitt et al. 2001, Dodds et al. 2008).

Wetlands, including fens, bogs, marshes, swamps and shallow open waters, represent approximately 2/3 of the landscape disturbed by open-pit mining (BGC Engineering 2010b, Rooney et al. 2012). Wetlands are an important feature of the boreal ecosystem because they help store water, increase biodiversity, accumulate carbon and improve water quality (Zedler and Kercher 2005, Rooney et al. 2012). The pre-mining landscape was predominantly composed of freshwater fens and bogs, which accumulate

large amounts of carbon in the form of peat and help store water in a region where evapotranspiration exceeds precipitation (Trites and Bayley 2009b). The formation of fens and bogs can take thousands of years and is largely dependent on water levels and the presence of low productivity vegetation species such as *Sphagnum* spp. and sedges (Warner and Asada 2006, Rooney et al. 2012). Due to large volumes of stockpiled overburden and large quantities of tailings material, there will be large scale conversion of wetland habitats to upland boreal forests (Audet et al. 2014). This change in topography will fundamentally alter the hydrology, biogeochemistry and productivity of the reclaimed landscape.

Open water marshes and end pit lakes (mines that have been filled with tailings and capped with fresh water) will largely replace fens as the dominant wetland type in the post mining landscape (Johnson and Miyanishi 2008, Rooney et al. 2012). Open water marshes and the littoral zone of end pit lakes (EPLs) and will play an important role in offsetting carbon losses due to the conversion of peatlands. The colonization of aquatic ecosystems constructed with oil sands process materials (OSPM) by diverse, native biota is impeded by elevated salinity (especially sodium) and the concentration of naphthenic acid fraction compounds (NAFCs) of tailings materials (Bendell-Young et al. 2000, Rooney and Bayley 2011, Raab and Rooney 2012, Kovalenko et al. 2013).

My research used field based mesocosms to evaluate a novel tailings treatment that reduces the concentration of NAFCs and their associated toxicity by using gamma irradiation (GI) to break down the chemical bonds and mineralize or catabolize the NAFCs into compounds that are more bioavailable to microbial degradation (Boudens et al. 2016, VanMensel et al. 2017). Both biodiversity and ecosystem functioning are

important reclamation criteria (Alberta Government 2014). I compared GI treated OSPM to untreated OSPM to determine if GI treated OSPM reinoculated with indigenous microbial communities underwent sufficient detoxification to promote the accrual of natural and diverse zooplankton communities. To determine if GI could stimulate ecosystem functioning and promote the development of systems that could potentially accumulate organic matter, I compared diel dissolved oxygen (used as a proxy for carbon) in GI treated OSPM mesocosms to untreated OSPM. In addition to NAFCs, research also suggests that the elevated salinity of OSPM will constrain developing wetland communities (Kovalenko et al. 2013). To determine the relative effects of salinity, I also compared communities that developed in OSPM mesocosms to communities that developed in freshwater and hyposaline water reference mesocosms.

Wetland ecosystems

Wetlands are transitional zones between upland areas and aquatic habitats defined by their ability to support water saturated soils, biogeochemical processes in the anaerobic sediment, and species, especially plants, that have adapted to thrive in these anaerobic conditions (Mitsch and Gosselink 2015). Despite a small global presence, wetlands are some of the most productive and valuable ecosystems worldwide, providing ecosystem services such as carbon storage, biodiversity, nutrient cycling, flood abatement and erosion control, food production, and recreation (Costanza et al. 1997, Zedler and Kercher 2005, Palmer and Filoso 2009).

The ecosystem services that wetlands provide are of high economic value (Costanza et al. 1997, Dodds et al. 2008). Wetlands currently cover approximately 9% of the world's land area, and it is estimated that over half of global wetlands have already

been lost (Zedler and Kercher 2005). Wetland restoration attempts to restore hydrology, biodiversity and ecosystem functioning lost following the destruction, drainage or conversion of wetlands (Zedler 2000). By comparison, wetland reclamation is defined as “the creation of wetlands on disturbed land where they did not formerly exist or where their previous form has been entirely lost” (Harris 2007).

Many wetland restoration studies focus on the recovery of biodiversity as a measure of success (Moreno-Mateos et al. 2012) Although there is a positive relationship between biodiversity and ecosystem function increases in biodiversity are not enough to ensure high ecosystem functioning (Meli et al. 2014). Meta-analyses by Rey Benayas et al. (2009) and Moreno-Mateos et al. (2012) have demonstrated that measures of biodiversity respond more quickly to restoration than measures of ecosystem functioning such as nutrient cycling, and carbon storage. Therefore, integrating measures of biodiversity and ecosystem functioning will help better inform restoration practices (Loreau et al. 2001).

Boreal forest wetlands

The boreal ecozone has a circumpolar distribution and is particularly rich with wetlands as well as natural resources such as petroleum, forestry, and mineral deposits (Foote and Krogman 2006). Wetlands of the western boreal forest extend from Alaska to Manitoba and are primarily peatlands, fens and bogs (Foote and Krogman 2006), which accumulate and store massive amount of carbon as peat, representing a significant global carbon sink (Vitt et al. 2001). Peat forms when rates of primary production exceed rates of decomposition, resulting in the partial decomposition of vegetation (Vitt et al. 2001, Trites and Bayley 2009b). Rates of net primary production are low for bogs and poor fens

but are offset by even slower rates of decomposition resulting in a net storage of carbon (Trites and Bayley 2009). Non-peat forming wetlands such as open water marshes have much higher rates of net primary production than peatlands but also tend to have higher decomposition rates due to fluctuating water levels re-aerating the soil, and higher litter quality (more N), making them more degradable by decomposers (Thormann et al. 1999). Although the reclamation of fen landscapes is being researched (Price et al. 2010, Ketcheson et al. 2016, Menard 2017) a large proportion of peatlands will be converted to open water marshes and end pit lakes (EPL).

Despite marsh wetlands representing only 7.5% of the total wetland area in the western boreal forest, they account for almost 20% of net primary production (Vitt et al. 2001). Open marsh wetlands in the region tend to be shallow (<2 m deep) and eutrophic making them highly productive (Bayley and Prather 2003). Shallow depths allow light to penetrate to the sediment and promotes the development of dense beds of submerged macrophytes. These submerged macrophytes beds provide an attachment site for epiphyton (Carpenter and Lodge 1986) and serve as an important refuge and food for zooplankton and aquatic macroinvertebrates (Hornung and Foote 2006). Both zooplankton (Norlin et al. 2006) and macroinvertebrates (Hornung and Foot 2006) serve as an important link between primary producers and higher trophic levels such as waterfowl, migratory birds, amphibians, and mammals (Foote and Krogman 2006).

Athabasca Oil Sands

During the mining process, the entire boreal landscape is removed to expose bitumen deposits, up to 75 m deep (Allen 2008), which are then harvested by shovel and transported to an extraction facility by truck or pipelines. A hot water digestion process

called the Clark Hot Water method is used to separate the entrapped bitumen from a sand, silt and clay matrix (Kasperski and Mikula 2011). Naturally occurring surfactants called naphthenic acids (NAs; hereafter termed NACFs), are released during the process which aid in bitumen recovery (Quagraine et al. 2005).

Each cubic meter of oil sands processed produces approximately four cubic meters of slurry waste (Quagraine et al. 2005; Kannel and Gan 2012). Mining companies are mandated by the Alberta government to operate under a “zero-discharge policy”, and any materials from the extraction process are held in settling basins designed to help the tailings stratify (Allen 2008). The sand particles settle out quickly, while the fines (particles less than 44 μm) stay suspended in a fluid layer termed fluid fine tailings (FFT) (Allen 2008). After three to five years the tailings consolidate to mature fine tailings reaching 30-40 wt% solids (Kasperski and Mikula 2011). Further consolidation of the FFT to a trafficable surface can take upwards of a century (MacKinnon et al. 2001). Technologies such as those that produce composite tailings which, mix gypsum with FFT and tailings sand to produce a non-segregating reclamation material that can then be capped with sand to create trafficable surfaces in less than a year have been developed (Matthews et al. 2002, BGC 2010a). However, during dewatering of the composite tailings particle free pore water with a similar composition to OSPW is released and must be reincorporated into the recycled water used in plant operations (MacKinnon et al. 2001).

To minimize water demand from the local rivers, process water (water that has come in contact with oil sands) is recycled through the extraction plant where it becomes increasingly enriched with metals, ions, salts and residual organic compounds (Clemente

and Fedorak 2004, Kasperski and Mikula 2011). The organic compounds include residual bitumen, polycyclic aromatic hydrocarbons (PAH), benzene, toluene, ethylbenzene and xylene (BTEX), and naphthenic acids all of which may interact to influence toxicity (Allen 2008, McQueen et al. 2017b). Tailings stocks continue to grow daily and are projected to reach approximately 1 billion m³ by 2025 (Quagarine et al. 2015).

Tailings toxicity

Naphthenic acid fraction compounds have been identified by a number of studies as the primary cause of acute and chronic toxicity (Holowenko et al. 2002, Clemente and Fedorak 2005, Allen 2008). The NAFCs are a diverse group of acid extractable compounds that includes classic naphthenic acids, with the chemical formula $C_nH_{2n+z}O_2$ where n is the number of carbons and z is representative of the degree of branching. Naphthenic acid fraction compounds are a group of carboxylic acids that range in structure from simple aliphatic compounds to polycyclic and multi-branched compounds, but that also includes other species containing sulphur and nitrogen, and varying degrees of unsaturation and aromaticity (Grewer et al. 2010, Headley et al. 2013, Headley et al. 2016, Huang et al. 2018). Differences in toxicity and residency time can be attributed to difference in the structure of the NAFCs (Chi et al. 2006, Frank et al. 2008, Kannel and Gan 2012, Toor et al. 2013, Brown and Ulrich 2015). The exact characteristics (pH, ionic concentrations, particle size, organic compounds) of fluid fine tailings in each tailings pond vary based on a variety of factors including the parent ore, the addition of chemicals to the extraction process, and the treatment of tailings (FTFC 1995). Furthermore, the mixtures of NAFCs in OSPW vary temporally and spatially within individual tailings ponds (Frank et al. 2016, Huang et al. 2018).

The NAFCs in OSPW are toxic to a wide range of organisms from bacteria to vertebrates and cause reduced survival (He et al. 2012, Lari et al. 2016, White 2017), reduced reproduction (Kavanagh et al. 2012, Lari et al. 2016), development delays (Hersikorn and Smits 2011, Anderson et al. 2012, Kennedy 2012), and behavioural changes (Anderson et al. 2012, Lari et al. 2016). An extensive review of OSPW toxicity is provided by Li et al. (2017). The most commonly used lab toxicity test organisms include the marine bacteria *Vibrio fisheri* (Clemente and Fedorak 2005, Frank et al. 2008, Zubot et al. 2012), standard zooplankton test species such as *Ceriodaphnia dubia* (White 2017) and *Daphnia pulex* or *D. magna* (Zubot et al. 2012, Lari et al. 2016), the dipteran larvae *Chironomus dilutus* (Anderson et al. 2012, White 2017), and fat head minnows (*Pimephales promelas*) (He et al. 2012, Kavanagh et al. 2012, Marentette et al. 2015). Although lab toxicity tests provide valuable information, the toxicity to marine organisms (Martin et al. 2010, Li et al. 2017) may not be applicable to freshwater organisms. Furthermore, the response of standard lab toxicity test species may differ from the response of native species (Schiffer and Liber 2017) and does not capture complex biotic interactions, such as compensation by more tolerant species (Leung et al. 2003, Vinebrooke et al. 2003).

In addition to residual acid extractable organic compounds, OSPW also has elevated concentrations of total dissolved solids and metals. The conductivity of OSPW can range from 1000 – 4000 $\mu\text{S}/\text{cm}$ and can have as large of an effect on organisms as NAFCs (Leung et al. 2003, Daly 2007, Rooney and Bayley 2011). The major ions present in OSPW are sodium, calcium, chloride, sulphate and bicarbonate (Leung et al. 2003; Kessler et al. 2010), and the ionic composition of the salinity has been shown to have a

direct effect on toxicity (Dwyer et al. 1992). However, complex interactions with other ions (White 2017) or NAFCs can mediate toxicity (Kennedy 2012, Kavanagh et al. 2012). White (2017) observed toxicity of *Ceriodaphnia dubia* to sodium salts was dependent on the accompanying anion. Kennedy (2012) observed an antagonistic effect of salinity and NAFCs on *Chironomus riparius* survival in lab toxicity tests and Kavanagh et al. (2012) noted a similar occurrence with the addition of NaHCO_3 , but not NaCl or Na_2SO_4 , reducing the toxicity of NAFCs.

Implications for reclamation

Wetlands will comprise a significant portion of the reclaimed landscape and will be important in restoring regional biodiversity and accumulating carbon (Rooney et al. 2012). To determine the effects of OSPM, on native wetland biota and processes, researchers have compared OSPM amended wetlands to natural and constructed wetlands within in the region (Bendell-Young 2000, Gardner-Costa 2010, Rooney and Bayley 2011, Kovalenko et al. 2013, Roy et al. 2016). Oil sands process materials affect all trophic levels from bacteria to vertebrates. Daly (2007) observed bacterial biomass was reduced in young OSPM wetlands compared to reference mesocosms, but stimulated in older OSPM wetlands compared to reference wetlands possibly as a result of an enriched carbon source from the NAFCs. However, lower bacterial production was observed in OSPM wetlands compared to reference wetlands, possibly due to elevated salinity.

Slama (2010) observed OSPM wetlands supported significantly less submerged macrophytes biomass compared to reference wetlands. Roy et al. (2016) and Rooney and Bayley (2011) observed distinct submerged macrophyte communities in OSPM wetlands compared to reference wetlands. Submerged macrophytes communities tended to have

fewer plant species that were more structurally simple, such as *Chara* sp. and *Potamogeton* sp. *Typha* stands grown in OSPM affected wetlands were smaller, and had less above and below ground biomass than *Typha* stands grown in reference wetlands (Mollard et al. 2013). Phytoplankton communities grown in microcosms had no differences in phytoplankton biomass over a range of NAFC concentrations and conductivities, but did support distinct communities which shifted to more tolerant phytoplankton species at higher NAFC concentrations (Leung et al. 2003).

In studies examining macroinvertebrate communities of OSPM wetlands, Kovalenko et al. (2013) observed reduced benthic macroinvertebrate biomass in younger OSPM wetlands compared to reference wetlands, but not in older OSPM wetlands. Younger OSPM wetlands supported a smaller biomass and less diverse benthic predator community. Oil sands process material wetlands were dominated by chironomids, having higher densities and biomass than reference wetlands (Bendell-Young et al. 2000, Kovalenko et al. 2013). Significant growth delays were also reported for tadpoles, reared in young OSPM wetlands compared to old OSPM wetlands and reference wetlands (Hersikorn and Smits 2011).

Aging of tailings reduces toxicity through microbial degradation from native communities that have developed *in situ* capable of aerobically and anaerobically degrading NAFCs in oil sands tailings (Herman et al. 1994, Holowenko et al. 2002, Han et al. 2009, Golby et al. 2012). Studies have shown a general decrease in acute toxicity as OSPW ages, which has been attributed to a decrease in NAFC concentrations (McCormick 2000, Leung et al. 2001, Anderson et al. 2012). Successful reclamation of FFT and OSPW will require the removal of NAFCs and elimination of the associated

acute and chronic toxicity, which will be achieved in part through enhanced bioremediation in wetland and lake habitats (Toor et al. 2013, Ajaero et al. 2018). However, there is a recalcitrant fraction of NAFCs resistant to microbial degradation that inhibits the reduction of NAFC concentrations to below 18 mg/L (Quagarine et al. 2005, Toor et al. 2013).

Degradation of NAFCs

Various bioremediation techniques are being researched to promote and enhance the breakdown of NAFCs. Bioremediation of OSPW has been studied in tailings ponds (Herman et al. 1994, Han et al. 2009), simulated wetlands (Toor et al. 2013, McQueen et al. 2017, Ajaero et al. 2018), and using microbial biofilms and bioreactors (Scott et al. 2005, Hwang et al. 2013, Xue et al. 2018). Although bioremediation is the most economical option and results in a reduction in NAFC concentration and acute toxicity (McQueen et al. 2017, Toor et al. 2013), mixtures of bio-persistent NAFC species and chronic toxicity remain within OSPW (Toor et al. 2013). Differences in the structure of individual NAFCs, the distinct microbial communities that develop within the different biological systems, and the conditions (pH, DO) in which the biological systems operate can all influence which NAFC species are degraded and which NAFC species persist (Xue et al. 2018).

To accelerate the breakdown of NAFCs, several advanced oxidative processes (AOPs) are being investigated (Scott et al. 2008, Kannel and Gan 2012, Hwang et al. 2013, Brown and Ulrich 2015, Quinlan et al. 2015). Advanced oxidative processes rely on the generation of strong oxidizing species, such as hydroxyl radicals, to completely mineralize NAFCs or break down persistent fractions to increase the biodegradability

(Kannel and Gan 2012, Hwang et al. 2013, Xue et al. 2018, Zhang et al. 2018). These processes include photocatalysis (Leshuk et al. 2016, McQueen et al. 2017), ozonation (Scott et al. 2008, Martin et al. 2010, Hwang et al. 2013, Zhang et al. 2018) and gamma irradiation (Boudens et al. 2016, VanMensel et al. 2017), which act to physically mineralize and catabolize NAFCs.

Ozonation has been demonstrated to be effective at reducing concentrations and increasing the biodegradability of the remaining NAFCs (Martin et al. 2010, Anderson et al. 2012, Hwang et al. 2013, and Zhang et al. 2018). At low doses (10 – 20 mg/L for less than 2 minutes), Martin et al. (2010) did not observe a reduction in toxicity following ozonation alone, but observed a reduction in toxicity following an incubation period with native microbial communities. High dose ozonation (30 mg/L) for 50 minutes by Scott et al. (2008) led to a 70% reduction in NAFC concentration and a complete elimination of toxicity using MicroTox assay, and a 96% reduction following ozonation for 130 minutes. Hwang et al (2013) observed the thicker and denser biofilm development following ozonation, which the authors attributed to an increase in bioavailable NAFCs following ozonation.

The increase in biodegradability of NAFCs exposed to ozone is most likely a result of the incomplete mineralization of more bio-persistent species, which are also more susceptible to ozone such as long carbon chains and cyclic NAFCs, into shorter chain, more bioavailable NAFCs (Martin et al. 2010, Zhang et al. 2018). Although pre-treatment using ozonation increases microbial degradation of NAFCs and reduces toxicity (Martin et al. 2010, Hwang et al. 2013, Zhang et al. 2018), the application of ozonation is limited by the high cost of generating enough ozone to treat the current

volume of tailings (Scott et al. 2008, Kannel and Gan 2012). The use of photocatalysis is limited by the need for particle free solutions, as UV is attenuated quickly by particulates (McMartin et al. 2004, Martin et al. 2010).

Although these methods have the potential to break down NAFCs and reduce toxicity, they have only been applied to OSPW. One novel treatment being explored to treat OSPW and the slurry FFT is the use of gamma irradiation. Gamma radiation is a form of ionizing radiation, a very high frequency electromagnetic radiation that reacts with water to produce highly reactive hydroxyl radicals (Getoff 1996). Cobalt⁶⁰ is commonly used in commercial gamma irradiation facilities to sterilize medical equipment, and prolong the shelf life of food. Gamma irradiation has also been employed industrially to remove a wide range of contaminants from waste water. These applications include the precipitation of heavy metals such as Pb²⁺ and Hg²⁺ from solution (Chaychian et al. 1998), reducing the total organic carbon in coking wastewater (Guo and Shen 2014), treatment of sewage (Borrely et al., 2000), and the breakdown of a model naphthenic acid (Jia et al. 2015). Gamma irradiation is favored because of its high-efficiency, low cost (Westoff 1996, Jia et al. 2015) and ability to penetrate slurry or sludge (Wang and Wang 2007).

Most recently, gamma irradiation has been used as a novel method of NAFC removal in both OSPW and FFT (Chen et al. 2013, Boudens et al. 2016, and VanMensel et al. 2017). Following gamma irradiation of tailings pond OSPW and FFT, Boudens et al. (2016) observed a reduction in NAFC concentrations of 85-97 % and 52-80% respectively. Similar to Martin et al. (2010), toxicity to MicroTox was not immediately reduced, but required an incubation period with native microbial populations, indicating

that GI likely broke down recalcitrant NAs into more biodegradable intermediates rather than fully mineralizing the organic compounds. This conclusion is further supported by VanMensel et al. (2017) who determined that GI stimulated microbial communities that were capable of biodegrading hydrocarbons most likely as a result of increased labile carbon. The observation of the genus *Ferruginibacter*, which is commonly associated with wetland environments, in GI treated OSPM but not untreated OSPM suggests that GI helps systems reach a pseudo-equilibrium more quickly.

Research scope and objectives

This thesis is part of a collaborative research effort in partnership with the labs of Dr. Christopher Weisener and Dr. Jan Ciborowski to provide proof of concept that GI provides sufficient detoxification to support natural biological communities and processes that allow biota to become established *in situ* in outdoor mesocosms constructed with gamma irradiated OSPM. This study was designed to determine if OSPM that has been gamma irradiated and reinoculated with indigenous microbial communities from tailings ponds and wetlands provides a suitable reclamation material that accelerates zooplankton and macrophyte colonization and increases the potential to accumulate carbon by reducing concentration of NAFCs. To address the suitability of GI as a reclamation treatment, the diel oxygen dynamics (used as a proxy for carbon) and zooplankton communities in mesocosms constructed from four different sources of tailings were tracked over a 33 month period. Tailings sources were chosen to be variable to determine how effective GI is on a range of tailings ponds. The development of GI as a treatment method could contribute substantially to the reclaiming and integration of tailings waste into the boreal landscape.

My second chapter will assess if GI reduces NAFC concentrations and the associated toxicity by tracking zooplankton community accrual in GI treated (G+) OSPM mesocosms reinoculated with indigenous microbial communities and compared to untreated (G-) OSPM mesocosms. To understand the effects of elevated salinity on zooplankton community accrual, OSPM mesocosms were compared to natural zooplankton communities collected from freshwater and hyposaline wetlands in the region. To date, no studies have determined what effect OSPM has on wetland zooplankton communities, and only one study has looked at the effects of OSPM on lake zooplankton communities in experimental mesocosms (McCormick 2000). Oil sands process material is toxic to model zooplankton species, but lab tests cannot predict community level effects, such as compensation by tolerant species (Leung et al. 2003, Vinebrooke et al. 2003). This study determined what effect OSPM had on wetland zooplankton communities, and if the detoxification of NAFCs made zooplankton communities in G+ OSPM mesocosms more similar to reference mesocosms in terms of biomass, density, and community composition.

The goal of my third chapter is to determine if GI can stimulate primary production and reduce mesocosm respiration. To achieve equal land capacity, reclaimed wetlands will have to function similarly to peatlands and accumulate carbon (Alberta Environment 2015). Carbon accumulation occurs when primary production is greater than respiration. Trites and Bayley (2009) demonstrated organic matter accumulation was possible in saline OSPM environments but rates of carbon accumulation are dependent on consistent water levels and slowly decomposing plant species. Wetlands constructed from OSPM tend to be less productive and support fewer and less diverse macrophytes than

reference wetlands (Slama 2010, Roy et al. 2016). NAFCs exhibit cytotoxic effects on macrophytes, reduce transpiration and growth (Trites and Bayley 2009), and inhibit germination (Crowe et al. 2002). In addition to low primary production, OSPM wetlands also tended to have higher rates respiration as a result of higher sediment oxygen demand (SOD) than reference mesocosms, as a result of increased chemical oxidation in the sediments (COD) (Gardner-Costa 2010, Slama 2010). Low productivity and high respiration will not be conducive to the accumulation of organic matter.

The majority of carbon that sustains microbial production in OSPM wetlands comes from hydrocarbons, which can support higher trophic levels such as *Daphnia* and chironomid larvae (Daly 2007). In reference wetlands, the carbon sustaining microbial populations largely comes from primary production. In order to make OSPM wetlands more similar to reference wetlands, and promote carbon accumulation, it will be important to promote primary production and minimize respiration.

Although GI may not directly stimulate primary production, a reduction in the concentration of NAFCs in OSPW and FFT (Boudens et al. 2016) could reduce cytotoxic effects and reduce the inhibition of macrophyte germination (Crowe et al. 2002) and growth. VanMensel et al. (2017) observed that in the laboratory gamma irradiation of OSPM stimulated microbial communities capable of degrading hydrocarbons and cycling nutrients compared to non-treated OSPM. In newly formed wetlands, biofilms are often the first colonizers and contribute to nutrient cycling, sediment stabilization, and supporting higher trophic levels (Frederick 2011). Biofilms are composed of both autotrophic and heterotrophic organisms which can partition resources and further facilitate the development of biofilms, and can contribute to the overall productivity of

shallow waters (Vadeboncoeur et al. 2006). Accelerated degradation of NAFCs by GI and the stimulation of the heterotrophic microbial community could facilitate the colonization of autotrophic microbial communities. Furthermore, in a study of the breakdown of a model naphthenic acid, Jia et al. (2015) observed that gamma irradiation effectively reduced COD. The efficiency of removal was positively correlated to the dosage, and negatively correlated to initial NA concentration. A reduction in COD, the major component of SOD in OSPM (Gardner-Costa 2010) could also lead to overall lower respiration which coupled with increased productivity could set GI treated OSPM on a trajectory to accumulate organic matter. My final chapter will be a general discussion that assess the potential to use GI as a reclamation treatment to accelerate the development of diverse and productive wetland communities and include limitations and recommendations for future research.

Chapter 2 - The Effects of Untreated and Gamma Irradiated Oil Sands Process Materials on Zooplankton Community Accrual in Field Based Mesocosms

Introduction

Zooplankton occupy a central position in lentic ecosystems, playing a key link in transferring nutrients from phytoplankton (primary producers) to heterotrophic consumers (Brett et al. 2009). Zooplankton are prey for almost all larval fishes (Sargent et al. 1995), benthic invertebrates (Hunt and Smith 2010), influence nutrient cycling through feeding and excretion (Wetzel 2001, Vanni 2002), and play an important role in maintaining clear water conditions (Jeppesen et al. 1999, Cottenie et al. 2001). Short generation times and ease of culturing make zooplankton model toxicity test organisms (Sánchez-Bayo 2006, Bownik 2017, McQueen et al. 2017, Schiffer et al. 2017, and White et al. 2017).

While single species toxicity tests are valuable for identifying constituents of concern, ecosystem interactions can mediate toxic effects observed in the lab (Shawn and Kennedy 1996). Ecotoxicological studies often use the cladoceran zooplankton, *Daphnia magna* and *Ceriodaphnia dubia* as model organisms, as they are often sensitive to toxic chemicals and are considered to be representative of relative ecosystem impacts (Hanazato 2001). However, single species toxicity testing may not be reflective of the ecological effects at the community level, because sensitivities have been found to differ among chemical compounds and different zooplankton species (Sanchez-Bayo 2006). For example, Sanchez-Bayo (2006) found that cladocerans were more sensitive to natural insecticides, PAHs, and aromatic hydrocarbons than copepods, while copepods were more sensitive to organochlorines and organohalogens than cladocerans.

Zooplankton community structure is influenced by physiochemical features such as pond area (Dodson 1992, Anas et al. 2014) and depth (Anas et al. 2014), salinity (Derry et al. 2003), turbidity (Lougheed and Chow-Fraser 1998), ionic composition (Waervaigen et al. 2002, Derry et al. 2003), pH (Arnott and Vanni 1993) and biotic interactions such as submerged aquatic vegetation cover (Lougheed and Chow-Fraser 1998, Cobbaert et al. 2015, Norlin et al. 2006), fish predation (Norlin et al. 2006), invertebrate predation (Hunt and Swift 2010), and competition (Lynch 1978).

Zooplankton communities are highly sensitive to anthropogenic and natural perturbations and respond rapidly through changes in the mode of reproduction (Nevalainen et al. 2011), and shifts in community structure (Vinebrooke et al. 2003, Jeziorski et al. 2015). Zooplankton are known to switch from parthenogenesis to the sexual production of diapausing eggs as a response to environmental and anthropogenic stressors which increases genetic diversity (Nevalainen et al. 2011). In soft water lakes of Ontario, declines in dissolved calcium have resulted in a decline of calcium rich *Daphnia* and an increase in calcium poor species such as *Holopedium gibberium* and *Bosmina* spp. This change in species composition alters the way nutrients such as calcium and phosphorus (both abundant in *Daphnia*) are transferred through the food web to higher trophic levels, such as fish (Jeziorski et al. 2015).

In response to elevated temperatures (MacLennan et al. 2015, Sorf et al. 2015), acidification (Vinebrooke et al. 2013), and chemical perturbations (Moore and Folt 1993, Hanazato 2001), zooplankton communities tend to shift from dominance by larger bodied *Daphnia* to smaller bodied cladocerans (*Bosmina* and *Chydorus*) and rotifers. Rotifer assemblages tend to be more diverse than cladoceran assemblages and contain tolerant

species within a community that can compensate for the loss of sensitive species (Hanazato 2001, Vinebrooke et al. 2003). Shifts in community size following warming are most likely a result of shorter generation times in small bodied zooplankton compared to larger zooplankton (Gillooly 2000), and a disproportionate increase in respiration by large bodied zooplankton resulting in energy deficits at elevated temperatures (Moore and Folt 1993).

Zooplankton in the western boreal forest zone

Despite the central position of zooplankton in aquatic ecosystems, zooplankton are a poorly studied component of the western boreal forest ecosystem (Swaddling et al. 2000, Norlin et al. 2005, 2006), especially in the Athabasca oil sands region (McCormick 2000, Anas et al. 2016). The reclamation of typical, self-sustaining wetland and lake ecosystems will be dependent on the establishment of zooplankton communities to sustain higher trophic levels. Patterns of zooplankton distribution in shallow ponds are largely linked to patterns in primary production (Pennak 1966, Jeppesen et al. 1999, Norlin et al. 2006, Vanderstukken et al. 2010).

Zooplankton community composition in shallow ponds, typically reflects one of two primary states - a clear water state and a turbid water state, which can alternate over time (Scheffer et al. 1993, Cobbaert et al. 2015). Ponds in the clear water state are characterized by extensive submerged aquatic vegetation (SAV) cover, relatively low chlorophyll *a* concentrations and a zooplankton community composed primarily of large grazers (*Daphnia*, *Simocephalus*) and small to medium-sized littoral zooplankton (*Ceriodaphnia* spp., Chydoridae) (Cottenie et al. 2001, Norlin et al. 2006). In contrast, ponds in a turbid state are characterized by low SAV cover, high concentrations of

chlorophyll *a*, and a zooplankton community dominated by rotifers and copepods and lacking in cladocerans (Jeppesen et al. 1999, Cottenie et al. 2001, Norlin et al. 2006).

During the clear water phase, macrophyte-rich ponds provide habitat for littoral/plant -associated zooplankters, and attachment sites for epiphytic algae and biofilm (Vanderstukken et al. 2010). Grazing by zooplankton keeps phytoplankton levels low, which in turn creates an adequate light environment for macrophyte growth (Scheffer et al. 1993). Macrophytes in turn stabilize the substrate, which minimizes sediment suspension (Jeppesen et al 1999). Conversely, turbid ponds are characterized by abundant phytoplankton, which limits light penetration, and reduces the depth of the photic zone inhibiting macrophytes development (Scheffer et al. 1993). Cobbaert et al. (2015) and Bayley and Prather (2003) also reported the presence of systems in intermediate states, some having both abundant SAV and high phytoplankton concentrations (co-rich); and others with little SAV and low phytoplankton concentrations (co-poor), which is most likely made possible by shallow depths of the studied wetlands allowing light for SAV growth and high nutrient levels reducing competition among macrophytes and phytoplankton.

Wetlands in the Athabasca Oil Sands region

The wetlands and ponds surrounding the Athabasca oil sands are primarily shallow (<2 m deep), fishless due to a lack of connectivity with larger waterbodies and harsh winter conditions (Tonn et al. 2004), and meso- to eutrophic (Bayley and Prather 2003, Norlin et al. 2005, Cobbaert et al. 2015). Research by Slama (2010), Rooney and Bayley (2011), and Roy et al. (2016) has shown that submerged aquatic vegetation communities in OSPM wetlands compared to reference wetlands are less diverse, contain

fewer species, support lower biomass, and tend to be monotypic. The species found to occur most often in OSPM amended wetlands are *Chara* and *Potamogeton*, which are tolerant of low nutrients, elevated salinity, and alkaline waters (Rooney and Bayley 2011). Wetlands with high ionic concentrations, or that were very turbid tended to lack submerged aquatic vegetation all together. Differences in SAV communities was attributed to increased concentration of oil sands constituents, elevated alkalinity, and total dissolved solids (salinity) (Cooper 2004, Rooney and Bayley 2011, Roy et al. 2016).

It is therefore reasonable to expect that zooplankton communities in OSPM amended wetlands would also differ. However, to our knowledge, there have been no published surveys of zooplankton communities in either OSPM amended wetlands or in reference wetlands within the oil sands region. If SAV is an essential component of zooplankton habitat and provides a surface for epiphytic algae, which is a food source for plant-associated zooplankton, the kinds of plankton communities (and higher trophic levels in a food web) that one can expect to occur in reclaimed wetlands will ultimately depend on a wetland's capacity to sustain productive and structurally complex SAV communities.

Toxicity of OSPW to zooplankton

Oil sands process water has acute and chronic effects on zooplankton including reduced fecundity, growth and feeding (Lari et al. 2016, Li et al. 2017). High concentrations of total dissolved solids (measured as salinity) and turbidity may also affect zooplankton and contribute to acute and chronic toxicity (Allen 2008). The dominant ions in OSPW are SO_4^{2-} , Cl^- , CO_3^- , and Na^+ , and concentration of specific ions, such as Cl^- and CO_3^- , exceed Canadian water quality guidelines (McQueen et al.

2017, White 2017), and may be at concentrations high enough to induce chronic effects (Allen 2008, Zubot et al. 2012). Elevated salinity may also exacerbate the toxic effects of NAFCs by inducing osmotic stress and disrupting the cell membrane (Quagarine et al. 2005). Daly (2007) attributed a decrease in the production:biomass ratios of planktonic microbial communities in OSPM affected wetlands compared to reference wetlands to be a result of elevated salinity. Examining phytoplankton in a series of test ponds with variable salinities, ionic compositions, and NA concentrations, Leung et al. (2003) determine salinity exerted as strong of an effect on structuring phytoplankton communities as NAFC concentrations. Furthermore, trace metals in OSPW such as vanadium occur at concentrations high enough to have acute and chronic effects on regional zooplankton species (Puttaswamy and Liber 2012, Schiffer and Liber 2017).

Lab based studies have observed an LC₅₀ ranging from 2% - 27% for OSPW (Li et al. 2017). Assuming an initial concentration of 120 mg/L that would correspond to an NAFC concentration of 2.5 - 32.4 mg/L. In a series of microcosms using OSPM materials of different ages that had undergone varying degrees of NAFC biodegradation, McCormick (2000) observed a significant reduction in total zooplankton biomass as a response to increasing NAFC concentrations. Microcosms constructed of aged material had lower NAFC concentrations and less of an effect on total zooplankton biomass than fresh material with higher NAFC concentrations. From this experiment, McCormick (2000) calculated a “no effect” NAFC concentration of 5 mg/L. Although single species toxicity tests are useful for determining toxicity, laboratory tests may not predict community level responses which are often modified by complex biotic interactions

(Cairns 1983). Therefore it is important to study and understand the effects OSPM may have on natural zooplankton community structure.

Objectives

The majority of previous OSPW studies have used single species assays to determine the toxicity of OSPW (Puttaswamy and Liber 2012, Zubot et al. 2012, Lari et al. 2016, McQueen et al. 2017, Schiffer and Liber 2017). To date, there is little research on the community level effects of OSPW on zooplankton (McCormick 2000). The objectives of this study are to 1) determine the effects of OSPM on colonization by zooplankton in field based mesocosms 2) if gamma irradiated OSPM undergoes sufficient detoxification to support the colonization of wetland zooplankton communities similar to reference mesocosms under natural conditions (freeze-thaw, rainfall, temperatures, and natural perturbations) in outdoor mesocosms. This research is a proof of concept of biological responses to determine if GI is a viable treatment to treat material used for oil sands reclamation in a natural setting. To quantify the effects of OSPM on zooplankton communities, the richness, biomass, and average zooplankter length were compared to freshwater (FW) and hyposaline (HSW) wetland zooplankton communities. To quantify the effects of a novel method of tailings treatment (gamma irradiated OSPM) zooplankton communities colonizing mesocosms containing treated OSPMW were compared to communities colonizing untreated OSPM. To determine if relative salinity was important in structuring zooplankton communities, GI treated OSPM zooplankton communities were compared to freshwater (FW) and hyposaline (HSW) wetland zooplankton communities. I also qualitatively assessed the relative abundance of

zooplankton community taxa to determine if OSPM mesocosms supported zooplankton communities similar to those in the FW and HSW mesocosm controls (Appendix B).

Zooplankton communities can vary among water bodies, either through differences in the abundance or mean size of individuals of a given species (Basińska et al. 2014) or through differences in species composition (Moore and Folt 1993). Smaller-bodied cladocerans and rotifers have shorter generation times, are less sensitive to toxic compounds, and have lower overall food requirements than large-bodied species, making them better competitors under stressed conditions (Moore and Folt 1993).

I predicted that:

- 1) Untreated OSPM mesocosms would have the lowest zooplankton biomass and would be dominated by zooplankton associated with turbid states and resistant to high levels of contaminants, primarily rotifers
- 2) If gamma irradiation is an effective treatment method for reducing OSPM toxicity, then I expected GI treated OSPM mesocosms to support similar diversity, biomass and, species composition of zooplankton in comparison to HSW mesocosms; I expected FW and HSW mesocosms to have similar communities, dominated by small bodied cladocerans and large-body daphnids. If GI is effective at treating tailings toxicity, I expected to see a shift from tolerant rotifers species, to less tolerant, larger bodied cladocerans such as *Daphnia*.
- 3) If salinity is a factor limiting zooplankton colonization, then I expect HSW mesocosms to have a lower abundance and biomass than FW mesocosms. Furthermore I expected salinity constraints to make the communities colonizing

gamma irradiated OSPM mesocosms more similar to HSW mesocosms than FW mesocosms.

Methods

Study site and donor materials

The experiment was setup north of Fort McMurray, AB at the Suncor Experimental Trenches Research Complex (56°58'50.0"N 111°30'22.8"W) (Fig. 2.1). The experimental trenches are 10 m wide x 50 m long x 1 m deep, lined reservoirs that were built in 1992 to study the effects of OSPM and OSPW (Gulley and Klym 1992), and since 2005, have contained water that supported wetland plant establishment (described further in Frederick 2011) and would provide a source of potential colonists. A little-used private access road formed the south boundary of the area. The north boundary was a stand of mature trees adjacent to a vegetated trench that received outflow from the experimental trenches. Mesocosms were arranged between two of the trenches in 3 columns and 8 rows. The allocation of treatment to mesocosms around the trenches was stratified-randomized using a random number generator and a schematic of the mesocosms set up is provided in Appendix 4.

The Trench Complex itself was surrounded by extensive wetlands that were also potential sources of invertebrate and plant colonists. The study site has mean summer and winter air temperatures of 14°C and -16°C, respectively, and evapotranspiration exceeds potential precipitation in the region with precipitation totaling 300 to 600 mm per year (Johnson and Miyanishi 2008). The study region experienced a period of unseasonably warm and dry weather in late April and early May 2016. This led to extensive forest fires,

which prevented access to the site until late June in 2016. At this time, some reference mesocosms had no standing water, but the sediment remained saturated. Data recovered from temperature loggers submersed in each mesocosms raises the possibility that evaporation may have resulted in complete loss of water from some of the reference, between May 14 2016 and June 26, 2016 but not from tailings mesocosms as there was sometimes a greater than 10°C difference among mesocosms in a single hour and extreme temperatures (35°C - 42°C); typically, among-mesocosm temperature differences were only 4-8°C at any given hour and the maximum water temperature did not exceed ambient air temperatures (maximum 30°C to 32°C).

Precipitation records were obtained from nearby weather stations set up and operated by Hatfield Consultants (1 – 2 km away from the study site) and otherwise empty mesocosms were used to collect and measure the volume of precipitation falling during the active sampling periods. To ensure that relatively constant water levels were maintained, distilled water was added to each mesocosm as needed, and the volume added was recorded. A more detailed record of water additions and precipitation is provided in Chapter 3.

In August 2014, water and sediment were collected from three freshwater wetlands (abbreviated FW1-3), three hyposaline water wetlands (abbreviated HSW1-3) and four tailings ponds (abbreviated OSPM1-4) to construct mesocosms (Fig. 2.1). The FW wetlands used are locally named Crescent (= Suncor Sand Pit) (56°54'05.3"N 111°24'20.9"W), Muskeg (57°08'11.1"N 111°36'07.4"W) and Shallow (57°04'52.8"N 111°41'27.2"W). The three HSW wetlands used are locally named Golden Pond (56°59'47.8"N 111°37'34.1"W), High Sulphate (56°59'50.7"N 111°33'11.8"W) and

Saline Marsh (56°59'37.3"N 111°32'08.8"W). The four tailings ponds used for OSPM were Syncrude's Mildred Lake Settling Basin (MLSB; 57°4'27"N 111°38'19"W), Suncor's Pond1A (P1A; 56°59'30.8"N 111°28'47.8"W), Suncor's South Tailings Pond (STP; 56°52'19.4"N 111°20'47.0"W) and Shell's Muskeg River Mine (MRM; 57°14'05.1"N 111°34'04.4"W), which was added to the experimental design at the beginning of September, 2015.

Approximately 80 L of water and sediment were collected from each of the 6 reference wetlands and stored in sealed 20-L polyethylene pails at ambient temperatures inside Syncrude's Environmental Complex Warehouse. Approximately 120 L of OSPW and FFT were collected by the oil sands companies from each of the four tailings pond. Extra OSPM was simultaneously collected for P1A, STP and MLSB for the construction of six additional mesocosms to parallel and scale up lab experiments performed by Boudens et al. (2016). Tailings materials from Syncrude and Suncor tailings ponds were collected in September 2014. Material from the Shell tailings pond was collected in August 2015 and set up in September 2015.

Half of all the material collected from reference wetlands and tailings ponds was shipped by ground freight and received by Roberta Pasuta of McMaster Institute of Applied Radiation Services (McIARS), Hamilton, Ontario, Canada for gamma irradiation. Irradiation was completed over a three week period from September 5 – September 26, 2014 using Cobalt-60 with the same methods as described in Boudens et al. (2016). Samples were rotated during irradiation to ensure a uniform deposition of the dose. The non-irradiated half of the materials were stored on site at the Syncrude Environmental Complex Warehouse at ambient temperatures. All materials were

transported to the Trench complex during the last week of September 2014 for mesocosm construction which took place over a three day period from October 3-5, 2014.

Donor wetlands were selected based on relative salinity (as measured by electrical conductivity) recorded during synoptic surveys of wetlands conducted as part of a separate monitoring program to assess the development of a reclaimed marsh and a reclaimed fen (COSIA 2017). Reference wetlands either formed opportunistically as a direct or indirect result of mining activities, or were constructed by oil sands mining companies. A summary of the wetlands and tailings ponds and select characteristics of each is provided in Appendix 1. The tailings ponds used in this study were variable in age and were designated as being relatively young tailings pond (12 to 15 years old and receiving fresh FFT and OSPW: STP, MLSB and MRM) or “aged” (~ 45 years old and not receiving fresh inputs of FFT, but continues to be used for the recycling of surface OSPW: P1A). Although MLSB was constructed in 1978, the FFT and OSPW collected for this experiment were obtained directly from the inflow pipe and were considered to be “fresh”.

In addition to differing in age, the chemical composition of tailings ponds can be quite variable pond to pond and the exact characteristics (pH, ion concentrations, particle size, organic compounds) of each tailings pond can vary based on a variety of factors including the parent ore, the addition of chemicals to the extraction process, and the treatment of tailings (FTFC 1995). Furthermore, mixtures of NAFCs in OSPW have been shown to vary temporally within an individual tailings pond, and spatially between tailings pond (Frank et al. 2016, Huang et al. 2018). From a NAFC perspective, the youngest tailings ponds would be expected to contain a full range of labile and persistent

NA congeners while the oldest tailings pond, which has not received any fresh inputs of FFT in decades, would be expected to contain only recalcitrant NA congeners that have not been biodegraded (VanMensel et al. 2017). The tailings ponds chosen in this study were chosen to represent a range of reclamation scenarios so that broader inferences on the efficacy of GI as a tailings treatment could be made.

Mesocosm construction

Rubbermaid Roughneck[®] totes (W 41 cm x L 61 cm x H 41 cm) made of low density polyethylene were used as experimental mesocosms. The units were kept open to the environment to allow natural colonization of wetland organisms and quasinatural conditions (sunlight, precipitation, freeze-thaw cycles, etc.). Each mesocosm was provisioned with sediment and water from a single tailings pond or wetland and each wetland had a G- and G+ complement, resulting in the creation of 18 experimental units (9 sources x 2 irradiation treatments) in October 2014, and 20 experimental units in September 2015 following the addition of the Muskeg River Mine tailings materials. Each mesocosms was filled with a 10-cm layer of sediment (~16L) and covered with a 15-cm water cap (~20 L).

Additional wetland materials were collected from each of the 6 reference wetlands in October 2014, and an aliquot of the non-irradiated FFT and OSPW from each tailings pond were combined in equal proportions to create a composite inoculum. Each mesocosm received an aliquot of sediment (1.25 L) and water (2 L) inoculum to provide similar starting communities and because all biota were presumably sterilized in GI treated materials, including microbial communities, plant fragments, aquatic

invertebrates, phytoplankton and zooplankton. The same inoculum was added to all G-mesocosms to ensure consistency in the experimental design.

To monitor the accumulation of organic matter being aerially deposited from the surrounding environment, three mesocosms were set up with a 25 cm of water (~37 L, which is equivalent to the amount of material used to construct the wetland/tailings pond replicates) and designated Blank 1, Blank 2 or Blank 3. Each mesocosm was nested within a 36" diameter wading pool made of durable plastic, which was itself placed inside of a 59" diameter wading pool made of durable plastic to catch any potential overflow during precipitation events. This minimized the risk of any tailings material coming in to contact with the environment (Fig 2.3). Mesocosms were actively monitored and maintained from mid-June to the end of August in 2015, from July to the end of August in 2016 and from early May to mid-June in 2017.

Experimental design

This study examined the effects of two factors on zooplankton colonization. The first was NAFC concentration using GI to reduce measured concentrations, mesocosms were designated as G- if they were untreated, or G+ if the material was gamma irradiated. The second factor was relative salinity (as measured by conductivity) which had three levels; freshwater reference (FW) n = 3, hyposaline reference wetlands (HSW) n = 3, and tailings ponds (OSPM) n = 3 in 2015, and n = 4 in 2016. Each individual wetland or tailings pond was considered a replicate. Both freshwater and hyposaline wetlands were considered to be reference treatments because although GI degrades NAFCs, salinity remains unchanged (Chen et al. 2013, Boudens et al. 2016), and is expected to influence developing wetland communities (Leung et al. 2003, Trites and Bayley 2009).

Non-irradiated (G-) OSPM mesocosms represent habitats that are constrained by both elevated salinity and elevated concentrations of NAFCs. Gamma irradiated (G+) OSPM mesocosms are constrained by elevated salinity, but have reduced levels of NAFCs. The HSW replicates are constrained by elevated salinity, but not by NAFCs. Finally, FW replicates represented habitats that were constrained by neither increased salinity nor NAFCs.

Zooplankton collection

Zooplankton samples were collected from mesocosms monthly in July and August 2015 and 2016 and biweekly in May and June of 2017. Samples from 2017 were archived because they didn't match the time frames of the other samples, and were sampled closer together to allow for future examination of zooplankton community growth. Samples were collected using an aquarium gravel vacuum with a PVC hose (diameter 5 cm) to siphon 2 L of water from each mesocosm (~10% of mesocosm volume) into a 2-L glass measuring cup. The sample was then poured through a 63- μ m mesh plankton net, rinsed into a 250-mL glass sample jar, and preserved with 70% ethanol. The filtered water was returned to the mesocosm so as to not change the volume or ionic balance. All sampling equipment was rinsed after each mesocosm was sampled in a bleach solution, then rinsed in distilled water to minimize the likelihood of transferring zooplankton and vegetation propagules among mesocosms.

Water chemistry, NAFCs, and environmental characteristics

Measurements of conductivity, dissolved oxygen concentration (DO) and salinity were made on each sampling date with a handheld YSI model 85 meter. Total suspended solids (TSS) were measured once in July 2015 (APHA 2540), and turbidity was measured

once in May 2017 (APHA 2130 A) to determine a relative level of water clarity. Weekly estimates of water clarity were made by putting a black polycarbonate ruler with white writing into the water and observing the depth at which the 0-cm mark could no longer be read. Chlorophyll *a* concentrations were measured in July of 2015 and 2016 (APHA 10200 H) to estimate phytoplankton biomass. Water samples were collected at 0, 9, 11, 22 and 31 months and sent to the Syncrude Canada Limited Analytical Laboratory (Edmonton, AB) to be analyzed for major ions, NAFCs and total alkalinity. HOBO Pendant[®] Temperature /Light 64K loggers (Onset Computer Corporation, Bourne, MA) were installed just above the sediment in each mesocosm to provide a continuous record of water temperature and of relative light intensity. Logging frequency was set to every 15 min over the course of the active sampling period and every 60 mins the rest of the time.

Dissolved oxygen loggers were used to record diel changes in DO, and are described in detail in Chapter 3. It was predicted that submerged aquatic vegetation would influence zooplankton communities. Estimates of submerged aquatic vegetation (SAV) relative cover (percent) were used to quantitatively assess zooplankton habitat multiple times per season (Appendix 2). The microbial biofilm, SAV, emergent macrophytes and roots were collected at the end of the study in June 2017 to determine biomass (Appendix 2). In addition to collecting zooplankton, macroinvertebrates were also sampled qualitatively using an aquarium net (3" long x 3" wide x 3" deep) with 0.25 mm mesh, with similar sampling efforts in all mesocosms. Macroinvertebrates were quantitatively sampled using artificial substrates by attaching aquarium plants resembling individuals of the genus *Elodea* to the unglazed side of 17.7 x 17.7 cm ceramic tiles and

leaving them *in situ* for 8 days (Scher et al. 2010). Both sweep and artificial substrate samples were archived for further analysis and will not be discussed further in this study.

Enumerating zooplankton samples

In the laboratory, zooplankton samples were poured through two nested sieves, 250 μm and 63 μm apertures. The fraction retained on the 250- μm sieve was counted as the crustacean zooplankton sample and the fraction retained on the 63- μm sieve was designated as the rotifer sample, preserved, and archived for future analysis. For the purpose of this study, only crustacean zooplankton found in the 250- μm fraction were identified, enumerated, and measured using a Wildco[®] acrylic Ward counting wheel 5-10 mL (Ben Meadows Company, Janesville WI) beneath a stereoscopic Wild M8 dissection microscope (6-50X magnification) with 20X eye pieces. Smaller zooplankton were wet mounted and examined beneath a Meiji ML2300 (40-100 X magnification) trinocular compound microscope to measure them. Rotifers in the 250- μm fraction were identified to genus but were not included in subsequent analyses due to difficulties and uncertainties in accurately measure them, furthermore *Brachionus* rotifers were typically observed occurring in masses that were difficult to separate and accurately count. However, because rotifers were the dominant taxa, especially in the OSPM mesocosms, they were included in the qualitative assessment of the zooplankton community (Appendix 2).

Crustacean zooplankton were identified to the lowest taxonomic resolution possible, usually to species, using the keys of Edmondson (1959). However, *Ceriodaphnia* and *Simocephalus* were only identified to genus due to difficulties in confidently assigning them to a species. Ostracods were enumerated and measured but

not identified further. Rotifers were enumerated, measured, and identified to genus except for members of Bdelloidea, which were not identified further, due to severe contraction in preserved specimens (Edmondson 1959).

Samples were transferred from the 250- μ m sieve into a volumetric beaker using a funnel, and stirred to ensure homogeneity. Two-mL aliquots were then drawn from the beaker using a marked pipette. Samples were subsampled and enumerated as per MacLennan et al. (2014). If a sample had fewer than 300 individuals it was counted in entirety. If there were more than 300 individuals then a minimum of two subsamples and 300 individuals, were counted such that the variance between subsamples was less than 10% of the mean number of individuals. To ensure that rare species were detected, twice the volume of the volume subsampled or at least one-half of the total sample volume was examined for rare species, identified as any species represented by fewer than 5 individuals counted from the total 300.

The first 15 individuals of each species and life stage encountered were photographed and measured using a SPOT[®] microscope camera and SPOT Imaging[™] advanced software. Length measurements were used to estimate weighted mean length of specimens in a sample and to convert measured lengths into biomass estimates using published length-weight regression formulae (Dumont et al. 1975, Bottrell et al. 1976, Rosen 1981, O’Gorman and Emmerson 2009). Males and “juveniles” were measured separately from mature females to reduce the variance in the estimates of average length for any given species before summing biomass. Juveniles were arbitrarily assigned based on size, except for *Daphnia* species, which were classified based on the development and size of the first abdominal process. This process is typically equal to or longer than the

second abdominal process in mature females. *Ceriodaphnia* and Ostracoda juveniles were individuals less than 0.5 mm long, *Simocephalus* juveniles were individuals measuring less than 0.8 mm, and *Daphnia* juveniles were individuals that did not have fully developed abdominal processes. A total of 68 zooplankton samples were enumerated and identified from experimental mesocosms n = 18 in July 2015, n = 18 in August 2015, n = 20 in July 2016, and n = 20 in August 2016. In addition 9 samples were enumerated and identified from the 3 “Blank” mesocosms used to track the aerially deposited organic matter from the environment, n = 3 in August 2015, n = 3 in July 2016 and n = 3 in August 2016. These samples were not included in further analyses but the density, total crustacean zooplankton biomass, and relative abundance were included in Appendix 3.

Statistical analysis

Linear mixed-model analyses were performed using the Mixed Models - Linear routine of IBM SPSS 24 (IBM version 24.0, IBM Corp.). GI Treatment, relative salinity and sampling date were treated as categorical fixed effects with date as the repeated measure and mesocosm as the subject. Although no random factors were used, mixed models were the best choice because they enable the author to select the proper variance-covariance model to account for correlation between repeated measures and do not require repeated measures to be evenly spaced as with traditional ANOVA analysis (Seltman 2015). Several covariance structures were tested and the one minimizing the AIC was used. Biomass ($\mu\text{g/L}$) and density (individuals/L) were $\log_2(x+1)$ transformed to improve model fit and to transform the scale into octaves so that an increase of one unit represents a doubling in the response variable. Mean weighted length (mm) and

richness were not transformed prior to analysis. To assess the functional aspect of community composition, each species was assigned to a feeding mode as well as a habitat to qualitatively observe structural differences in zooplankton communities based on observed ecology (Balcer et al. 1984, Rautio et al. 2006, Fryer 2009).

Biomass, and richness were fitted with a first order auto-regressive (AR1) covariance structure. The first order auto-regressive covariance structure assumes homogeneous variance but allows the covariance to vary with distance or time between samples so that samples measured closer in time tend to be more highly correlated (Littell et al. 2000). The mean weighted length and richness models had a diagonal covariance structure that allowed for heterogeneous variance. Pairwise comparisons with a Bonferroni adjustment were run despite a non-significant main effect for GI treatment because I expected GI would have an effect on OSPM mesocosms but not on FW or HSW mesocosms.



Fig. 2.1: Google Earth image of Alberta showing Fort McMurray (yellow star) and the study area (yellow box). Red bar at bottom left measures 100 km.



Fig. 2.2: Google Earth image of reference sites (yellow dots – freshwater, blue dots – hypersaline water) and tailings ponds (red dots), and the experimental trenches (pink dot) in relation to Fort McMurray. Red bar at bottom left measures 10 km.



Fig. 2.3: Mesocosms set up at the Experimental Trench Complex showing the 3 x 10 experimental setup, the precipitation mesocosms and the DO calibration mesocosms used in Chapter 3 and additional mesocosms constructed for a parallel study by Boudens et al. (2016).

Results

Water chemistry, NAFCs and temperature

Mean \pm SE electrical conductivities for untreated FW, HSW and OSPM mesocosms were $371.5 \pm 99.38 \mu\text{S/cm}$, $1406.5 \pm 480.3 \mu\text{S/cm}$, and $1934.8 \pm 711.3 \mu\text{S/cm}$ respectively. Mean \pm SE electrical conductivities for GI treated FW, HSW and OSPM mesocosms were $380.9 \pm 142.8 \mu\text{S/cm}$, $1117.6 \pm 518.2 \mu\text{S/cm}$ and $2033.5 \pm 757.5 \mu\text{S/cm}$ respectively. The concentration of NAFCs in all reference wetlands was below 8 mg/L (Appendix 1). Initial mean \pm SE NAFC concentration in untreated OSPM mesocosms was $62.3 \pm 2.7 \text{ mg/L}$ in OSPW and $45 \pm 14.3 \text{ mg/L}$ in FFT. Following gamma irradiation of OSPM the mean \pm SE NAFC concentration of OSPW was $10.1 \pm 6.4 \text{ mg/L}$ and $25.3 \pm 3.9 \text{ mg/L}$ in FFT. The reduction in NAFC concentration was not consistent across OSPM replicates (Table 2.1, 2.2). Gamma irradiation of younger OSPM mesocosms resulted in a greater than 90% reduction in measured NAFC concentrations, compared to a 54.7% reduction in aged OSPW (Table 2.1). Natural aging of the OSPW in the younger tailings pond mesocosms did not result in any further reductions in NAFC concentrations, but rather NAFC concentrations appeared to increase around months 9 - 11, before decreasing again (Table 2.1). The concentration of NAFCs in aged OSPW continued to decline over the duration of the experiment (Table 2.1). The mean \pm SE NAFC concentration in OSPW on the final day of the experiment for GI treated OSPM mesocosms was $12.5 \pm 5.6 \text{ mg/L}$. In untreated OSPM mesocosms NAFC concentrations in OSPW steadily decreased until the end of the experiment where a final mean \pm SE of $12.9 \pm 0.8 \text{ mg/L}$ was reached. The reduction in NAFC concentrations of FFT also appeared to be dependent on the replicate. NAFC concentrations were reduced in the two

OSPM mesocosms with the highest initial concentrations from (71 mg/L to 27 mg/L in P1A and from 68 mg/L to 32 mg/L in MLSB) (Table 2.2). The concentration of NAFCs in STP and MRM remained relatively unchanged.

Daily mean \pm SE temperatures were calculated from the continuous temperature record by each of the n = 18 HOBO Pendant[®] loggers in 2015 and n = 20 loggers in 2016 and 2017, respectively (Appendix 4). Daily mean \pm SE temperatures in July and August were 20.8 \pm 0.1°C (n = 31 days) and 19.4 \pm 0.1°C (n = 31 days). In 2015, the maximum recorded temperature was 33.1°C in July, and 33.9°C in August. Temperatures in 2016 were slightly warmer on average than in 2015 with mean \pm SE maximum temperatures of 22.5 \pm 0.1°C (n=31 days) and 20.2 \pm 0.1°C (n=31 days), in July and August respectively. In 2016, the maximum recorded temperature was 34.7°C in July and 33.4°C in August. Daily mean \pm SE temperatures for May and June 2017 were 16.1 \pm 0.1°C (n=31 days) and 20.7 \pm 0.1°C (n=30 days) respectively. In 2017, the maximum recorded temperature was 32.6°C in May and 34.4°C in June.

Chlorophyll *a* concentrations were all below detection limits indicating that phytoplankton was not a significant component in the mesocosms. All reference mesocosms developed and maintained macrophyte communities for the duration of the study. Fresh and saline reference communities developed natural plant communities consisting of common and fast colonizing wetland species. Untreated OSPM replicates G- MRM and G- MLSB supported macrophytes (*Schoenoplectus*) in the first year of the study, but failed to persist after the first winter. Gamma irradiated OSPM replicates G+ P1A, G+ MLSB and G+ MRM supported *Schoenoplectus* in the first year of the study but only persisted in G+ MLSB and G+ MRM mesocosms in subsequent sampling years. In

2015, *Myriophyllum* was observed in a single tote but after the winter of 2015 only *Chara* and *Potamogeton* (*P. foliosus* and *P. pusillus*) were observed in the SAV community. Water plantain (*Alisma*) was recorded in 9 of 21 mesocosms in 2015, 3 of 24 totes in 2016 and absent in 2017. *Typha* was observed in 6 of 21 mesocosms in 2015, 3 of 24 totes in 2016 and absent in 2017. *Schoenopelctus* was found to occur in 13 of 21 mesocosms in 2015, 12 of 24 totes in 2016 and 10 out of 24 totes in 2017. *Eleocharis* was only ever found in Shallow (G- and G+) and occurred in all three years.

Plant communities were structurally simple, composed of thin and single branching SAV species and macrophyte species, % cover of macrophytes was recorded several times during each growing season and is presented in Appendix 2. Taxonomic richness of vegetation communities decreased during the experiment as totes became dominated by either emergent macrophytes or SAV. Following low water levels in 2016 and warmer than normal temperatures, there was abundant epiphyton in the majority of totes, and epiphyton made up 30-100% cover. After maintaining stable water levels for the summer of 2016 and overwinter into the spring of 2017, heavy epiphyton cover was still observed in 2017. Emergent macrophytes, roots, submerged aquatic vegetation (including epiphyton) and microbial biofilms were harvested and dried to determine dry weight (g), results are presented in Appendix 2.

Total suspended solids and turbidity were used to determine relative water clarity. Total suspended solids analyzed in 2015 were highly variable among mesocosms ranging from 0.7 – 96.08 mg/L. Gamma irradiated mesocosms tended to have marginally higher median TSS than their G- counterparts despite high variability ($Z = -1.955$, $p = 0.051$) (Table 2.3). Total suspended solids had a mean \pm SE of 42.25 \pm 27.13 mg/L in G+ OSPM

mesocosms, 19.65 ± 9.85 mg/L in G-OSPM mesocosms, 20.09 ± 12.56 mg/L in G+ HSW mesocosms, 4.85 ± 0.55 mg/L in G- HSW mesocosms, 28.65 ± 21.66 mg/L in G+ FW mesocosms and 4.2 ± 2.06 mg/L in G- FW mesocosms. (Table 2.3). Turbidity analyzed in 2017 was variable among mesocosms ranging from 1.35 – 49.8 NTU. Turbidity was higher and more variable in G+ OSPM mesocosms compared to G- OSPM mesocosms (Table 2.3). With the exception of one reference mesocosm (G- Muskeg, 26.2 NTU), turbidity in reference mesocosm was typically below 10 NTU. With the exception of two G+ OSPM mesocosms (MLSB 7.43 NTU and MRM 6.60 NTU) turbidity in OSPM mesocosms was typically greater than 10 NTU.

Table 2.1: Concentration of Naphthenic acid fraction compounds in OSPW from untreated and gamma irradiated OSPM mesocosms.

Months post setup	NAFC concentration (mg/L)		Percent reduction
	Untreated	GI-treated	
P1A			
0	64	29	54.7
9	50	25	50.0
11	42	24	42.9
23	27.5	21.1	23.3
31	12.9	23.2	-79.8
STP			
0	69	6	91.3
9	40	13	67.5
11	29	16	44.8
23	37.4	14.0	62.6
31	11.4	9.9	13.2
MLSB			
0	57	5	91.2
9	39	35	10.3
11	25	25	0.0
23	23.5	15.2	35.3
31	14.3	4.5	68.5
Shell			
0	59	1	98.3
12	14.1	5.7	59.6
20	11.1	1.9	82.9

Table 2.2: Concentration of Naphthenic acid fraction compounds in FFT from untreated and gamma irradiated OSPM mesocosms at setup (time 0).

	NAFC concentration (mg/L)		Percent reduction
	Untreated	GI-treated	
P1A	71	27	62.0
STP	26	28	-7.7
MLSB	68	32	52.9
MRM	15	14	6.7

Table 2.3: Total suspended solids and turbidity by GI and relative salinity.

		TSS (mg/L)		Turbidity (NTU)	
		Untreated	Treated	Untreated	Treated
FW	Mean±SE	4.2±2.06	28.65±21.66	12.13±7.04	5.61±1.58
	Range	0.7 – 7.83	5.80 – 71.9	4.73 – 26.2	3.33 – 8.64
HSW	Mean±SE	4.85±0.55	20.09±12.56	3.08±0.87	4.27±0.17
	Range	3.91 – 5.82	2.46 – 44.41	1.35 – 3.99	4.01 – 4.60
OSPM	Mean±SE	19.65±9.85	42.25±27.13	13.14±1.29	18.01±5.68
	Range	10.05 – 38.82	9.35 – 96.08	10.47 – 16.1	7.43 – 34.1

Community composition and species richness

A total of 21 taxa were observed in mesocosms including 13 taxa of cladocera, 1 taxon of arthropoda, 1 taxon of ostracoda, and 6 taxa of rotifers. Only 7 taxa made up at least 5% of the total zooplankton abundance in at least 5% of the mesocosm across all sampling dates (n = 68 samples). Appendix 2 shows the total abundance of zooplankton taxa including rotifers and *Chaoborus* larvae, for each mesocosm on each of the four sampling dates, as well as the total crustacean zooplankton biomass (cladocerans and ostracods). The most commonly observed zooplankton were *Chydorus sphaericus* (n = 49 samples), ostracods (n = 45 samples), *Alona rectangulara* (n = 29 samples), *Ceriodaphnia* sp. (n=25 samples), *Brachionus* sp. (n = 14 samples), *Simocephalus* sp. (n = 9 samples) and *Lecane* sp. (n = 8 samples). In both FW and HSW mesocosms, *C. sphaericus*, ostracods, and *A. rectangulara* were the most commonly observed taxa, whereas ostracods, *Brachionus* sp. and *Ceriodaphnia* sp. were the most commonly observed taxa in OSPM mesocosms.

At the beginning of the study, crustacean zooplankton were frequently absent in G- OSPM mesocosms. Species richness in G- OSPM mesocosms remained low for the duration of the study, and G- OSPM zooplankton samples were frequently composed of a single taxa (*Brachionus* or ostracods). Species richness was initially low in G+ OSPM mesocosms but increased over the duration of the study, and in 2016 richness was not significantly different in G+ OSPM mesocosms compared to G+ FW and G+ HSW references. The zooplankton taxa observed in G+ OSPM mesocosms appeared to be tolerant taxa. The only taxa that was more common in OSPM mesocosms than reference mesocosms was the rotifer *Brachionus*. Richness was highest in G- HSW mesocosms in

August 2015 due to the presence of rare sediment associated taxa (*Leydigia quadrangularis*, *Streblocercus sericaudatus*) and many plant associated cladocerans. Richness in G-HSW mesocosm declined slightly in 2016 which may have been due to high water temperatures and mesocosms potentially drying up.

Gamma irradiation had no significant overall effect on species richness ($F_{1,64} = 0.186$, $p = 0.668$) (Table 2.4). However, there was a significant interaction between GI and relative salinity ($F_{2,64} = 8.811$, $p > 0.001$). A test of the simple effects using pairwise comparisons with a Bonferroni adjustment suggests there were no significant difference in species richness between G+ OSPM mesocosms and G- OSPM mesocosms in July ($F_{1,18} = 0.155$, $p = 0.698$) or August 2015 ($F_{1,18} = 1.125$, $p = 0.303$). However, G+ OSPM mesocosms had significantly higher species richness than the G- OSPM counterparts in July 2016 ($F_{1,20} = 20.000$, $p > 0.001$) and August 2016 ($F_{1,20} = 4.615$, $p = 0.044$) (Fig 2.2).

Relative salinity had a highly significant effect on zooplankton species richness ($F_{2,31} = 41.942$, $p < 0.001$) (Table 2.4). Untreated OSPM mesocosms had lower zooplankton richness than all reference mesocosms, with the exception of G- SW mesocosms in July 2015 (Fig. 2.4). Gamma irradiated OSPM mesocosms had lower zooplankton richness than reference mesocosms in 2015, but in 2016, species richness in G+ OSPM mesocosms was equivalent to species richness in all G+ reference mesocosms (Fig 2.2). Untreated FW and HSW mesocosm had slightly higher species richness than G+ FW and HSW reference mesocosms. However, these results were only statistically significant for G- FW mesocosms in July 2016 ($F_{1,20} = 6.667$, $p = 0.018$). Date significantly influenced mean zooplankton richness ($F_{3,41} = 15.193$, $p < 0.0001$). Mean

species richness was lowest in all mesocosms at the start of sampling in July 2015 (Fig. 2.4). Mean species richness was highest in reference mesocosms in August 2015. In OSPM mesocosms, the number of species observed in a sample tended to increase through time

Zooplankton biomass

Crustacean zooplankton were absent from G- OSPM mesocosms when mesocosms were first sampled in July 2015. Biomass increased from July 2015 to August 2015 in G- OSPM mesocosm but mean zooplankton biomass remained significantly lower than biomass in reference mesocosms. Crustacean zooplankton biomass in G+ OSPM mesocosms was immediately increased following GI and continued to increase throughout the study (Fig. 2.5). By the end of the study crustacean zooplankton in G+ OSPM mesocosms was statistically equivalent to the biomass observed in reference mesocosms due to an increase in zooplankton biomass in G+ OSPM mesocosms, and variable biomass among reference mesocosm replicates.

There was a significant effect of relative salinity on mean zooplankton biomass ($F_{2, 22} = 30.764$, $p > 0.001$). Untreated OSPM mesocosms contained significantly lower zooplankton biomass than were found in reference mesocosms (Table 2.4, Fig. 2.5). Initial mean zooplankton biomass in untreated FW and HSW mesocosms was $17.17 \mu\text{g/L}$ 95% CI [$1.793 \mu\text{g/L}$, $117.26 \mu\text{g/L}$] and $46.12 \mu\text{g/L}$ 96% CI [$7.14 \mu\text{g/L}$, 271.91] respectively and in gamma irradiated FW and HSW mesocosms, the initial mean zooplankton biomass was $7.48 \mu\text{g/L}$ 95% CI [$7.48 \mu\text{g/L}$, $54.18 \mu\text{g/L}$] and $198.17 \mu\text{g/L}$ 96% CI [$23.27 \mu\text{g/L}$, $1633.52 \mu\text{g/L}$], respectively. No crustacean zooplankton were observed in G- OSPM in July 2015. Crustacean zooplankton biomass peaked at a

maximum of 24.22 $\mu\text{g/L}$ 95% CI [4.01 $\mu\text{g/L}$, 125.94 $\mu\text{g/L}$] in July of 2016, and declined in August 2016 for a final mean recorded biomass of 17.61 $\mu\text{g/L}$ 95% CI [2.70 $\mu\text{g/L}$, 92.69 $\mu\text{g/L}$] in August 2016.

Untreated OSPM mesocosms always had significantly lower zooplankton biomass than either FW or HSW mesocosms (Fig. 2.5). Mean crustacean biomass in August 2016 was 1125.5 $\mu\text{g/L}$ 95%CI [172.123 $\mu\text{g/L}$, 7329.1 $\mu\text{g/L}$] and 1252.2 $\mu\text{g/L}$ 95%CI [215.4 $\mu\text{g/L}$, 7256.2 $\mu\text{g/L}$] for G- FW and G- HSW mesocosms, respectively and 2235.9 $\mu\text{g/L}$ 95% CI [342.8 $\mu\text{g/L}$, 14554.4 $\mu\text{g/L}$] and 7333.4 $\mu\text{g/L}$ [1126.2 $\mu\text{g/L}$, 47723.6 $\mu\text{g/L}$] for G+ FW and G+ HSW mesocosms respectively. Untreated OSPM contained on average 98.4 – 99.8% lower zooplankton biomass than did reference mesocosms.

Gamma irradiation had a significant overall effect on mean zooplankton biomass ($F_{1,22} = 9.149$, $p = 0.006$). Pairwise comparisons suggest gamma irradiation of OSPM did not have an immediate effect on zooplankton biomass (July 2015, $F_{1,76} = 3.142$, $p = 0.08$; August 2015, $F_{1,76} = 0.192$, $p = 0.66$) (Fig. 2.3). The initial mean biomass of zooplankton in G+ OSPM mesocosms was 3.09 $\mu\text{g/L}$ 95% CI [0 $\mu\text{g/L}$, 22.80 $\mu\text{g/L}$]. Mean zooplankton biomass increased in G+ OSPM mesocosms over the course of the experiment reaching a mean maximum value of 491.19 $\mu\text{g/L}$ 95% CI [96.21 $\mu\text{g/L}$, 2490.96 $\mu\text{g/L}$] in August 2016. Pairwise comparisons of G- and G+ OSPM mesocosms revealed there was significantly higher zooplankton biomass in G+ OSPM mesocosms compared to G- OSPM mesocosms by 2016 (July [$F_{1,76} = 5.318$, $p = 0.024$] and August [$F_{1,76} = 5.847$, $p = 0.018$]) of 2016. By August 2016, mean zooplankton biomass in G+ OSPM mesocosms was 27.8 times greater than the mean zooplankton biomass in G- OSPM mesocosms. Mean zooplankton biomass in G+ OSPM mesocosms by August

2016 was not significantly different from any of the reference mesocosms due to high variability among reference mesocosms (Fig. 2.5). Overall, gamma irradiated mesocosms overall supported a larger mean zooplankton biomass than their G- mesocosm compliments (Fig. 2.3).

Mean weighted length

The majority of reference mesocosms were dominated by a high density of small bodied chydorids which measured 0.3 – 0.5 mm in length and a low-moderate density of *Ceriodaphnia* measuring 0.5 – 0.8 mm in length. Large cladocerans measuring greater than 1 mm, such as *Simocephalus* and *Daphnia* were not frequently observed in reference mesocosms nor OSPM mesocosms. Ostracods were present in almost all reference mesocosm on every date, and in approximately half of the OSPM mesocosms, and reached a typically measured 0.3 – 0.7 mm in length. Overall all mesocosm were dominated by small and medium sized zooplankton. Had rotifer measurements been included in the analysis, it is likely that mean weighted length in OSPM mesocosms would have been considerably smaller.

Although there was a significant overall effect of GI on the mean size of crustacean zooplankton ($F_{1, 42} = 6.20, p = 0.017$), the significant GI*Date interaction ($F_{3, 31} = 3.692, p = 0.022$) indicates that the effects were not consistently expressed through time (Table 2.4). Mean zooplankton body size was larger in G- OSPM mesocosms compared to G+ OSPM mesocosms in August 2015 but smaller in G- OSPM mesocosms than G+ OSPM mesocosms in 2016 (Fig. 2.6). Differences were a result of very low densities of zooplankton and each measured individual have a large effect on the overall mean weighted length. Overall, the mean body size of crustacean zooplankton was less

than 1mm in all mesocosms. The largest average crustacean zooplankton length was observed in G+ HSW mesocosms in July 2015, the mean \pm SE crustacean zooplankton length was 0.88 \pm 0.12 mm and was the result of a few large ostracods (> 1 mm) dominating 2 of 3 G+ HSW replicates.

Density

Mean zooplankton density was uniformly low at the beginning of the study in July 2015. Mesocosms constructed with OSPM always had the lowest density (Fig. 2.7), and G- OSPM mesocosms maintained the lowest mean density for the duration of the study, although differences among G-/G+ OSPM mesocosms were not statistically significantly different. Densities in reference mesocosms were highly variable and attributed to differences in SAV % cover (Appendix 2). Untreated HSW mesocosms had the highest zooplankton densities and tended to have the highest %SAV cover (Appendix 2) which was attributed to a very high density of small, plant associated chydorid zooplankton and a high density of benthic detritivores (ostracods). By August 2016, G+ OSPM mesocosms had zooplankton densities that were statistically equivalent to G+ FW mesocosms due to high variability in zooplankton reference mesocosms, and increased zooplankton densities in G+ OSPM mesocosms. By the end of the experiment G+ OSPM mesocosms had a higher mean density of zooplankton compared to their G- counterparts, but the results were not statistically significant and G- OPSM mesocosms remained statistically different from G- reference mesocosms.

GI treatment did not have a significant overall effect on mean crustacean zooplankton density in mesocosms ($F_{1, 15} = 2.766$, $p = 0.118$; Fig. 2.7). Relative salinity had a significant overall effect on crustacean zooplankton density ($F_{2, 15} = 26.530$, $p =$

<0.0001, Table 2.4), with OSPM inhibiting overall zooplankton density. Untreated OSPM mesocosms had the lowest crustacean zooplankton density of all the treatments reaching a maximum mean density of 5 individuals/L 95% CI [1, 17 zooplankton/L] by August 2016. Gamma irradiated OSPM mesocosms also had lower crustacean zooplankton density than reference mesocosms reaching a maximum mean density of 30 zooplankton/L 95% CI [10, 93 zooplankton/L] (Fig. 2.7). Pairwise comparison of zooplankton density in G-/G+ OSPM mesocosms showed that by August 2016, zooplankton density was not statistically higher in G+ OSPM mesocosms compared to G- OSPM mesocosms ($F_{1, 38} = 3.276$, $p = 0.078$) which was due to high variability in zooplankton densities in G- OSPM mesocosms (Fig. 2.7). Pairwise comparisons suggest that by August 2016 the mean zooplankton density in G+ OSPM mesocosms was statistically equivalent to G+ FW mesocosms which had a mean of 188 zooplankton/L 95% CI [53, 659 zooplankton/litre] ($p = 0.252$). Zooplankton density in G- OSPM mesocosms was still statistically less than both G- FW mesocosms ($p = < 0.0001$) and G- HSW mesocosms ($p < 0.001$). Zooplankton densities in FW and HSW mesocosms were highly variable and typically spanned an order of magnitude (Fig. 2.7).

Table 2.4: Results of the mixed model analysis for the fixed effects of GI treatment, relative salinity level (FW, HSW, OSPM), and sample date. P-values in bold indicate statistical significance at $\alpha=0.05$.

Fixed effect	Mean weighted length		Biomass		Richness		Density	
	F	p	F	p	F	p	F	p
GI Treatment	6.20	0.017	9.149	.006	0.186	0.668	2.766	0.118
Salinity	2.150	0.129	30.764	<0.0001	42.674	<0.0001	26.530	<0.0001
Date	2.599	0.070	48.659	<0.0001	15.194	<0.0001	24.053	<0.0001
GI*Salinity	1.648	0.205	2.058	0.151	8.811	<0.0001	0.990	0.395
GI*Date	3.692	0.022	0.197	0.898	0.482	0.697	1.653	0.195
Salinity*Date	8.611	<0.0001	1.413	0.230	1.923	0.110	1.646	0.164
GI*Salinity*Date	3.403	0.011	1.196	0.325	0.961	0.468	0.416	0.864

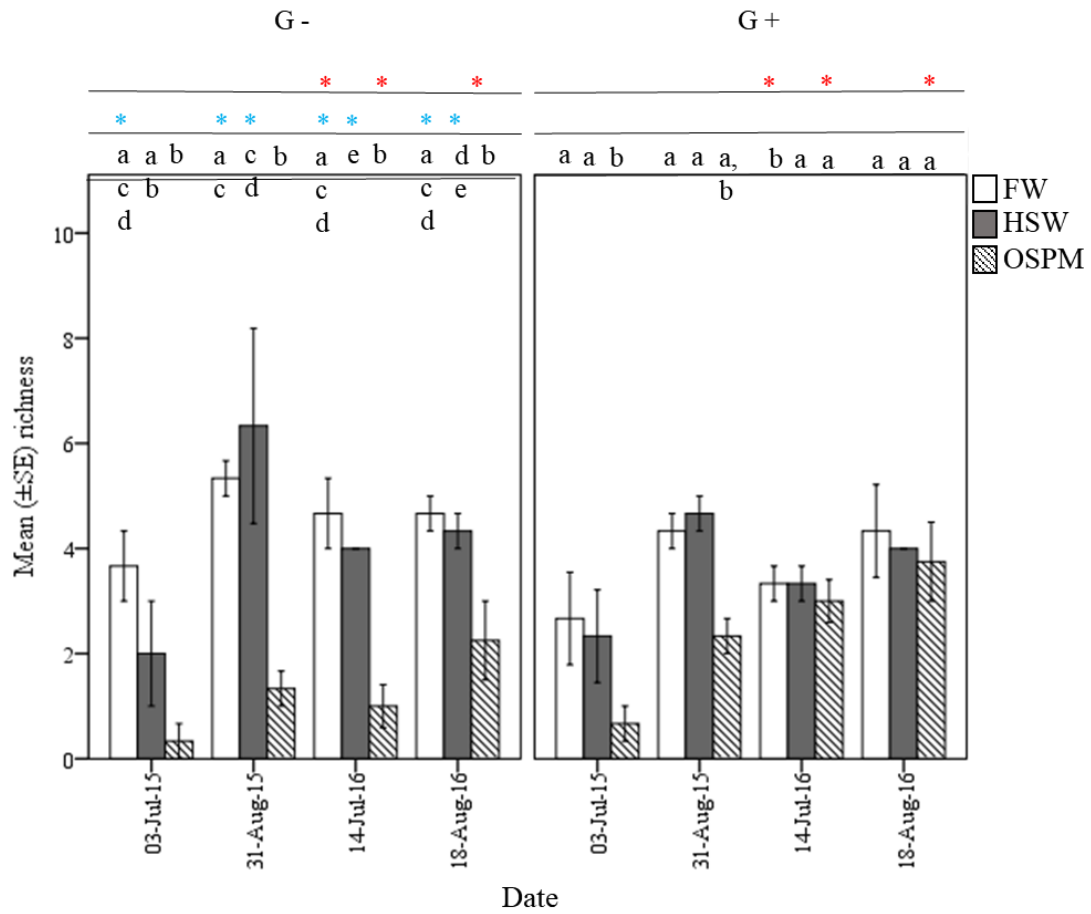


Fig. 2.4: Mean (\pm SE) crustacean zooplankton richness among sampling dates (x-axis). Open bars represent FW mesocosms, gray bars represent HSW mesocosms, and crosshatched bars represent OSPM mesocosms. Blue asterisks indicate where there is a significant effect of source pond (comparing OSPM mesocosms to FW and HSW mesocosms). Red asterisks indicate dates on which the differences between G- and G+ pairs were significant. Letters indicate dates on which richness differed among FW, HSW, and OSPM mesocosms within the G- treatment (left panel) or the G+ treatment (right panel). Mesocosms that share a letter were not significantly different from each other.

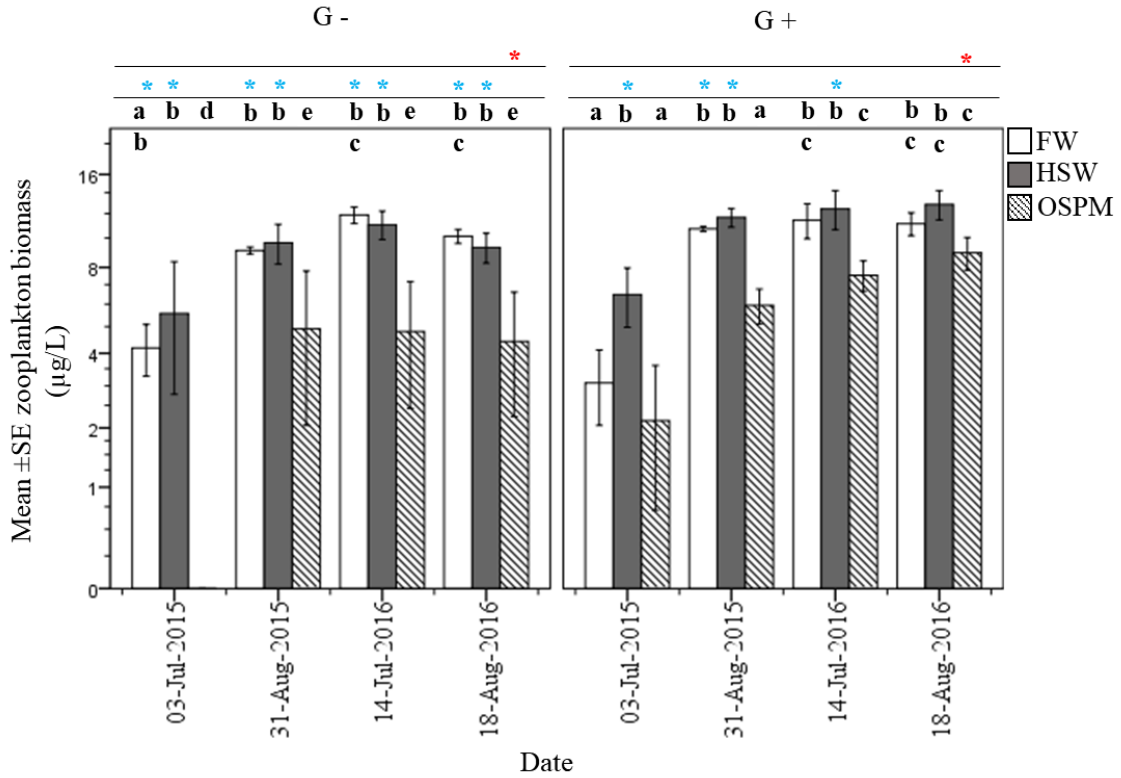


Fig. 2.5: Mean \pm SE zooplankton biomass ($\mu\text{g/L}$) (note the \log_2 scale) for $n=4$ dates in G- mesocosms; left panel and G+ mesocosms; right panel. Open bars represent FW mesocosms, gray bars represent HSW mesocosms, and crosshatched bars represent OSPM mesocosms. Red asterisks indicate where there is a significant pairwise effect of GI treatment. Blue asterisks indicate where there is a significant effect of source pond (comparing OSPM mesocosms to FW and HSW mesocosms). Letters indicate dates on which richness differed among FW, HSW, and OSPM mesocosms within the G-treatment (left panel) or the G+ treatment (right panel). Mesocosms that share a letter were not significantly different from each other.

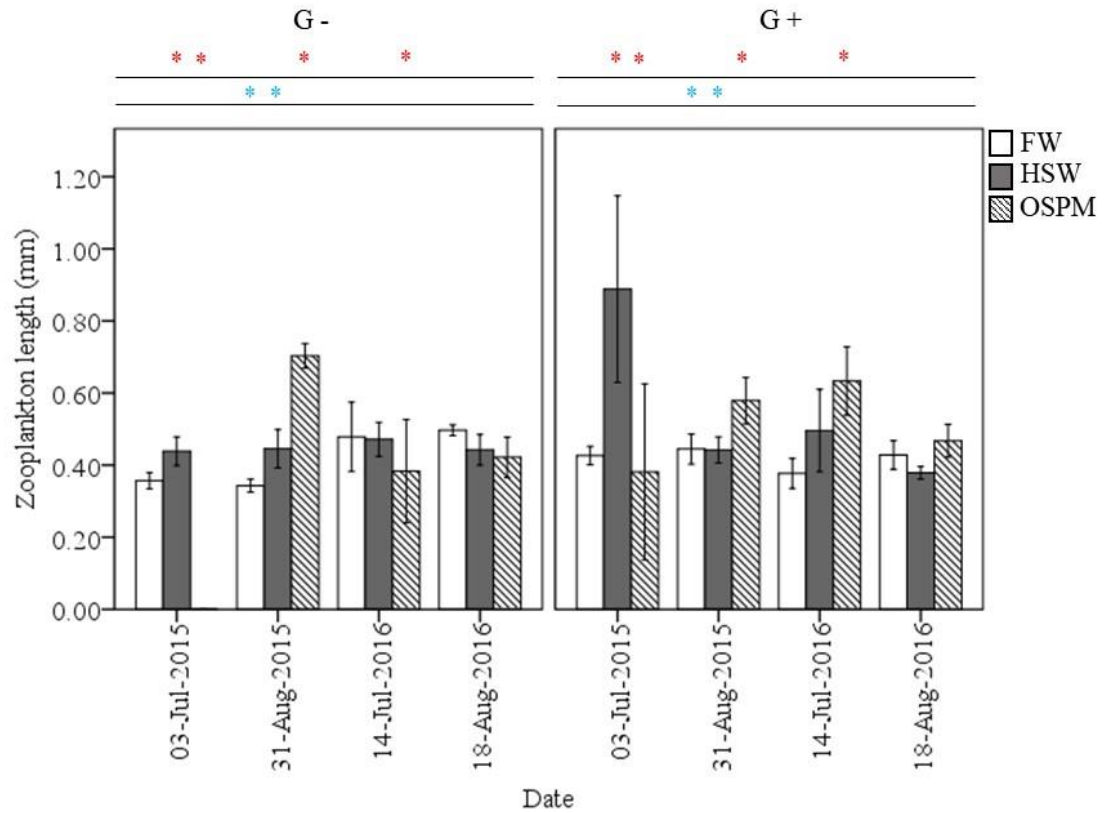


Fig. 2.6: Mean (\pm SE) weighted length (mm) - a measure of the mean length of individuals within a sample for $n = 4$ sampling dates. G- mesocosms; left panel. G+ mesocosms; right panel. Open bars represent FW mesocosms, gray bars represent HSW mesocosms, and crosshatched bars represent OSPM mesocosms. Red asterisks indicate where there is a significant pairwise effect of GI treatment. Blue asterisks indicate where there is a significant effect of source pond (comparing OSPM mesocosms to FW and HSW mesocosms).

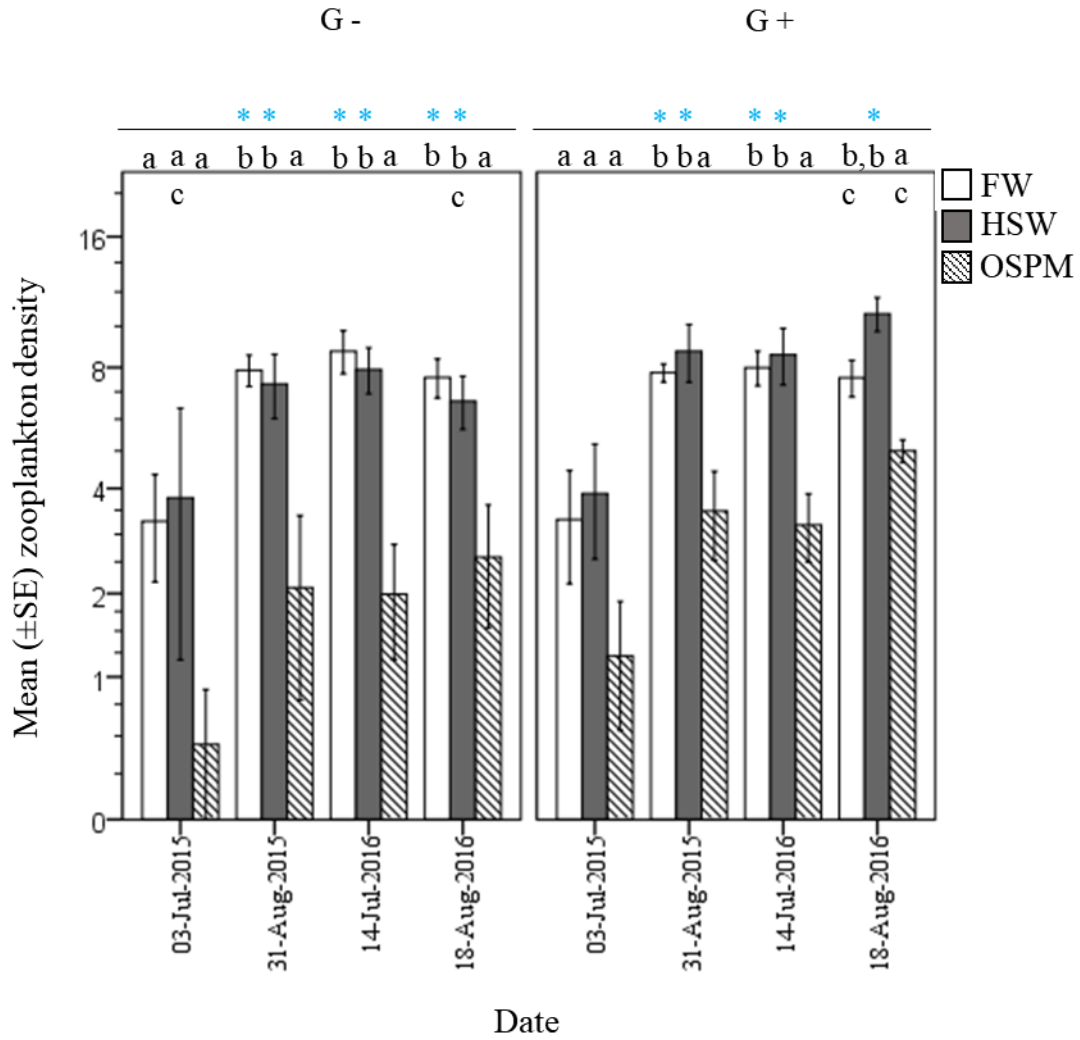


Fig. 2.7: Mean (\pm SE) zooplankton density (note the log₂ scale) measured as the number of individual crustacean zooplankton L⁻¹ of water for n = 4 sampling dates. G-mesocosms; left panel. G+ mesocosms; right panel. Blue asterisks indicate pairwise differences in tailings pond mesocosms compared to FW and HSW reference mesocosms. Letters indicate dates on which density differed among FW, HSW, and OSPM mesocosms within the G- treatment (left panel) or the G+ treatment (right panel). Mesocosms that share a letter were not significantly different from each other.

Discussion

Effects of GI on NAFC concentrations

To my knowledge, this study is one of two studies to document the effects of OSPM on wetland zooplankton communities in a quasinatural setting (but see also McCormick 2000) and the first study to assess the effects of GI treated OSPM on zooplankton communities to determine if the treatment of OSPM can accelerate the development of natural biological systems. Gamma irradiation of OSPM immediately reduced the concentration of NAFCs by 54.7 – 98.3% in OSPW and by 0 – 62% in FFT. The reductions in NAFC concentrations in this study were more variable than those reported by Boudens et al. (2016) who observed an 85 – 97% reduction in OSPW and a 52 – 80% reduction in FFT immediately following GI. Differences in the observed efficacy of GI to breakdown NAFCs could be a result of the FTIR method used to measure them, or to differences in the initial NAFC congeners present in the OSPM. Although Fourier transformed infrared spectrum (FTIR) has become the industry standard for measuring NAFC concentrations, in comparisons between FTIR and gas chromatography – mass spectrometry, Scott et al. (2010) and Grewer et al. (2010) found that the less specific FTIR method overestimated NAFC concentrations. Differences in the efficacy of GI could also be related to the spatial and temporal heterogeneity of NAFCs within and among tailings ponds (Frank et al. 2016).

A collaboration with Environment Canada is underway to better characterize the NAFC fingerprints of the tailings ponds using liquid chromatography quadrupole time-of-flight mass spectrometry (LC-QToF-MS). Preliminary results suggest that GI reduces the diversity of compounds to a suite that is isometrically homogeneous among samples

regardless of the initial NAFC composition (Richard Frank, Environment and Climate Change Canada, Burlington, ON, personal communication). Characterizing the changes in NAFC speciation will be an important next step in developing this technology. NAFC concentrations had become comparable in G- OSPM and G+ OSPM mesocosms by the end of the study, with a mean \pm SE of 12.9 \pm 0.8 mg/L and 12.5 \pm 5.6 mg/L respectively. However, despite the similarity of final concentrations there were significant differences in zooplankton biomass, and differences in density approaching statistical significance between G- and G+ OSPM mesocosms. Zooplankton in G+ OSPM mesocosms had become similar to the assemblages in reference mesocosms, suggesting that GI detoxified OSPM and accelerated the accrual of zooplankton taxa and the development of a diverse community. However, zooplankton community richness, biomass and density only approached values observed in reference mesocosms after 1.5 years, suggesting that microbial biodegradation played an important role in detoxifying the G+ OSPM mesocosms.

Effects of OSPM on zooplankton communities

There have been relatively few studies documenting the effects of OSPM on zooplankton (Mahaffey and Dubé 2017) but lab toxicity assays show that NAFCs, salinity, and trace metals may all contribute to zooplankton toxicity (Puttaswamy 2012, Zubot et al. 2012, Schiffer and Liber 2017). Oil sands process affected water reduces survival and reproduction, and impair *Daphnia* feeding (Lari et al. 2016). Early in this study, OSPM mesocosms supported only 5 – 30% of the crustacean zooplankton biomass observed in reference mesocosms. By August 2016 mean crustacean zooplankton biomass in G- OSPM mesocosms was still less than 2% of the mean crustacean

zooplankton biomass observed in reference mesocosms. Maximum mean zooplankton biomass was observed in July 2016 and was still only 24 µg/L in G- OSPM mesocosms. Similarly, a microcosm experiment using lake zooplankton communities exposed to fresh OSPW (NAFC concentration 62.7 mg/L) by McCormick (2000) showed a 97 – 98.5% reduction in zooplankton biomass during the one week experiment, with zooplankton biomass being correlated to both NAFCs and conductivity.

As expected, zooplankton communities in G- OSPM mesocosms were frequently dominated by *Brachionus* rotifers and ostracods. This observation was in agreement with McCormick (2000), who observed that increasing NAFCs changed zooplankton community composition and resulted in an increase in biomass of *Brachionus rubens*, such that increases in *B. rubens* were able to compensate for the loss of cladoceran zooplankton, resulting in no net difference in total zooplankton biomass. Unlike McCormick (2000), *Daphnia pulex* was rarely encountered in the present study. *Daphnia* are large bodied filter feeders, which typically inhabit the open waters of lakes, and have been shown to be negatively impacted by high % SAV cover (Norlin et al. 2006). Norlin et al. (2006) observed zooplankton communities dominated by small bodied cladocerans and lacking *Daphnia* in western boreal ponds with > 75 % SAV cover. *Daphnia* may have been selected against in OSPM mesocosms due to high TSS (Lougheed and Chow-Fraser 1998). High turbidity in OSPM has been shown to interfere with *Daphnia* feeding (Lari et al. 2016).

In contrast to OSPM mesocosms, reference mesocosms were dominated by small-bodied, Chydoridae, which are primarily associated with substrates and plants rather than being truly planktonic; they live in or on bottom sediments and feed on detritus, or they

are epiphytic, living on or associated with vegetation (Fryer 1968). High percent cover of *Chara sp.* and periphyton in reference mesocosms (Appendix 3) most likely supported the development of chydorids, especially *Chydorus sphaericus* and *Alona rectangula*, and plant associated cladocerans such as *Simocephalus sp.* (Pennak 1966, Wade 1969). Crustacean zooplankton richness was consistently low in both G- and G+ OSPM mesocosms, because of the presence of a few tolerant species and a lack of habitat heterogeneity (i.e. aquatic vegetation). This is further supported by increased zooplankton richness in the G+ MRM replicate which had both the most abundant and diverse macrophyte (discussed further in Chapter 3) and zooplankton communities of the OSPM replicates (Appendix 2)

I had expected G- OSPM mesocosms on average to be composed of smaller zooplankton than reference mesocosms, however this prediction did not hold true. Untreated OSPM mesocosms tended to have zooplankton communities composed of medium-sized ostracods and relatively few small bodied *C. sphaericus*. Reference mesocosms on the other hand had a very high abundance of small, plant associated chydorids which reduced the average size of the crustacean zooplankton community. Overall, both OSPM and reference communities tended to be dominated by small bodied zooplankton. The relatively warm mean water temperatures of the mesocosms during the (20 - 25°C), may have also favoured rapid development of small-bodied zooplankton in mesocosms (Moore and Folt 1993, MacLennan et al. 2015). Furthermore, Steiner (2004) observed a negative correlation between *Daphnia* biomass and increasing temperature, and a positive correlation between small cladocerans and increasing temperatures. The presence of *Chydorus sphaericus* in OSPM mesocosms is not surprising as it has been

observed to be a highly tolerant species dominant in waters impacted by mining (Leppänen 2018), and furthermore is capable of feeding on detritus (Fryer 1968).

Rotifer measurements were not included in mean weighted length calculations because I could not accurately measure them, the *Brachionus sp.* rotifers that were commonly encountered in OSPM samples tended to be clumped together and were difficult to separate. The inclusion of rotifers in the assessment of zooplankton mean body size in future studies would most likely have an effect on overall zooplankton community size structure. Rotifers were dominant in OSPM mesocosms but tended to be relatively rare in reference mesocosms.

Effects of GI treated OSPM on zooplankton communities

Gamma irradiated OSPM mesocosms supported higher crustacean zooplankton biomass than their G- OSPM counterparts from the first date of sampling. However the difference did not become statistically significant until the second year of the study. Gamma irradiated OSPM mesocosms also supported greater crustacean zooplankton density than their G- OSPM counterparts. However, the results only approached significance by August 2016, zooplankton biomass is frequently highest in the spring (Steiner 2004) and the enumeration of zooplankton samples from May and June 2017 could help further strengthen the patterns observed so far. Experimental results supported my hypothesis that gamma irradiation of OSPM mesocosms would support greater zooplankton abundance and biomass and make G+ OSPM mesocosms more similar to reference mesocosms. However the results were not immediate. It took 1.5 years for G+ OSPM mesocosms to become sufficiently detoxified so that zooplankton

communities achieved crustacean zooplankton biomass and density comparable to those of reference mesocosms.

Martin et al. (2010) studied the use of ozone to break down NAFCs in OSPW and observed no immediate reduction in toxicity. Rather detoxification increased in ozone treated OSPW following incubation with indigenous microorganisms over the course of the 100 day experiment. Scott et al. (2008) also observed that the concentration of total organic carbon remained relatively unchanged following ozonation, indicating NAFCs were oxidized to other organic compounds rather than being completely mineralized to carbon dioxide. It appeared that microbial degradation was important in detoxifying G+ OSPM mesocosms following gamma irradiation, a conclusion also reached by Boudens et al. (2016) in laboratory studies.

Although G+ OSPM mesocosms had a statistically higher species richness compared to G- OSPM mesocosms, and were not statistically different from G+ reference mesocosms, species richness in G+ OSPM mesocosms still tended to be ~ 25% lower than species richness in reference mesocosms. In a mesocosms study of the effects of different salinities on zooplankton communities, Brock et al. (2005) found no difference in zooplankton richness for salinities less than 1 ppt, but species richness was reduced at salinities greater than 2 ppt. In my study, mesocosms constructed from OSPM had salinities between 1.0 – 1.8 ppt whereas reference mesocosms had salinities between 0.1 – 1.1 ppt. Thus, elevated salinity could possibly have continued to constrain zooplankton richness, or interacted with NAFC concentrations (Leung et al. 2003). White (2017) in an analysis of the water quality of Base Mine Lake, an end pit lake constructed from OSPW and FFT identified Na^+ , Cl^- and HCO_3^- as posing a high toxicity risk to aquatic organisms.

Although NAFC concentrations are reduced following GI, salinity remains unchanged, which may persistently limit the development of zooplankton communities.

Zooplankton biomass was highly variable among reference mesocosms, which were created with materials from a range of wetlands within the AOS. By the end of 2016, biomass in G+ OSPM mesocosms was not significantly different from FW mesocosms. I had expected G+ OSPM mesocosms to be more similar to HSW mesocosms than to FW mesocosms due to the elevated salinity of OSPM and I expected FW mesocosms to have the greatest biomass and highest density of zooplankton because there were no salinity constraints. However, the maximum zooplankton biomass and densities were observed in G+ HSW mesocosms. Examination of the macrophyte communities that developed in the mesocosms (Appendix 2) shows that G+ HSW mesocosms had a greater percent cover and biomass of submerged aquatic vegetation than other mesocosms treatments, providing more habitat for epiphytic species such as *Ceriodaphnia* sp., *Simocephalus* sp. and *C. sphaericus* (Vanderstukken et al. 2010). In two of three G+ HSW mesocosms *Chara* sp., which is tolerant of elevated salinities, and high alkalinity, formed dense monotypic beds with nearly 100% cover. In contrast, the freshwater mesocosms tended to have a higher percent cover and biomass of emergent macrophytes and a lower percent cover and biomass of SAV. Contrary to my expectations reference mesocosms did not support populations of *Daphnia*. In an observational study of shallow English lakes, Stansfield et al. (1997) found that *Daphnia* were abundant in May and June but in waterbodies with high macrophyte cover and low fish predation were replaced in July and August by *Ceriodaphnia* sp. and *Simocephalus* sp. I observed that, similar to observation of Norlin et al. (2006), mesocosms with

extensive cover of SAV contained communities dominated by Chydoridae and *Ceriodaphnia*. Taken together, differences among zooplankton biomass and density between G+ OSPM mesocosms and reference mesocosms may also be attributed to the lack of a developed macrophyte community.

In conclusion, this research demonstrates that GI was effective at reducing NAFC associated toxicity in G+ OSPM mesocosms, and accelerated the development of zooplankton communities. However, other constraints such as elevated salinity and lack of macrophytes may impede the development of zooplankton communities that are similar to reference wetlands.

Chapter 3 – The Effects of Untreated and Gamma Irradiated Oil Sands Process Materials on Ecosystem Metabolism in Field-Based Mesocosms

Introduction

Approximately 65% of the landscape disturbed by mining activities in the AOS are or were formerly comprised by wetlands including peatlands (Rooney et al. 2012). Wetlands provide many important ecosystem services such as flood abatement, improvement of water quality, carbon management, and supporting biodiversity (Zedler and Kercher 2005). Assessing current mine closure and reclamation plans, a net loss of 67% of pre-mining peatland habitat will be lost (Rooney et al. 2012). Peatlands began to form in the western boreal forest approximately 9000 years ago following deglaciation when rates of primary production exceeded rates of decomposition (Vitt et al. 2000).

The cool, moist climate of the boreal ecoregion promotes slow rates of decomposition (Vitt et al. 2001). It is estimated that Canada's continental peatlands contain 2.1% of the world's terrestrial carbon pool (Vitt et al. 2000). Fens tend to accumulate carbon due to high productivity whereas bogs tend to accumulate carbon because of very slow decomposition (Trites and Bayley 2009, Rooney et al. 2012, Roy et al. 2016). Peat also has the ability to retain water, and hydrological connectivity among peatland-wetland complexes is important for maintaining water levels in a region where evapotranspiration exceeds precipitation (Ferone and Devito 2004).

The large scale conversions of peatlands to open water marshes that are part of oil sands mining closure plans will result in a lower potential for the post-mining landscape to sequester carbon (Rooney et al. 2012). Furthermore, the elevated salinity of OSPM and sodic overburden used in the reclamation landscape will preclude the development of

Sphagnum mosses, which are characteristic of many peatlands (Rooney et al. 2012, Graf and Rochefort 2009). Therefore, it will be important for mining companies to create wetlands that have the ability to accumulate peat for the long term maintenance and success of the reclaimed landscapes (Trites and Bayley 2009). Consequently, there is a need to understand how wetland processes, such as net ecosystem production, develop in newly constructed wetland habitats amended with organic rich OSPM.

In a study of organic matter accumulation in saline western boreal wetlands along a salinity gradient and OSPM affected wetlands, Trites and Bayley (2009) observed the net accumulation of carbon was possible but was largely dependent on stable water levels and slowly decomposing plant species. Mollard et al. (2013) found that production, measured as above and belowground biomass was significantly lower in *Typha latifolia* stands growing in OSPM amended wetlands compared to stands growing in natural wetlands. Both NAFCs, which are cytotoxic and inhibit germination (Crowe et al. 2002), and elevated salinities (Trites and Bayley 2009) have been shown to reduce plant production. Similarly, several studies have observed reduced species richness, plant cover, and biomass in OSPM amended wetlands compared to unamended or natural wetlands (Slama 2010, Kovalenko et al. 2010, Rooney and Bayley 2011, Roy et al. 2014, Roy et al. 2016). In a study of the carbon dynamics of OSPM amended wetlands, Kovalenko et al. (2013) determined that even after 20 years, OSPM amended wetlands were functionally impaired and did not accumulate organic matter, measured as biomass, similar to reference wetlands of an equal age. Assessing ecosystem functioning of reclaimed wetlands will be important in ensuring that productive landscapes are built and guiding future reclamation practices.

One way of assessing ecosystem functioning is by determining the metabolic status of an ecosystem and whether the ecosystem is net autotrophic (production >respiration) or net heterotrophic (production <respiration). Net ecosystem production (NEP), is the imbalance between gross primary production (GPP) and ecosystem respiration (ER) (Chapin et al. 2006). Net ecosystem production is typically defined in terms of carbon- the total autotrophic conversion of inorganic carbon to organic carbon (GPP) and the total oxidation of organic carbon to inorganic carbon (R) (Staeher et al. 2012). However, NEP can also be inferred from diel free-water changes in dissolved oxygen (Odum and Odum 1955). Dissolved oxygen concentrations increase during the day as a result of photosynthesis, and decrease at night as a result of respiration (Staeher et al. 2010). One benefit of free-water measurements is that it captures the processes occurring in the entire ecosystem and avoids container artifacts that accompany measurements made in small bottles or chambers.

The diel free-water method has been frequently employed in streams, oceans and lake ecosystems (Odum and Odum 1955, Odum 1956, del Giorgio 1999, Cole et al. 2000, Coloso et al. 2008, Laas et al. 2012, Staeher et al. 2010) to estimate the metabolic status. More recently, the diel free-water method has been applied to wetland restoration research to assess the recovery of ecosystem functioning (Reeder 2011, Espanol 2013, Bortolotti 2016), which has been shown to recover more slowly than measures of biodiversity or community structure (Moreno-Mateos et al. 2012). In this study I quantified and compared the production, respiration and net ecosystem production in untreated (G-) OSPM, gamma irradiated (G+) OSPM, freshwater wetland (FW) and hyposaline water wetland (HSW) mesocosms to determine if GI could stimulate

production by reducing NAFC concentrations, and to determine if GI stimulates aerobic respiration by making NAFCs more biodegradable. Elevated NAFC concentrations have been shown to inhibit both macrophyte (Mollard et al. 2013, Roy et al. 2014) and bacterial production (Daly 2007). A reduction in NAFC concentrations may therefore be expected to increase production, although elevated salinities may still constrain production (Trites and Bayley 2009).

In a 52-week lab microcosm study, Boudens et al. (2016) found that aerobic microbial respiration was stimulated in gamma irradiated aged OSPM collected from Suncor's Pond 1A compared to untreated OSPM from weeks 4 – 52 with, peak respiration observed at week 8 and the greatest stimulation occurring at week 20. Gamma irradiation of fresh OSPM collected from Suncor's South Tailings Pond also stimulated aerobic microbial respiration between weeks 4 and 20, with peak respiration at week 8, but there was no observable difference between respiration rates in G- and G+ microcosms between weeks 20 – 52. Boudens et al. (2016) attributed the increase in aerobic respiration to either an increase in labile carbon as a result of gamma irradiation breaking down recalcitrant NAFCs, or an increase in the chemical oxidation in the anaerobic FFT.

A parallel study by VanMensel et al. (2017) supported the conclusion that increases in DO flux were a result of increased aerobic microbial respiration. They observed an increase in the relative abundance of microorganisms capable of degrading hydrocarbons and cycling nutrients in both aerobic and anaerobic GI-treated OSPM microcosms compared to untreated OSPM. The genera of microorganisms stimulated differed between fresh and aged OSPM, reflecting differences in native microbial

populations among tailings ponds. Furthermore, a 52-week lab microcosm study conducted by Reid et al. (2016) using materials from the same tailings ponds (P1A and STP) partitioned the sediment oxygen demand into the biological and chemical components. They concluded that increases in oxygen flux to the sediments were largely driven by biological processes. In fresh FFT, biological DO flux declined from week 2 – 52, and chemical oxidation increased from week 2 – 52. By week 52 chemical oxidation exceeded biological oxidation. In aged FFT, biological DO flux increased at 20 weeks before reaching a steady state at week 52. Although increased aerobic microbial respiration is desirable from a NAFC breakdown view point, a long-term increases in respiration would be detrimental for the accumulation of organic matter.

Patterns of dissolved oxygen and production in shallow ponds

Oxygen is produced via photosynthesis and is depleted by the aerobic respiration of plants, animals and bacteria, and the chemical oxidation of compounds in the sediment (Wetzel 2001). Dissolved oxygen concentrations are not uniform within shallow ponds, and oxygen gradients develop largely as a result of changes in plant communities (Frodge et al. 1990, Carpenter and Lodge 1986, Chimney et al. 2006). Emergent and floating leaf macrophytes have aerial foliage and exchange metabolic gases with the atmosphere whereas submerged aquatic vegetation (SAV) exchanges metabolic gases directly with the water column and sediment (Wetzel 2001).

In dense stands of *Typha* and floating aquatic vegetation, Chimney et al. (2006) observed consistently low concentrations of DO (<4 mg/L) and small diel fluctuations in DO. The hypoxia was attributed to increased microbial respiration as a result of the decomposition of plant materials (Carpenter and Lodge 1986), shading of the water

column, which reduces photosynthesis by periphyton, and reduced reaeration of the water column from the atmosphere during physical mixing. Conversely, during the daytime DO tends to be high in SAV beds due to direct exchange of photosynthetic products with the water column (Carpenter and Lodge 1986). As a result, areas with dense SAV often exhibit oxygen supersaturation and large diel fluctuations in DO concentrations and are less prone to anoxia (Frodge et al. 1990, Chimney et al. 2006). Submerged aquatic vegetation also acts as a substrate and nutrient source for the development of epiphytic communities which can contribute substantially to primary production (Vadeboncoeur et al. 2006). In open water habitats dominated by phytoplankton, diel DO fluctuations tend to be smaller (<1 mg/L) than those in vegetated habitats (Lauster et al. 2006, Chimney et al. 2006) and were less prone to anoxia (Chimney et al. 2006, Reeder 2011). Therefore, the extent of the littoral zone and the composition of macrophytes can have significant effects on ecosystem production and diel DO patterns.

Objectives

The purpose of this experiment was to assess the effects of untreated OSPM and gamma irradiated OSPM on mesocosm metabolism in comparison to freshwater and hyposaline water reference mesocosms to determine if GI stimulated the development of ecosystem metabolism representative of wetlands.

- 1) In order to function at a land capacity equivalent to premining conditions, OSPM amended wetlands must be able to accumulate organic matter (Trites and Bayley 2009). I assessed the metabolic status of G- and G+ OSPM mesocosms to determine if they were net autotrophic or net heterotrophic. VanMensel et al. (2017) observed that GI treated FFT stimulated microbial

communities capable of degrading hydrocarbons and cycling nutrients, and in aerobic microcosms constructed with P1A FFT, also observed the presence of a genus commonly associated with wetlands.

- 2) Wetlands amended with OSPM have reduced plant diversity and percent cover compared to reference wetlands as a result of elevated NAFCs and salinity (Crowe et al. 2002, Trites and Bayley 2009, Slama 2010, Roy et al. 2016). Crowe et al. (2002) observed plant death at high NAFCs concentrations (>60 mg/L), and delayed seed germination, as well as slower plant growth in OSPM amended wetlands. Decreased microbial production (Daly 2007), macrophyte production (Mollard et al. 2013) phytoplankton and periphyton production (Chen 2011) has also been observed in OSPM amended wetlands. Based on these findings, I expected mesocosms constructed from OSPM to exhibit the lowest primary production.
- 3) High concentrations of NAs reduced plant growth (Armstrong 2009) and germination (Crowe et al 2002), I predict that a reduction in NAFC concentrations in G+ OSPM mesocosms would result in increased plant growth and primary production compared to G- OSPM mesocosms.
- 4) Research by Boudens et al. (2016) demonstrated that GI stimulates DO flux at the water/FFT interface most likely due to an increase in labile carbon over a period of 8 – 20 weeks, I predict that GI would stimulate respiration in G+ OSPM over the first year of the study compared to G- OSPM, presumably while the most labile carbon is available. Respiration was greater in G+ Aged FFT than in G- Aged FFT at week 52 whereas, rates of respiration in G+

Fresh FFT and G- Fresh FFT converged around week 36. I predicted that higher rates of residual NAFCs in FFT would cause an increase in the length of time that respiration in G+OSPM mesocosms is stimulated compared to G-OSPM mesocosms.

- 5) Based on work by Trites and Bayley (2009) who observed a negative relationship between salinity and production, I did not expect find a difference in production or respiration among FW and HSW mesocosms as the range of conductivities are relatively small (0.3 – 1.4 mS/cm) in comparison to Trites and Bayley (2009) (0.5 – 13.5 mS/cm).

Methods and Materials

Study site

Measurements of NEP were made from July 13- September 2, 2015, July 13- September 7, 2016, and May 8 – June 13, 2017 in the mesocosms described in Chapter 2. Due to logistic constraints, it was not possible to track DO over the course of an entire field season (May – September). In 2015, DO loggers (described below) were not received until early July. In 2016, the site was inaccessible until July 1 due to extensive forest fires in the region. In 2017, mesocosms were monitored beginning in early May but monitoring was concluded in mid-June at the end of the study.

Water levels were monitored and maintained at a constant depth through the course of the study to ensure a suitable and stable habitat for the growth of aquatic macrophytes. This was achieved by adding water to a depth 15 cm above the substrate at the time of setup in October 2014, marking the level on the mesocosm wall, and

replenishing water to that level to account for evapotranspiration when necessary. Some consolidation of the sediment occurred, to account for this, new markings were placed at the beginning of each sampling season. Two empty mesocosms were used to measure the volume of precipitation collected during the active sampling periods. Temperature and relative light intensity were recorded using HOBO Pendant[®] Temperature/Light 64K Data Loggers (Onset[®] Bourne, MA) Pendant loggers were weighted with monofilament fishing line attached to aluminum washers coated in Tremclad rust paint so that they were suspended 2.5 cm above the substrate in each mesocosm.

Emergent and submerged macrophyte development was qualitatively tracked throughout the duration of the experiment by estimating percent cover (Appendix 4), and the species composition was described briefly in Chapter 2. Mesocosms were typically dominated by bulrushes (*Schoenoplectus* sp.), *Chara* sp., pondweed (*Potamogeton* sp.) and in one wetland replicate by spike-rushes (*Eleocharis* sp.). Following low water levels and unseasonally warm temperatures in May and June 2016, algae, primarily *Spirogyra* sp. became dominant, growing as epiphyton. At the end of the study, macrophytes were collected, divided into emergent vegetation, roots, and submerged aquatic vegetation and dried in an oven to determine dry weight. Visible microbial biofilm was removed from the walls of the mesocosms and from the sediment surface, and dried in an oven to determine dry weight. Macrophytes were dried in a muffle furnace to determine ash free dry weight (carbon content) and are also reported in Appendix 2.

Diel oxygen method

Dissolved oxygen concentration was measured at 15-min intervals in mesocosms with HOBO U26 Dissolved Oxygen and Temperature Data Loggers (Onset[®], Bourne,

MA). In 2015, 7 loggers were deployed and rotated among mesocosms using brackets made of 3 mm thick aluminum strips 1.25 cm wide x 45 cm long. Brackets were bent so that the logger would sit 5 cm from the wall, and hung from the lip of the mesocosm so that the DO loggers were suspended ~7.5 cm above the sediment surface, midway in the water column. A 6.35-cm diameter PVC saddle clip was attached to the aluminum bracket with two screws to hold the logger horizontally in the water column (Figure 3.1). Sondes were equipped with an optical O₂ sensor and temperature sensors and calibrated weekly in water-saturated air using a wet sponge placed inside the calibration boot. In 2015 and 2016, six data loggers were rotated every 3 days among 6 mesocosm replicates, providing for one round of sampling of all 18 experimental totes every 9 days in 2015, and in 2016 with one round of sampling for all 20 experimental totes occurring every 12 days. In 2017 the addition of eight loggers allowed for near continuous monitoring of DO in the tailings pond mesocosms with the remaining 6 loggers rotated among the FW and HSW controls every 2 – 4 days, depending on access to the sampling site - a schematic of the mesocosm layouts is provided in Appendix 4. The total number of sonde days logged is recorded in Table 3.1.

After each deployment, loggers and brackets were rinsed in a mild bleach solution and scrubbed with a toothbrush to remove any adhering material, then rinsed in clean water and allowed to air dry before being installed the next mesocosm to limit the transfer of propagules between mesocosms. In 2015, loggers were randomly assigned to the mesocosms. However, inspection of that data showed high day to day variability in metabolic estimates so paired sampling (G- and G+ complements for each

wetland/tailings pond replicate) was used for 2016 and 2017 so that direct comparisons could be made between G- and G+ complements.

The diel oxygen method for calculating NEP is based upon the change in daytime dissolved oxygen (photosynthesis and both autotrophic and heterotrophic respiration), the change in nighttime dissolved oxygen (respiration only) and oxygen exchanged with the atmosphere (Odum 1956). The governing equation used to calculate NEP comes from Odum (1956):

$$\Delta O_2/\Delta t = GPP - R - F \quad (1)$$

Where the change in DO over a given time step is equal to the oxygen produced by photosynthesis (GPP), the oxygen respired by all autotrophic and heterotrophic organisms, and chemical oxidation (R), and the flux of atmospheric oxygen (F).

Atmospheric flux (F) is calculated using a coefficient k which describes gas exchange at a specific temperature, and is primarily a function of wind speed. However there is great uncertainty in estimating k (Liss 1973, Turney et al. 2005) so k_{600} is used as a constant to estimate gas exchange (Cole et al. 2000, Bortolotti et al. 2016). Initial calculations of NEP in this study used a k_{600} and wind speed to estimate F, but the atmospheric fluxes were larger than the actual measured changes in DO. I then performed the calculations assuming a near negligible F because the water's surface in the mesocosms was typically protected by the wall of the mesocosm itself and instead used the change in DO/h in a mesocosms filled with distilled water (DO_{Blank}) and changed weekly, to determine the atmospheric flux assuming that it sustained no biological activity. This was confirmed by the diel change in DO in the DO_{Blank} which followed daily temperatures. Oxygen

increased at night when the water was cooler and decreased during the day when water temperatures increased. Diel changes in the DO_{Blank} were typically less than 1 mg/L.

In order to use equation 1, it is necessary to assume that daytime R is equivalent to nighttime R however Karakaya (2011) modelled daytime R as a function of temperature and pH and demonstrated that daytime R is higher than nighttime R because respiration is temperature dependent. As a result the magnitude of GPP and R are often underestimated, but NEP estimates are unaffected (Cole et al. 2000). By assuming equal daytime and nighttime R, we can estimate hourly respiration by calculating the mean change in DO/hour at night, daytime R by multiplying the nighttime hourly respiration by the number of daylight hours, and finally, we can calculate daily R by multiplying the nighttime hourly respiration by 24 hours.

To determine hourly NEP, I calculated the mean change in DO/h during daylight hours and subtracted the F constant calculated from the DO_{Blank}

$$NEP_{\text{hour}} = \text{mean } \Delta DO \text{ during the day} - F_{DO_{\text{Blank}}} \quad (2)$$

The hourly NEP was then multiplied by the number of daylight hours to determine daytime NEP (Staehr et al. 2010). Gross primary production cannot be measured directly, but rather we use daytime NEP and R to calculate it.

$$GPP = NEP_{\text{daytime}} - R_{\text{daytime}} \quad (3)$$

In order to avoid having to change the sign, daytime R, which is always negative as it the amount of oxygen consumed, was subtracted from daytime NEP to determine GPP. To determine daily NEP, and to avoid having to change the sign, daily R is added to daily

GPP. Positive values of daily NEP indicate a system that is net autotrophic, while a negative NEP indicates a system that is net heterotrophic.

Relative light intensity data from HOBO Pendant® loggers were used to determine the number of daylight and nighttime hours. Algal cells can continue to photosynthesize for short periods following sunset (Staeher et al. 2010). As a result, daytime hours are calculated as the interval between one hour post-sunset until dawn. A value of 54 lux, which is equivalent to one photon ($\mu\text{moles}/\text{m}^2/\text{s}$) was arbitrarily chosen, to represent daytime hours, as a single photon can initiate the process of photosynthesis.

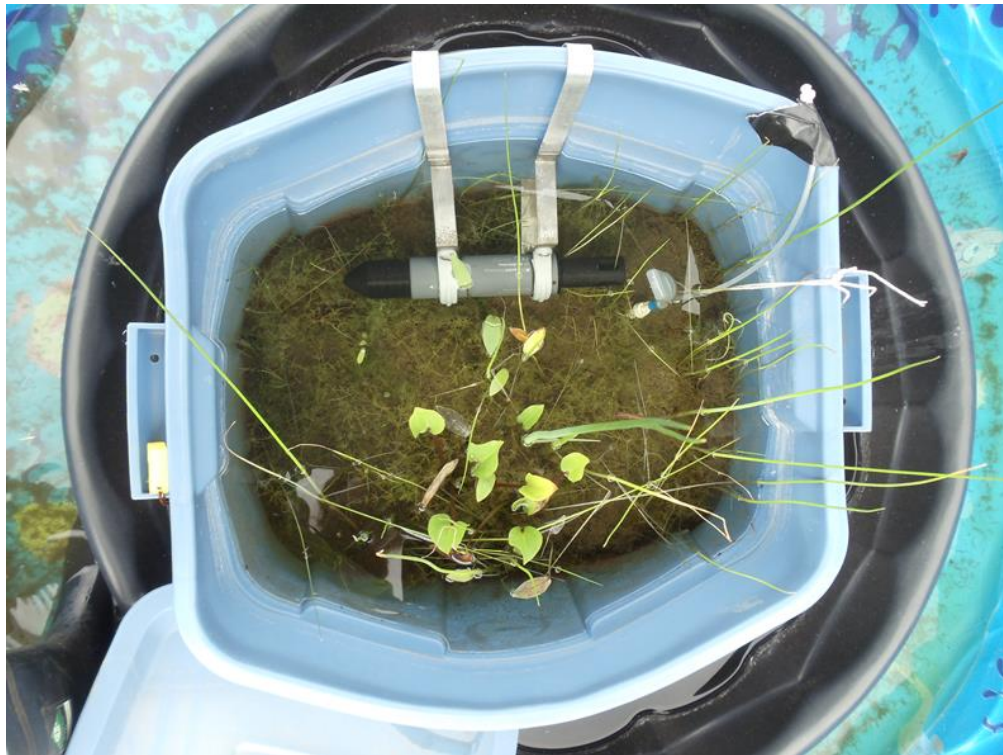


Fig. 3.1: A mesocosm showing the dissolved oxygen logger and the brackets that were used to deploy them, as well as the position of the HOBO light logger in the upper right corner. The tube extending out of the sediment is a Rhizon® sediment pore water sampler.

Outliers and data clean up

Each DO curve was examined for outliers and abnormal readings (sudden or erratic changes in DO concentrations). Precipitation events cause a physical disruption of the air-water interface, increasing the efflux of oxygen to the air and disrupts the diel pattern of DO. Precipitation events were determined from the volume of water observed in precipitation mesocosms in combination with data from nearby meteorological stations (provided by Hatfield Consultants Inc.) to determine which sampling dates needed to be excluded due to rain (2 dates in 2015 and 3 dates in each of 2016 and 2017).

Statistical analysis

I used the Mixed Models - Linear routine of IBM SPSS 24 (IBM version 24.0, IBM Corp.) with restricted maximum likelihood estimation to evaluate trends in GPP, R, and NEP for each sampling year. The use of mixed models allows for the correct selection of the variance-covariance matrix to account for correlation between measurements and account for the unevenly spaced repeated measuring of mesocosms (Littell et al. 2000). GI Treatment (G- or G+) and relative salinity freshwater (FW), hyposaline water (HSW), and tailings ponds (OSPM) were treated as categorical fixed effects. Date could not be included as a factor because it used too many degrees of freedom.

Daily rates of metabolism estimates were calculated and averaged among replicates in each treatment by sampling year. Post-hoc comparisons were run on all analyses regardless of overall significance to examine the simple effects of treatment and conductivity, and to examine differences between OSPM mesocosms and FW and HSW

mesocosms, because we did not expect GI to have a significant effect on reference mesocosms, but did expect significant difference between G+ and G- OSPM mesocosms. Several covariance structures were tested and the one minimizing the Akieke Information Criterion (AIC) was used. A first-order auto-regressive covariance structure was ultimately used, which assumes homogeneous variance between two observations on an individual mesocosm to be more highly correlated the closer together in time the measurements are taken (Littell et al. 2000). Results from linear mixed models were reported as the marginal means and 95% confidence intervals (Bortolotti et al. 2016)

Table 3.1: Total number of sonde days recorded for each GI treatment and relative salinity combination for each sampling year. Numbers in parentheses are the number of replicate mesocosms sampled. FW – freshwater reference, HSW – hyposaline water reference, OSPM – tailings ponds

Treatment	Pond source	Year		
		2015	2016	2017
G-	FW	39 (n=3)	46 (n=3)	32 (n=3)
	HSW	47 (n=3)	52 (n=3)	25 (n=3)
	OSPM	40 (n=3)	101 (n=4)	117 (n=4)
G+	FW	48(n=3)	58 (n=3)	32 (n=3)
	HSW	42(n=3)	52 (n=3)	27 (n=3)
	OSPM	45(n=3)	104 (n=4)	125 (n=4)

Results

Water quality and environmental factors

In 2015 mean \pm SE monthly water temperatures in mesocosms were 20.24 \pm 0.13°C and 18.78 \pm 0.14°C in July and August respectively, and ranged from 8.18 – 31.83°C in July and 4.41 – 32.09°C in August 2015. In 2016, mean monthly temperatures were 21.24 \pm 0.11°C and 18.69 \pm 0.10°C in July and August, respectively, and ranged from 8.12 – 32.67°C in July and 6.41 – 31.77°C in August. In 2017, mean monthly temperatures were 14.29 \pm 0.1°C and 18.86 \pm 0.13°C in May and June respectively, and ranged from 4.62 – 29.31°C in May and 8.90 – 30.88°C in June. The growing season was estimated as the length of time when mean daytime water temperatures were consistently above 4°C, as plants become dormant below 4°C (Stein and Hook 2005). The estimated growing seasons were from April 8 – October 3 in 2015, April 15 – October 4 in 2016 and April 1 until the end of the study in 2017. In 2017, temperatures rose above 4°C from April 1 – 9 then decreased to a mean of 3-5°C from April 8 – 25 after which point mean temperatures remained above 4°C. The continuous temperature record and the recorded water temperatures for the sampling seasons are provided in Appendix 4.

Dissolved oxygen concentrations were highly variable among treatments, FW and HSW had higher mean DO max and larger diel fluctuations in DO than OSPM mesocosms (Appendix 4). Maximum diel changes in DO were 7 – 10 mg/L in FW mesocosms and 10 – 15 mg/L in HSW mesocosms, compared to 2 – 3 mg/L in OSPM mesocosms. In G- FW and HSW mesocosms and G+ FW mesocosms, minimum DO concentrations reached a mean of 5 – 7 mg/L (below saturation) whereas minimum DO concentrations reached a mean 3 – 5 mg/L (hypoxia) in G+ HSW mesocosms. Minimum

DO concentrations in OSPMW mesocosms typically had a mean value of 7 – 10 mg/L (at or just below saturation). Both G- and G+ HSW mesocosms periodically experienced nighttime anoxia, with DO reaching concentrations of 0 mg/L.

Water collected by precipitation mesocosms amounted to 180 mm of rain in 2015, 190 mm of rain in 2016 and 227 mm snowmelt and rain in 2017. Distilled water was added to mesocosms to make up for differences between evapotranspiration and precipitation. Overall FW and HSW mesocosms had much higher rates of evapotranspiration and required the addition of approximately 29 – 43% more distilled water to maintain water levels than OSPM mesocosms. In 2015 and 2016, reference mesocosms required an additional 32 – 51 L of distilled water compared to 23 – 31.75 L of distilled water added to OSPM mesocosms (Appendix 4).

Submerged aquatic vegetation was an important feature of many of the mesocosms and was often observed with adherent gas bubbles, indicating supersaturation of DO (personal observation). Submerged aquatic vegetation was observed in only one pair of OSPM mesocosm replicates (MRM) in 2016. In 2017, trace amounts of SAV were observed in the same G+ OSPM replicate (MRM), but not in the G- replicate (Appendix 4). In 2015, SAV was equally abundant in G-/G+ pairs of FW mesocosms and HSW mesocosms. In 2016, SAV was equally abundant in G-/G+ FW mesocosms, but tended to be more abundant in G+ HSW mesocosms than their G- HSW counterparts. Following low water levels at the beginning of 2016 due to restricted access to the study site, there was an increase in the abundance of epiphytic algae which was prominent in 2017 as well. Algal cover was included in SAV estimates because it exchanges metabolic gasses directly with the water, had a significant % cover within the mesocosms, and frequently

grew attached to the SAV. Emergent macrophytes were also a prominent feature in reference mesocosms accounting for 0 – 20% of the percent cover. Emergent macrophytes were more common in mesocosms that had a smaller % SAV cover and tended to be absent from mesocosms with 100% SAV cover.

Emergent macrophytes were observed in G- OSPM (MLSB and MRM) mesocosms during the first growing season but were absent from G- OSPM mesocosms in subsequent years. Emergent macrophytes were observed in three G+ OSPM replicates (P1A, MLSB, and MRM) during the first growing season, but only persisted in MLB and MRM replicates in subsequent years (Appendix 2). Emergent macrophytes were greatly reduced in both the number and size of stems compared to reference mesocosms (unpublished data). Microbial biofilm was the dominant feature in G- and G+ OSPM mesocosms, and was observed on multiple separate occasions floating to the top of mesocosms supersaturated in oxygen bubbles in P1A, MLSB, and MRM replicates. STP replicates were very turbid for the duration of the study and no macrophytes or microbial biofilm could be observed. At the end of the study, biofilm was collected from the walls of the mesocosms and the sediment surface. Biofilm was observed in all G-/G+ OSPM replicates with the exception of G- STP (Appendix 2).

Mesocosm production

Estimates of production were highly variable within a sampling season (Fig. 3.2) and among wetland replicates (Fig. 3.3), but consistent across years. Mesocosm production appeared to be related to the extent of SAV cover (Appendix 2) and water temperatures (Appendix 4). Production was highest when water temperatures were warmest, which was at the beginning of my sampling in 2015 and 2016, and at the end of

my sampling in 2017 (Fig. 3.2). Relative salinity had a significant effect on production across all years (2015 $F = 64.251$, $p = <0.0001$; 2016 $F = 66.634$, $p <0.0001$; 2017 $F = 3.449$, $p = 0.036$; Table 3.2) and production was significantly higher in FW and HSW mesocosms compared to OSPM mesocosms (Table 3.3). Gamma irradiation had no significant effect on production across years (2015: $F = 1.185$, $p = 0.283$; 2016: $F = 1.019$, $p = 0.320$; 2017: $F = 0.010$, $p = 0.920$). The greatest difference in production between G-/G+ pairs of mesocosms was in 2016 in G- and G+ HSW reference mesocosms when mean production was $528.6 \mu\text{mol O}_2/\text{L/day}$ [378.6, 678.5] and $644.3 \mu\text{mol O}_2/\text{L/day}$ [491.7, 796.9] respectively, which corresponds to G+ HSW mesocosms having twice as much SAV compared to G- HSW mesocosms (Appendix 2).

In 2015, production in reference mesocosms ranged from a low of $465.8 \mu\text{mol O}_2/\text{L/day}$ [380.3, 551.3] in G- FW mesocosms to a high of $544.5 \mu\text{mol O}_2/\text{L/day}$ [465.2, 623.8] in G+ HSW mesocosms (Table 3.3). Production in G- and G+ OSPM mesocosms was $115.8 \mu\text{mol O}_2/\text{L/day}$ [38.3, 1933.3] and $130.3 \mu\text{mol O}_2/\text{L/day}$ [50.4, 210.4] respectively. In 2016 production in reference mesocosms ranged from a low of $431.8 \mu\text{mol O}_2/\text{L/day}$ [279.1, 584.6] in G- FW mesocosms to a high of $644.3 \mu\text{mol O}_2/\text{L/day}$ [491.7, 796.9] in G+ FW mesocosms. In 2016, production in G- OSPM mesocosms and G+ OSPM mesocosm was $152.6 \mu\text{mol O}_2/\text{L/day}$ [28.5, 276.7] and $188.4 \mu\text{mol O}_2/\text{L/day}$ [64.5, 312.3], respectively. In 2017, production in reference mesocosms ranged from a minimum of $546.5 \mu\text{mol O}_2/\text{L/day}$ [358.0, 735.0] in G- HSW mesocosms to a high of $600.4 \mu\text{mol O}_2/\text{L/day}$ [413.0, 787.8] in G+ HSW mesocosms. In 2017, production in G- OSPM mesocosms and G+ OSPM mesocosms was $208.7 \mu\text{mol O}_2/\text{L/day}$ [59.1, 358.2] and $178.6 \mu\text{mol O}_2/\text{L/day}$ [31.0, 326.1] respectively.

Mesocosm respiration

Estimates of respiration were highly variable within a season but consistent across years (Fig. 3.4), and variable among replicates within a treatment (Fig. 3.4, Fig. 3.5). As with production, estimates of respiration appeared to be related to both % SAV cover (Appendix 2) and temperature (Appendix 4) and followed the same trends as production. Respiration was highest when water temperatures were warmest, which was at the beginning of sampling in 2015 and 2016, and at the end of sampling in 2017 (Fig. 3.4, Appendix 4). Gamma irradiation did not have a statistically significant effect on respiration in any sampling year (2015: $F = 1.582$, $p = 0.218$; 2016: $F = 1.848$, $p = 0.183$; 2017: $F = 0.027$, $p = 0.871$) (Table 3.2). As with production, the greatest difference in respiration between G-/G+ pairs occurred in HSW mesocosms in 2016, $-514.2 \mu\text{mol O}_2/\text{L}/\text{day}$ $[-367.9, -660.6]$ and $-673.0 \mu\text{mol O}_2/\text{L}/\text{day}$ $[-524.0, -317.3]$, respectively, which coincided with the largest difference in % SAV cover (Appendix 2).

Relative salinity had a highly significant effect on respiration (Table 3.2) across years (2015: $F = 66.634$, $p < 0.001$; 2016: $F = 21.486$, $p < 0.0001$; 2017: $F = 18.592$, $p < 0.0001$). Both FW and HSW mesocosms respired more than OSPM mesocosms across all sampling years (Table 3.3, Fig. 3.3.4). In 2015, respiration in reference mesocosms was lowest in G- FW mesocosms $-498.4 \mu\text{mol O}_2/\text{L}/\text{day}$ $[-408.8, -588.1]$ and highest in G+ HSW mesocosms $-611.1 \mu\text{mol O}_2/\text{L}/\text{day}$ $[-527.3, -649.9]$ compared to $-144.8 \mu\text{mol O}_2/\text{L}/\text{day}$ $[60.6, -229.0]$ in G- OSPM mesocosms and $-124.0 \mu\text{mol O}_2/\text{L}/\text{day}$ $[-41.8, -206.1]$ in G+ OSPM mesocosms. In 2016, respiration was lowest in G- FW mesocosms $-437.0 \mu\text{mol O}_2/\text{L}/\text{day}$ $[-287.9, -586.2]$ and highest in G+ HSW mesocosms $-673.0 \mu\text{mol O}_2/\text{L}/\text{day}$ $[-317.3, -524.0]$, compared to $-154.7 \mu\text{mol O}_2/\text{L}/\text{day}$ $[-33.79, -275.6]$ in G-

OSPM mesocosms and $-196.6 \mu\text{mol O}_2/\text{L/day}$ $[-75.9, -317.3]$ in G+ OSPM mesocosm. In 2017, respiration in reference mesocosms was lowest in G- HSW mesocosms $-573.1 \mu\text{mol O}_2/\text{L/day}$ $[-388.9, -757.3]$ and highest in G+ HSW mesocosms $-635.2 \mu\text{mol O}_2/\text{L/day}$ $[-828.2, -452.2]$ compared to $-213 \mu\text{mol O}_2/\text{L/day}$ $[-68.6, -358.1]$ in G- OSPM mesocosms and $-187.8 \mu\text{mol O}_2/\text{L/day}$ $[-45.1, -330.5]$ in G+ OSPM mesocosms.

Rates of Net ecosystem production

Metabolic status switched between net heterotrophy and net autotrophy throughout the sampling season across all years (Fig. 3.6). In 2015, NEP ranged from $-214.09 \mu\text{mol O}_2/\text{L/day}$ to $113.91 \mu\text{mol O}_2/\text{L/day}$ in G- FW mesocosms, from $-150.09 \mu\text{mol O}_2/\text{L/day}$ to $87.51 \mu\text{mol O}_2/\text{L/day}$ in G- HSW mesocosms, $-41.88 \mu\text{mol O}_2/\text{L/day}$ to $22.60 \mu\text{mol O}_2/\text{L/day}$ in G- OSPM mesocosms, $-185.58 \mu\text{mol O}_2/\text{L/day}$ to $122.51 \mu\text{mol O}_2/\text{L/day}$ in G+ FW mesocosms, $-377.32 \mu\text{mol O}_2/\text{L/day}$ to $162.04 \mu\text{mol O}_2/\text{L/day}$ in G+ HSW mesocosms and from $-95.86 \mu\text{mol O}_2/\text{L/day}$ to $52.19 \mu\text{mol O}_2/\text{L/day}$ in G+ OSPM mesocosms. In 2016, NEP ranged from $-65 \mu\text{mol O}_2/\text{L/day}$ to $98.76 \mu\text{mol O}_2/\text{L/day}$ in G- FW mesocosms, $-238.45 \mu\text{mol O}_2/\text{L/day}$ to $144.38 \mu\text{mol O}_2/\text{L/day}$ in G- HSW mesocosms, $-54.69 \mu\text{mol O}_2/\text{L/day}$ to $91.88 \mu\text{mol O}_2/\text{L/day}$ in G- OSPM mesocosms, $-246.76 \mu\text{mol O}_2/\text{L/day}$ to $143.45 \mu\text{mol O}_2/\text{L/day}$ in G+ FW mesocosms, $-185.32 \mu\text{mol O}_2/\text{L/day}$ to $148.13 \mu\text{mol O}_2/\text{L/day}$ in G+ HSW mesocosms and $-71.78 \mu\text{mol O}_2/\text{L/day}$ to $79.07 \mu\text{mol O}_2/\text{L/day}$ in G+ OSPM mesocosms. In 2017, NEP ranged from $-102.37 \mu\text{mol O}_2/\text{L/day}$ to $60.01 \mu\text{mol O}_2/\text{L/day}$ in G- FW mesocosms, $-80.41 \mu\text{mol O}_2/\text{L/day}$ to $77.54 \mu\text{mol O}_2/\text{L/day}$ in G- HSW mesocosms, $-56.73 \mu\text{mol O}_2/\text{L/day}$ to $62.85 \mu\text{mol O}_2/\text{L/day}$ in G- OSPM mesocosms, $-217.20 \mu\text{mol O}_2/\text{L/day}$ to $113.38 \mu\text{mol O}_2/\text{L/day}$ in G+ FW

mesocosms, $-266.43 \mu\text{mol O}_2/\text{L}/\text{day}$ to $84.60 \mu\text{mol O}_2/\text{L}/\text{day}$ in G+ HSW mesocosms, and $-74.92 \mu\text{mol O}_2/\text{L}/\text{day}$ to $57.83 \mu\text{mol O}_2/\text{L}/\text{day}$ in G+ OSPM mesocosms.

Gamma irradiation had no effect on NEP across all sampling years (Table 3.2) (2015: $F = 2.021$, $p = 0.159$; 2016: $F = 2.701$, $p = 0.102$; 2017: $F = 0.286$, $p = 0.594$). Relative salinity had a significant across all years on NEP (2015: $F = 3.449$, $p = 0.036$; 2016: $F = 4.027$, $p = 0.019$; 2017: $F = 4.199$, $p = 0.017$). Mean NEP tended to be heterotrophic across all years and treatments, with G- OSPM mesocosms and G+ OSPM mesocosms having a smaller magnitude of heterotrophy than reference mesocosms (Table 3.3). Mean NEP in G- OSPM mesocosms ranged from $-2.0 \mu\text{mol O}_2/\text{L}/\text{day}$ $[-8.5, 4.4]$ and $-6.8 \mu\text{mol O}_2/\text{L}/\text{day}$ $[-31.3, 17.8]$ across all sampling years compared to G- reference mesocosms which had a mean NEP between $-3.8 \mu\text{mol O}_2/\text{L}/\text{day}$ $[-14.7, 7.0]$ and $-23.8 \mu\text{mol O}_2/\text{L}/\text{day}$ $[-48.7, 1.1]$ in G- reference mesocosms across all sampling years (Table 3.3). Mean NEP in G+ OSPM mesocosms ranged from $-3.0 \mu\text{mol O}_2/\text{L}/\text{day}$ $[-9.3, 3.2]$ to $-6.8 \mu\text{mol O}_2/\text{L}/\text{day}$ $[-14.2, 0.5]$ across all sampling years compared to G+ reference mesocosms which had a mean NEP between $-61.1 \mu\text{mol O}_2/\text{L}/\text{day}$ $[-84.9, -37.2]$ and $-10.6 \mu\text{mol O}_2/\text{L}/\text{day}$ $[20.5, 0.6]$, across all sampling years.

There were no consistent patterns in the number of days mesocosms were net autotrophic across sampling years (Table 3.4). In 2015, the mean \pm SE percentage of days net autotrophy was observed in G- and G+ OSPM mesocosms was $45\pm 7.9\%$ $n = 40$ days, and $40\pm 4.3\%$ $n = 45$ days respectively. Comparatively, reference mesocosms in 2015 were net autotrophic $37.5\pm 7.0\%$ $n = 48$ days in G+ FW mesocosms to $46.1\pm 8.0\%$ $n = 39$ days in G+ FW mesocosms. In 2016, net autotrophy was observed $38.4\pm 4.9\%$ $n = 99$ days in G- OSPM mesocosms and $33.7\pm 4.6\%$ $n = 104$ days in G+ OSPM mesocosms.

Reference mesocosms in 2016 were net autotrophic between $39.1 \pm 7.2\%$ $n = 46$ days in G- FW mesocosms and $46.0 \pm 7.0\%$ $n = 50$ days in G- HSW mesocosms. In 2017, net autotrophy was observed $41.9 \pm 4.6\%$ $n = 117$ days in G- OSPM mesocosms and $42.4 \pm 4.4\%$ $n = 125$ days in G+ OSPM mesocosms. In 2017 net autotrophy was observed occurring between $36.0 \pm 9.6\%$ $n = 25$ days in G- HSW mesocosms and $53.1 \pm 8.8\%$ $n = 32$ days in G- FW mesocosms.

Table 3.2: Results of mixed model fixed effects analyses of effects of GI treatment and source pond type on metabolism estimates across year; GPP (upper panel), R (middle panel), and NEP (lower panel). P-values in bold indicate a statistically significant effect at $\alpha = 0.05$.

Gross primary production						
Fixed effect	2015		2016		2017	
	F	p	F	p	F	p
GI	1.185	0.283	1.019	0.320	0.010	0.920
Salinity	64.251	<0.001	20.264	<0.0001	16.047	<0.0001
GI*Salinity	0.600	0.554	0.244	0.785	0.134	0.875

Respiration						
Fixed effect	2015		2016		2017	
	F	p	F	p	F	p
GI	1.582	0.218	1.848	0.183	0.027	0.871
Salinity	66.634	<0.001	21.486	<0.0001	18.592	<0.0001
GI*Salinity	1.137	0.333	0.519	0.600	0.155	0.857

Net ecosystem production						
Fixed effect	2015		2016		2017	
	F	p	F	p	F	p
GI	2.021	0.159	2.701	0.102	0.286	0.594
Salinity	3.449	0.036	4.027	0.019	4.199	0.017
GI*Salinity	2.890	0.061	0.202	0.817	0.207	0.814

Table. 3.3: Estimated mean±SE O₂ μmol /L/day produced (upper panel), respired (middle panel), and net ecosystem production (bottom panel) among GI treatment, salinity, and sampling year.

		Gross Primary Production		
GI	Relative Salinity	2015	2016	2017
G-	FW	465.8 [380.3, 551.3]	431.8 [279.1, 584.6]	580.6 [391.6, 769.7]
	HSW	487.6 [412.0, 563.2]	528.6 [378.6, 678.5]	546.5 [358.0, 735.0]
	OSPM	130.3 [50.4, 210.4]	152.6 [28.5, 276.7]	208.7 [59.1, 358.2]
G+	FW	528.3 [450.5, 606.2]	453.0 [305.3, 600.8]	578.1 [389.1, 767.1]
	HSW	544.5 [465.2, 623.8]	644.3 [491.7, 796.9]	600.4 [413.0, 787.8]
	OSPM	115.8 [38.3, 193.3]	188.4 [64.5, 312.3]	178.6 [31.0, 326.1]
		Respiration		
GI	Relative Salinity	2015	2016	2017
G-	FW	-498.4 [-408.8, -588.1]	-437.0 [-287.9, -586.2]	-601.8 [-417.1, -786.5]
	HSW	-510.0 [-430.0, -590.0]	-514.2 [-367.9, -660.6]	-573.1 [-388.9, -757.3]
	OSPM	-144.8 [-60.6, -229.0]	-154.7 [-33.79, -275.6]	-213.3 [-68.6, -358.1]
G+	FW	-544.7 [-462.7, -626.7]	-463.8 [-319.7, -607.9]	-598.5 [-413.8, -783.2]
	HSW	-611.1 [-527.3, -694.9]	-673.0 [-524.0, -317.3]	-635.2 [-828.2, -452.2]
	OSPM	-124.0 [-41.8, -206.1]	-196.6 [-75.9, -317.3]	-187.8 [-45.1, -330.5]
		Net Ecosystem Production		
GI	Relative Salinity	2015	2016	2017
G-	FW	-23.8 [-48.7, 1.1]	-3.8 [-14.7, 7.0]	-13.2 [-26.5, 0.0]
	HSW	-14.6 [-37.3, 8.0]	-13.2 [-23.5, -2.9]	-11.8 [-25.3, 1.7]
	OSPM	-6.8 [-31.3, 17.8]	-3.3 [-10.8, 4.1]	-2.0 [-8.5, 4.4]
G+	FW	-18.8 [-41.4, 3.7]	-10.6 [-20.5, -0.6]	-12.7 [-25.9, 0.6]
	HSW	-61.1 [-84.9, -37.2]	-22.4 [-32.7, -12.1]	-18.9 [-31.9, -5.9]
	OSPM	-6.7 [-29.8, 16.4]	-6.8 [-14.2, 0.5]	-3.0 [-9.3, 3.2]

Table 3.4 Mean±SE percentage of sonde days (number of days in brackets) calculated as autotrophic (GPP>R) among source pond, GI treatment, and sampling year. A sonde day is one 24 hour sampling period within a single mesocosm replicate.

Treatment	Type	Year		
		2015	2016	2017
G-	Fresh	46.1±8.0 (39)	39.1±7.2 (46)	53.1±8.8 (32)
	Saline	38.3±7.1 (47)	46.0±7.0 (50)	36.0±9.6 (25)
	Tailings	45.0±7.9 (40)	38.4±4.9 (99)	41.9±4.6 (117)
G+	Fresh	37.5±7.0 (48)	39.7±6.4 (58)	46.9±8.8 (32)
	Saline	42.9±7.6 (42)	40.4±6.8 (52)	51.9±9.6 (27)
	Tailings	40.0±7.3 (45)	33.7±4.6 (104)	42.4±4.4 (125)

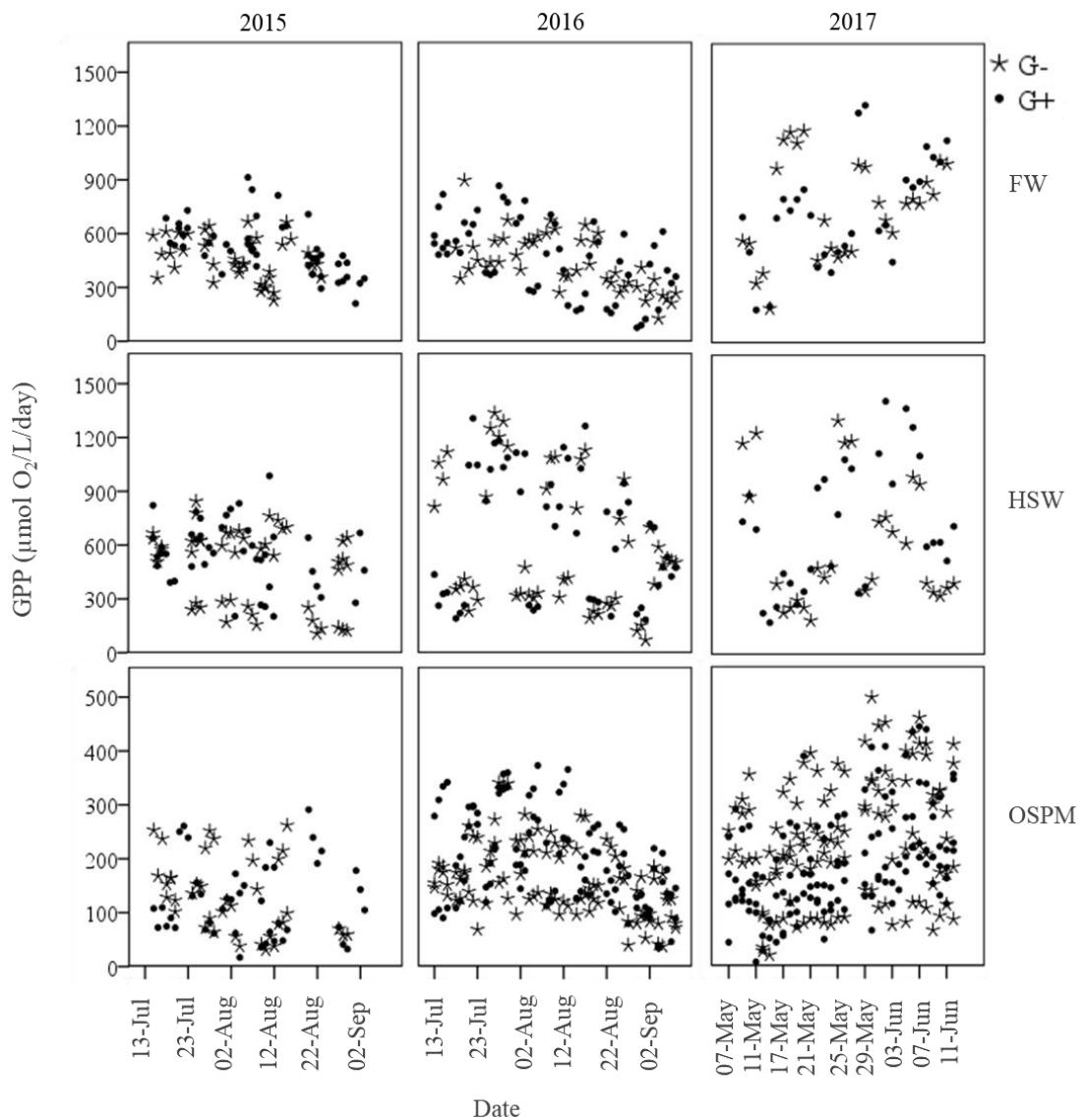


Fig. 3.2: Gross primary production ($\text{O}_2 \mu\text{mol} / \text{L}/\text{day}$) among relative salinity (panels): freshwater mesocosms (top panel), hyposaline water mesocosms (middle panel) and tailings pond mesocosms (bottom panel) among sampling years, note the difference in x and y-scales. Black asterisks represent one sonde day in a G- mesocosm replicate and black circles represent one sonde day in a G+ mesocosm replicate.

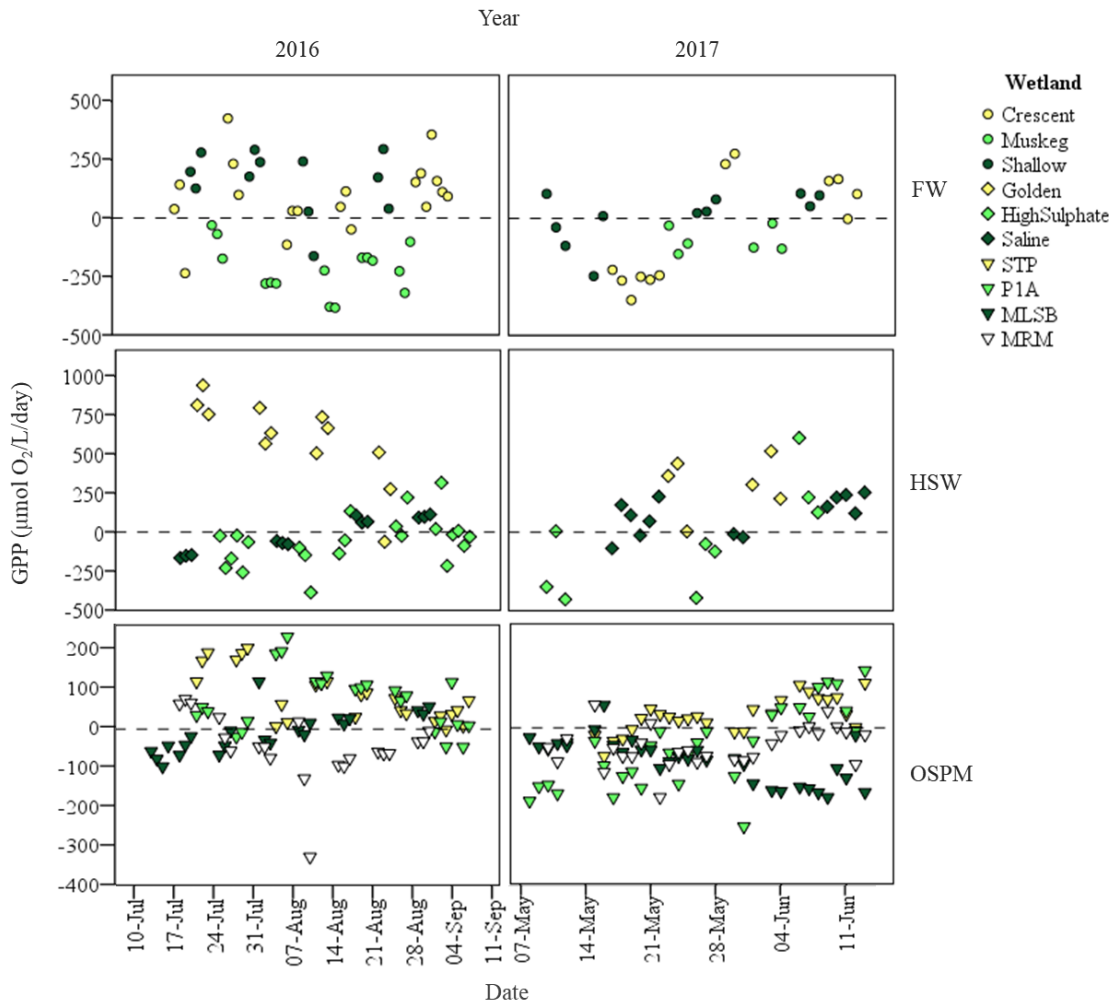


Fig. 3.3: Difference in daily estimates of O_2 $\mu\text{mol}/\text{L}/\text{day}$ produced between G+/G- pairs for individuals replicates within each level of relative salinity (panels): freshwater mesocosms (top panel), hyposaline water mesocosms (middle panel) and oil sands process material mesocosms (bottom panel), for paired sampling in 2016 (left) and 2017 (right). Note the difference in scale on the y-axis and the x-axis. G+ mesocosms are more productive than their G- counterparts when observed values of GPP are greater than 0.

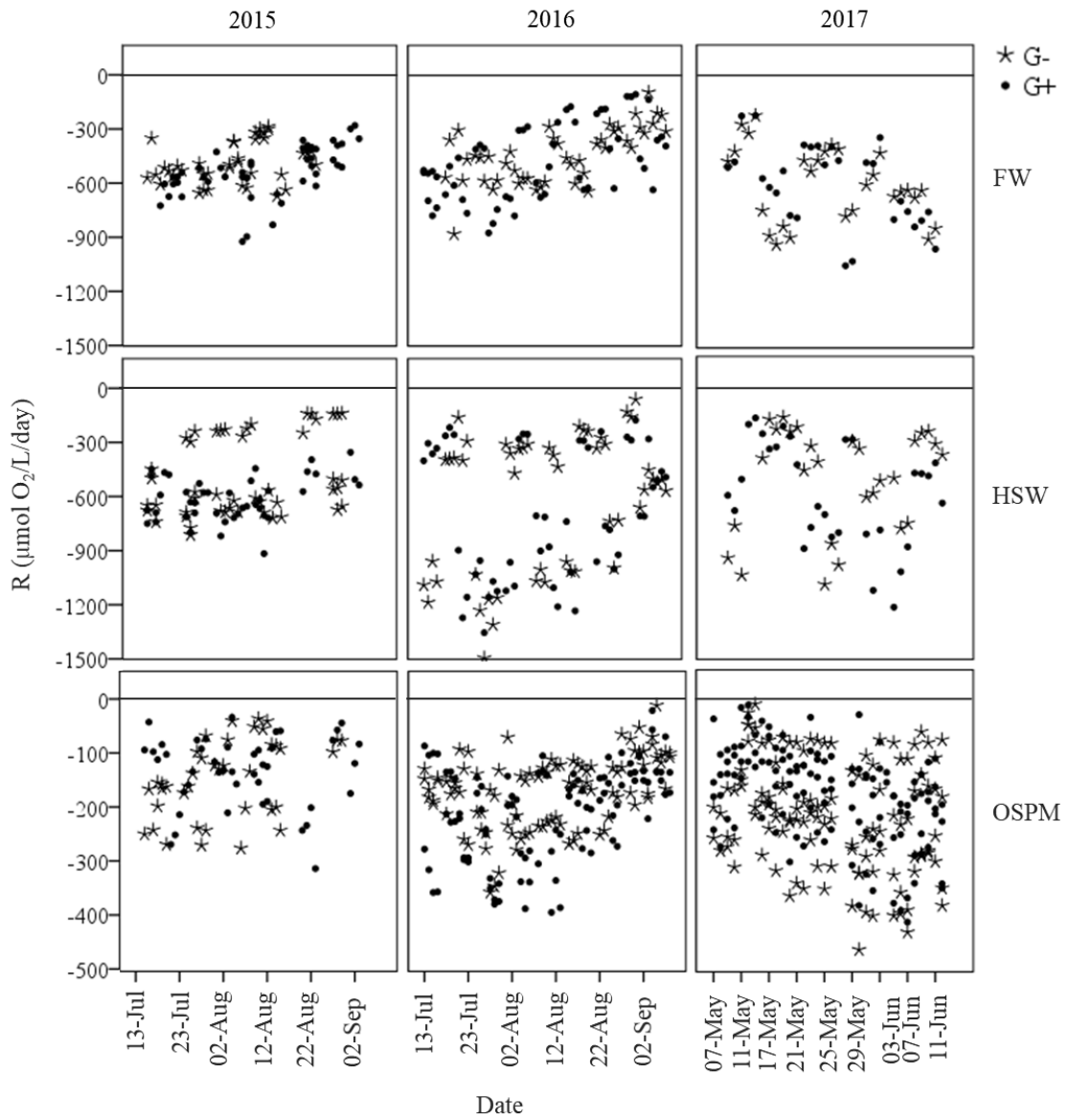


Fig. 3.4: Respiration ($O_2 \mu\text{mol} / \text{L} / \text{day}$) among source pond type (panels): freshwater mesocosms (top panel), hyposaline water mesocosms (middle panel) and OSPM mesocosms (bottom panel) among sampling years, note the difference in y-scales between reference mesocosms and OSPM mesocosms. Blank asterisks represent one sonde day in a single G- mesocosm replicate, and circles asterisks represent one sonde day in a single G+ mesocosm replicate.

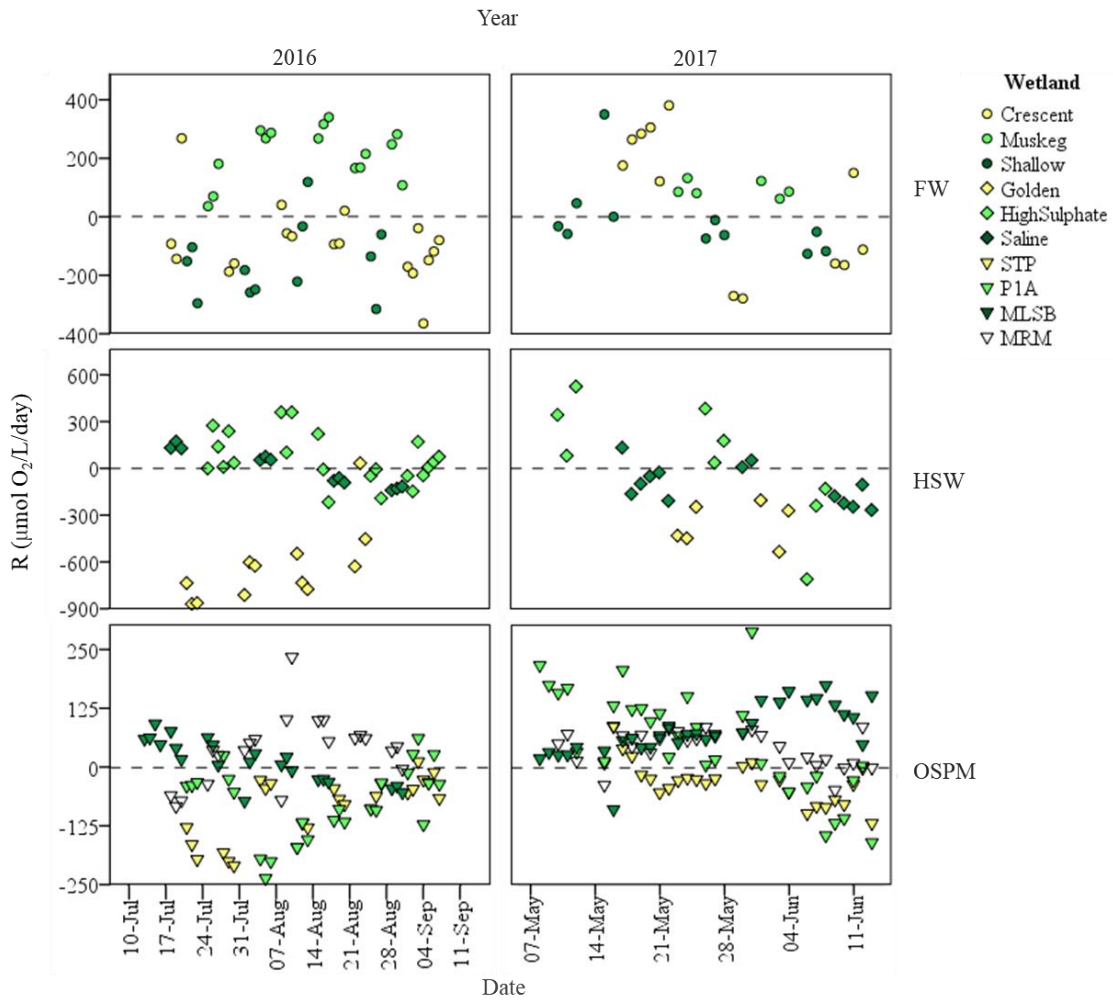


Fig. 3.5: Difference in respiration ($\text{O}_2 \mu\text{mol /L/day}$) between G+/G- pairs of wetland replicates (panels): Freshwater mesocosms (top panel), hyposaline water mesocosms (middle panel) and OSPM mesocosms (bottom panel), for paired sampling in 2016 (left) and 2017 (right). Note the difference in scale in both the x and y axis. GI stimulates mesocosm respiration in G+ mesocosms when calculated values of R are less than 0 (more negative).

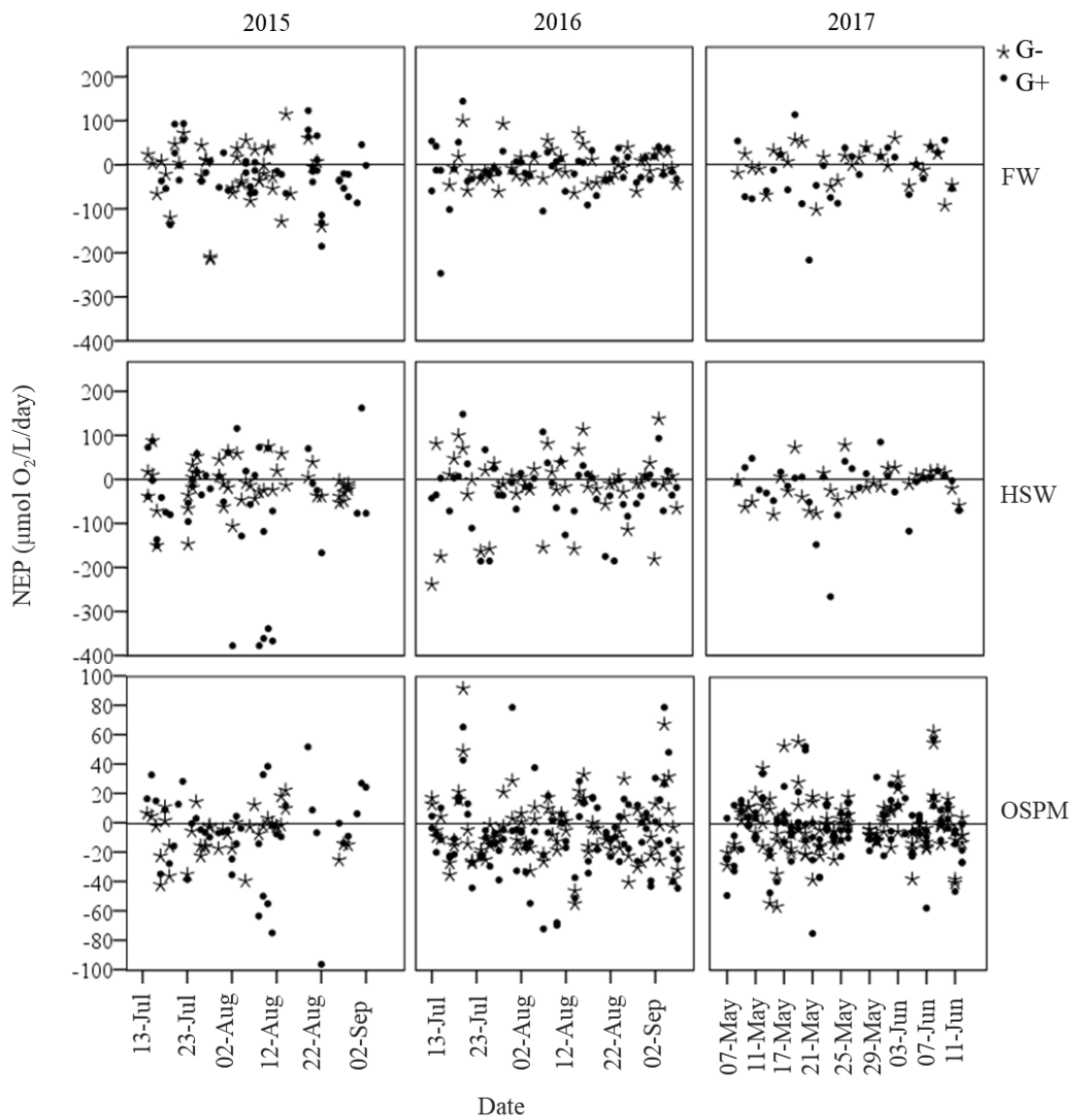


Fig. 3.6: Net ecosystem productivity ($O_2 \mu\text{mol /L/day}$) among relative salinity (panels): freshwater reference mesocosms (top panel), hyposaline water mesocosms (middle panel) and tailings pond mesocosms (bottom panel) among sampling years (columns), note the difference in y-scales. Black asterisks represent one sonde day in a G- mesocosm replicate, and black circles represent one sonde day in a G+ mesocosm replicate.

Discussion

Production

Reference mesocosms established plant communities that tended to be comprised of submerged species that quickly colonize newly constructed wetlands such as *Chara*, and *Potamogeton* (Bayley and Prather 2003) (Appendix B). Mesocosms also supported rushes (*Schoenoplectus*), which are common in wetlands in the area. All of these plant species have been observed growing in OSPM wetlands within the study region (Cooper 2004). Plants continued to grow and proliferate throughout the length of the experiment resulting in high overall primary production. Reference mesocosms had large diel fluctuations in DO that were attributed to a high % SAV cover. As expected OSPM mesocosms had the lowest overall rates of production and OSPM mesocosms were typically dominated by microbial biofilm (Appendix 2).

Patterns of DO in mesocosms were similar to patterns one would expect to find in newly constructed and natural wetlands. In a study comparing the DO dynamics of floating and submerged aquatic vegetation mats, Frodge et al. (1990) consistently observed diel DO fluctuations between 20 - 26 mg/L near the surface of SAV beds, similar to values that I observed in mesocosms dominated by SAV. In a comparison of production in the littoral and pelagic habitats of a lake, Lauster et al. (2006) observed that daily fluctuations in DO were larger in macrophyte beds in comparison to pelagic areas (3 mg/L per day vs. 1 mg/L per day). Difference between DO fluctuation in this study and the study by Lauster et al. (2006) are most likely a function of water depth.

In an assessment of three vegetation habitats in a set of restored wetlands, Reeder (2011) observed the smallest diel DO changes and production in SAV and the largest diel DO changes and production in emergent macrophytes. This is contrary to the results of this experiment where production and diel DO changes were highest in SAV and lower in mesocosms with emergent macrophytes. Emergent macrophytes exchange respiratory products directly with the atmosphere, so their metabolic products are not captured by the diel free-water oxygen technique but their decomposition is (Rejmánková 2011). One possible explanation for the differences observed between this study and Reeder (2011) is differences in the % cover of submerged and emergent macrophytes. Bunch et al. (2010) observed higher diel DO fluctuations and greater likelihood of anoxia as the % cover of emergent macrophytes increased from 50% - 95%.

When emergent macrophytes were the dominant vegetation in mesocosms, they still covered only ~10 – 20% of the mesocosm. Macrophyte % cover was <10% in OSPM mesocosms for the duration of the study. Diel DO fluctuations in OSPM mesocosms were similar to those observed in open water habitats (Lauster et al. 2006). Production estimates were also within values reported in the literature. Reeder and Binion (2001) reported GPP estimates of 247 $\mu\text{mol/L/day}$ in a shallow, eutrophic wetland with ~33% submerged macrophyte cover. Estimates of GPP for a clear water oligotrophic lake and a eutrophic lakes, both with little SAV, were 232 $\mu\text{mol/L/day}$ and 3831 $\mu\text{mol/L/day}$ respectively (Staehr et al. 2010). In littoral zones of shallow lakes that ranged from oligotrophic to eutrophic, Lauster et al. (2006) reported GPP values of 168 $\mu\text{mol/L/day}$ to 943 $\mu\text{mol/L/day}$. In the littoral zone of a clear, oligotrophic lake with little to no SAV,

Coloso et al. (2008) estimated GPP between 12 – 17 $\mu\text{mol/L/day}$. However whole lake GPP was 411.2 $\mu\text{mol/L/day}$. Estimated GPP values from reference mesocosms are well within the range reported in the literature, and values from OSPM mesocosms are typically lower than the reported literature values with the exception of the unproductive littoral zone reported in Coloso et al. (2008).

Contrary to my predictions, a reduction in NAFC concentrations following GI (Chapter 2) did not promote the extensive growth of macrophytes. Macrophytes were observed in two of the four G+ OSPM replicates at the end of the experiment (Appendix 2). Macrophytes were initially observed growing in a third G+ OSPM replicate (P1A) in 2015. In 2016, the apparent cloudiness of the water had increased and the bottom of the mesocosms could no longer be seen. Given that macrophytes in OSPM mesocosms were only observed in mesocosms where the water was clear enough to see the bottom (low TSS and turbidity) it is possible that light limitation could have also been a factor inhibiting the growth of macrophytes in this study. Furthermore, the macrophytes that did develop in OSPM mesocosms were much smaller than those observed in reference mesocosms (personal observation). The growth of both *Typha* (Mollard et al. 2013) and *Carex* (Mollard et al. 2012) were reduced when grown in OSPM amended wetlands, resulting in smaller sized macrophytes. Trites and Bayley (2009) observed productivity declined along a salinity gradient, implying that the salinity of OSPM materials will most likely continue to constrain the development of macrophytes even if NAFCs become degraded and do not inhibit growth.

Respiration

Respiration values reported from the mesocosms are typical of values reported in the literature. Lauster et al. (2006) reported R values between -204 and -1126 $\mu\text{mol/L/day}$ in the littoral zones of shallow lakes ranging from oligotrophic to eutrophic. Respiration rates in a shallow eutrophic wetland with minimal SAV were reported as -157.8 $\mu\text{mol/L/day}$ (Reeder and Binion 2001). Studies of sediment respiration in unvegetated sediments in OSPM amended wetlands reported values of approximately 0.02 $\mu\text{mol/L/day}$ in OSPM wetlands and 0.002 $\mu\text{mol/L/day}$ in reference wetlands when sediment respiration rates were multiplied by the depth of water (Gardner-Costa 2010). Chemical oxidation was the dominant form of oxygen consumption in both OSPM amended and reference wetlands (Gardner – Costa 2010). However, in highly productive waters, chemical oxidation is most likely masked by high biological respiration (Wetzel 2001).

Respiration in OSPM mesocosms was primarily attributed to microbial activity as macrophytes were scarce or absent, but extensive microbial biofilms were frequently observed. Daly (2007) observed lower bacterial production in young OSPM wetlands compared to aged OSPM wetlands and reference wetlands. Bacterial biomass in OSPM wetlands was lower than in reference wetlands of a similar age, but higher in older OSPM wetlands compared to reference wetlands of a similar age. Despite older OSPM wetlands having higher bacterial biomass, bacterial production was less than 50% of bacterial production in reference wetlands of a similar age. This reduction in bacterial production was attributed to elevated salinity (Daly 2007).

I predicted that respiration would be stimulated in G+ OSPM mesocosms during the first year to the study due to an increase in labile carbon for microbial communities to consume, similar to lab observations made by Boudens et al. (2016). Contrary to my predictions though, GI did not appear to stimulate respiration in OSPM mesocosms during the first year of the study, as respiration in G+ OSPM mesocosms was marginally less than in G- OSPM mesocosms in 2015. Respiration in G+ OSPM mesocosms was slightly higher in than G- OSPM mesocosms in 2016, with mean values of -196.6 $\mu\text{mol/L/day}$ 95% CI [-75.9, -317.3] and -154.7 $\mu\text{mol/L/day}$ [-33.79, -275.6], respectively. In 2017, respiration was higher in G- OSPM mesocosms compared to G+ OSPM mesocosms with a mean respiration of -213.3 $\mu\text{mol/L/day}$ [-68.6, -358.1] and -187.8 $\mu\text{mol/L/day}$ [-45.1, -330.5] respectively. Although respiration was marginally higher in G- OSPM mesocosms compared to G+ OSPM mesocosms, the dry mass of microbial biofilm (Appendix 2) collected from G+ OSPM mesocosms at the end of experiment was on average only 1/3 of the biomass in G- OSPM mesocosms. VanMensel et al. (2017) found that GI stimulated the development of microbial communities adapted to hydrocarbon degradation and nutrient cycling in lab-based OSPM microcosms. Given the fact that microbial biofilm biomass in G+ OSPM mesocosms was 1/3 of the biomass in G- OSPM mesocosms, it suggests that microbial production was stimulated by GI perhaps favouring communities that are more efficient (lower biomass:production) (Daly 2007). Alternatively, difference could be due to a reduction in chemical oxidation in G+ OSPM mesocosms. Jia et al. (2015) observed a decrease in chemical oxygen demand following gamma irradiation of a model naphthenic acid with varying GI doses, and

varying initial chemical concentrations. The authors noted that the decrease in chemical oxygen demand were positive correlated to an increase in GI dose and negatively correlated to increasing initial naphthenic acid concentrations, resembling a pseudo first order reaction. Similarly, Guo and Shen (2014) observed a decrease in the measured chemical oxygen demand following gamma irradiation of coking wastewater. However, the authors observed the largest decrease in COD at a GI dose of 3kGy, with a slight increase in COD at GI doses of 5.0 and 7.0 kGy. However, patterns in OSPM respiration follow patterns in OSPM production indicating that differences are most likely attributable to the biological component.

Metabolic status

All mesocosms switched between net autotrophy and net heterotrophy within a growing season and across years, but mesocosms were predominantly heterotrophic. Hyposaline water mesocosms tended to have the most variable NEP, and OSPM mesocosms had the least variable NEP. In a study of never restored, older restored, and newly restored prairie wetlands Bortolotti et al. (2016) observed that wetlands in all three categories switched between net autotrophy and net heterotrophy within a sampling season. They observed net autotrophy on 13% of days in both sampling years of their study in young restored wetlands compared to 28% (n=18) in year one and 61% (n=138) in year two in the natural wetland. The number of autotrophic days (sonde days where $GPP > R$) sampled in experimental mesocosms in this study are within the same range as natural wetlands in Bortolotti et al. (2016), with net autotrophy being observed on 33-55% of sampling days in the current study. The lack of macrophyte development in

OSPM mesocosms will impede OSPM wetlands from being able to accumulate organic matter. However, the presence of roots in G+ FFT indicates that if plants can become established, slow decomposition of roots could lead to the accumulation of organic matter.

Mean NEP in mesocosms in this study was also within the range observed by Bortolotti et al. (2016). The authors observed a maximum mean NEP rate of 16.9 ± 98.7 $\mu\text{mol O}_2/\text{L}/\text{day}$ for natural wetlands, -59.7 ± 118.1 $\text{O}_2 \mu\text{mol}/\text{L}/\text{day}$ for older restored wetlands and -79.6 ± 76.3 $\mu\text{mol O}_2/\text{L}/\text{day}$ for older restored wetlands. In comparison, values in this study ranged between -2.0 [$-8.5, 4.4$] $\mu\text{mol O}_2/\text{L}/\text{day}$ in G- tailings type mesocosms to -61.1 $\mu\text{mol O}_2/\text{L}/\text{day}$ [$-84.9, -37.2$] in G+ saline type mesocosms. G+ HSW mesocosms tended to have the most heterotrophic estimates of mean NEP. One possible explanation for high rates of net heterotrophy in reference mesocosms could be a result of the percent cover of emergent macrophytes. Emergent macrophytes exchange metabolic gasses directly with the atmosphere, but their decomposition is partially captured in measures of respiration. Therefore the inclusion of the metabolic gasses from macrophytes would likely increase NEP and the overall observance of net autotrophy. Based on the emergent macrophyte biomass at takedown (Appendix 2) and the ash free dry weight of emergent macrophyte shoots, between 0.12 and 1.9 mol O_2 would have been added to overall mesocosm NEP estimates. If we assume a similar carbon content in both macrophytes shoots and roots, an additional 0.5 to 11.4 mol O_2 would have been added to overall mesocosm NEP estimates. With the inclusion of macrophytes estimates added to NEP estimates, it is likely these systems would have been autotrophic. Another

possible explanation for high net autotrophy especially in G+ HS mesocosms, which always had the most negative estimate of NEP could be related to very high abundances of zooplankton resulting in high heterotrophic respiration.

Synopsis

This study revealed considerable natural variation measures of ecosystem metabolism among wetland replicates. As predicted, OSPM mesocosms were the least productive owing to a lack of macrophyte development. I predicted that GI would promote the development of macrophytes in G+ OSPM mesocosms by degrading and reducing concentrations of NAFCs which, exhibit cytotoxic effects (Crowe et al. 2002). In two of the G+ OSPM replicates (MLSB and MRM), GI promoted limited development of emergent macrophytes. However they were considerably smaller and less numerous than those found in reference mesocosms, similar to the findings of Mollard et al. (2013, 2014). In the other two G+ OSPM replicates that did not accrue macrophytes (P1A and STP), it appeared this was potentially a result of light limitation, as mesocosms were so turbid that the sediment could not be viewed.

Contrary to what I predicted, respiration was not increased in G+ OSPM mesocosms. However, considering that microbial biofilm dry weight in G+ OSPM mesocosms was 1/3 of the biomass in G- OSPM, it seems likely that the productivity of bacterial cells in G+ OSPM mesocosms is higher than those in G- OSPM mesocosms. Future studies should aim to quantify bacterial biomass and production to elucidate the effects of GI on microbial development. Respiration in both G- and G+ OSPM

mesocosms was several orders of magnitude higher than respiration reported by Gardner-Costa (2010) and paralleled production relatively closely, indicating that respiration was most likely dominated by biological processes as opposed to chemical oxidation. The biggest impediment to the development of productive macrophyte communities appears to be related to water clarity. However, emergent macrophytes growing in OSPM mesocosms were still smaller than those grown in reference mesocosms. Future research should aim to determine if the addition of organic material, such as peat (Roy et al. 2014), or improving the texture of the predominantly clay FFT, in addition to GI to reduce NAFC concentrations, supports the development of natural wetland macrophyte assemblages.

Chapter 4 - Synopsis, Implications of Findings, and Recommendations for Future Research

Significance

This study was the first demonstration that GI can stimulate the development of multicellular biological communities in a field based setting. Gamma irradiation is the first advanced oxidative process to be used to treat both OSPW and FFT slurry. Gamma irradiation was effective at reducing NAFC concentrations in the OSPW, but more variable in its efficacy to treat FFT (Chapter 2) resulting in a 0 – 54% reduction in NAFC concentrations. In terms of treating FFT, GI appeared to have an effect when initial NAFC concentrations were highest, which may be a function of the physical structure of individual NAFC congeners. It has been hypothesized that higher weight NAFCs with a higher degree of branching or ring structures (a higher number of tertiary carbons) are more susceptible to hydrogen abstraction due to an increase in the number of hydrogen atoms (Quinlan and Tan 2015). After 1.5 years, zooplankton biomass and density in G+ OSPM mesocosms was numerically equivalent to zooplankton biomass and density in reference mesocosms. By the end of study, measured NAFC concentrations were similar in G- and G+ OSPM mesocosms, but G+ OSPM mesocosms had a numerically higher biomass and density of zooplankton than their G- OSPM counterparts, and zooplankton biomass and density in G- OSPM was significantly reduced compared to reference mesocosms (Chapter 2). This suggests that GI not only reduces NAFC concentrations but changes chemical species present which appears to affect toxicity (Frank et al. 2008).

The reduction in NAFC concentration and presumed cytotoxicity alone was not enough to promote the development of substantial macrophyte communities in all G+ OSPM replicates. Turbidity and may have also been an important additional factor inhibiting the development of macrophytes (Cooper 2004). The diel dissolved oxygen method was used as a proxy to measure carbon and the potential for organic matter accumulation. Despite no apparent effects of GI on production or respiration in G+ OSPM mesocosms compared to G- OSPM mesocosms, production and respiration were equivalent in G- and G+ OSPM mesocosms while G+OSPM mesocosms supported roughly 1/3 of the microbial biomass in G- OSPM mesocosms, suggesting that microbial communities in G+ OSPM mesocosms are more productive than communities in G- OSPM mesocosms.

Major findings

Despite variability in NAFC speciation among different tailings ponds (Frank et al. 2016), GI appears to break down NAFCs into a common, shared carbon pool regardless of tailings pond age, type, or company source (Richard Frank, Environment and Climate Change Canada, Burlington, ON, personal communication). The oxidation of NAFCs by GI was not consistent among tailings pond replicates, which is most likely related to initial NAFC composition. Treatments such as ozonation have been shown to be more effective at reducing the proportion of higher weight recalcitrant NAFCs (Scott et al. 2008, Quinlan and Tam 2015). However, in both this study and a study by Boudens et al. (2016), GI was less effective at reducing NAFCs in P1A, (considered to be an aged tailings pond as it no longer receives inputs of FFT) which has undergone natural

biodegradation and is composed primarily of refractory NAFCs (Holowenko et al. 2002, Scott et al. 2005). Despite GI potentially creating a shared carbon pool, the biological responses to GI differed by replicate (Chapter 2). This is most likely as a result of initial NAFC characteristic, and the ability of microbial communities to further degrade them (VanMensel et al. 2017), or a result of differences in the physical environment such as particle size, conductivity, major ions, turbidity/suspended solids etc. (Reid et al. 2016). One of the key next steps will be the characterization of NAFCs following GI to elucidate the physical, chemical, and toxicological differences among ponds (Bartlett et al. 2017). Collaborations are underway to characterize the NAFC composition of samples from this study using liquid chromatography quadrupole time-of-flight mass spectrometry (LC-QToF-MS) (R. Frank et al. Environment Canada, Burlington, ON, pers. Comm.).

Zooplankton communities in OSPM mesocosms were made up of a subset of zooplankton from reference mesocosms with the exception of *Brachionus* rotifers, which were unique to OSPM mesocosms. The most pronounced differences among OSPM mesocosms and reference mesocosms were related to the relative amount of macrophyte cover (Chapter 2, Appendix 2). Emergent macrophytes colonized only 2 of the 4 G+ OSPM replicates, and SAV was only observed in Shell MRM replicates. *Potamogeton foliosus* was observed growing in both G- and G+ MRM replicates in 2016, but was observed only in G+ MRM replicates in 2017, G+ MRM replicates also supported *Chara*. By 2016 zooplankton communities in G+ OSPM mesocosms were equivalent in biomass, and density to freshwater reference mesocosms, in part due to large natural variability in the productivity of reference mesocosms. Zooplankton biomass in mesocosms filled with

25 cm of water to observe the passive accumulation of organic matter was similar to biomass in G+ OSPM mesocosms, which is an indication that the remaining differences in zooplankton biomass and abundance are due to habitat heterogeneity i.e. macrophyte cover rather than inhibitory properties of the materials in the OSPM mesocosms themselves. Zooplankton species assemblages in reference mesocosms supported assemblages similar to those found typically found in shallow ponds or wetlands (Cottenie et al. 2001, Norlin et al. 2006, and Kurek et al. 2012).

All mesocosms developed diel DO rhythms (Odum 1956) but the amplitude of the rhythms varied among mesocosm replicates. Net autotrophy and net heterotrophy was observed in all mesocosms but mesocosms were more often than not heterotrophic (Chapter 3). Patterns of diel O₂ were a function of the dominant primary producers, with reference mesocosms with high SAV cover being the most productive and OSPM mesocosms with predominantly microbial primary production being the least productive. Although GI did not have an apparent effect on production or respiration in G+ OSPM mesocosm compared to G- OSPM mesocosms, the microbial biofilm collected from G+ OSPM mesocosms was approximately 1/3 of the dry weight of biofilm collected from G- OSPM mesocosms. Daly (2007) observed decreased production:biomass ratios in young OSPM wetlands which she attributed to increased salinity, and observed higher production:biomass ratios in reference wetlands. The equivalent production in G+OSPM mesocosms despite a lower biomass taken in concert with the findings of VanMensel et al. (2017) who observed the stimulation of microbial degraders and the presence of a genus of bacteria frequently associated with freshwater sediments and wetland

environments suggests that GI stimulates the development of microbial communities on track with successful wetland reclamation. However the establishment of macrophyte communities is still impeded and will be important for carbon accrual and habitat for higher trophic levels

Recommendations for future studies

One of the next steps to develop GI as a treatment option for the remediation of OSPM is to characterize the NAFC congeneric composition to determine if GI can be optimized to reduce NAFC concentrations in all tailings ponds, or if is better suited to tailings ponds with specific NAFC characteristics. Ozonation of NAFCs has been shown to most likely follow a pseudo first order reaction with the pseudo first order rate constant increasing in proportion as the number of rings and branching of NAFCs increases (Quinlan and Tam 2015). Jia et al. (2015) observed a decrease in COD following gamma irradiation of cyclohexane butyric acid (a model naphthenic acid), with increasing GI dose, but a decrease in the efficacy as the initial concentration of the target compound increased. In order to optimize GI as a treatment option for OSPM, it will be important to determine how NAFC concentration and speciation, and GI dose interact.

The accrual of zooplankton biomass and diversity in G+ OSPM mesocosms was not immediate, possibly because of residual toxicity that required the activity of indigenous microbial communities to reduce it. It took approximately 1.5 years before mesocosms supported zooplankton communities. In order to apply GI as a treatment option to develop functioning aquatic ecosystems, the next studies could investigate the

use of a biphasic inoculation to determine the ideal time to introduce biological propagules to increase survival and proliferation. The first phase would be introducing indigenous microbial communities immediately after GI and the second phase would be introducing a biological inoculum (plants, zooplankton), after sufficient detoxification and conditions (water clarity) has occurred (1.5 years, according to this study).

The application of GI as a treatment method offers multiple potential benefits such as the ability to treat slurry, the elimination of the need for particle free water, and the ability of GI to form hydroxyl radicals with water in the sample as opposed to the need to add of expensive oxidizing agents such as ozone. The volume of tailings that need to be treated are large, and GI would most likely need to be applied to the tailings as they are moved out of the settling basins. Although GI is effective at reducing NAFC concentrations, water quality (salinity, TSS, other residual organics) will likely remain an important challenge the oil sands industry has to face (McQueen et al. 2017, White 2017). Gamma irradiation will likely have to be combined with other treatments to create sustainable landscapes that incorporate mine waste materials.

References

- Alberta Government (2015) *Lower Athabasca region tailings management framework for the mineable Athabasca Oil Sands*.
- Ajaero C., Peru K.M., Simair M., Friesen V., O'Sullivan G., Hughes S.A., *et al.* (2018) Fate and behavior of oil sands naphthenic acids in a pilot-scale treatment wetland as characterized by negative-ion electrospray ionization Orbitrap mass spectrometry. *Science of the Total Environment* **631–632**, 829–839.
- Allen E.W. (2008) Process water treatment in Canada's oil sands industry: I. Target pollutants and treatment objectives. *Journal of Environmental Engineering and Science* **7**, 123–138.
- Anas M.U.M., Scott K.A., Cooper R.N. & Wissel B. (2014) Zooplankton communities are good indicators of potential impacts of Athabasca oil sands operations on downwind boreal lakes. *Canadian Journal of Fisheries and Aquatic Sciences* **71**, 719–732.
- Anderson J., Wiseman S.B., Moustafa A., Gamal El-Din M., Liber K. & Giesy J.P. (2012) Effects of exposure to oil sands process-affected water from experimental reclamation ponds on *Chironomus dilutus*. *Water Research* **46**, 1662–1672.
- APHA, 1989. *Standard Methods for the Examination of Water, Sewage, and Wastewater*. 17th Ed. American Public Health Association, Washington, D.C.
- Armstrong S.A., Headley J. V., Peru K.M. & Germida J.J. (2009) Differences in phytotoxicity and dissipation between ionized and nonionized oil sands naphthenic acids in wetland plants. *Environmental Toxicology and Chemistry* **28**, 2167–2174.
- Arnott S.E. & Vanni M.J. (1993) Zooplankton assemblages in fishless bog lakes :influence of biotic and abiotic factors. *Ecology* **74**, 2361–2380.
- Audet P., Pinno B.D. & Thiffault E. (2015) Reclamation of boreal forest after oil sands mining: anticipating novel challenges in novel environments. *Canadian Journal of Forest Research* **45**, 364–371.
- Bartlett A.J., Frank R.A., Gillis P.L., Parrott J.L., Marentette J.R., Brown L.R., *et al.* (2017) Toxicity of naphthenic acids to invertebrates: Extracts from oil sands process-affected water versus commercial mixtures. *Environmental Pollution* **227**, 271–279.
- Basińska A.M., Antczak M., Świdnicki K., Jassey V.E.J. & Kuczyńska-Kippen N. (2014) Habitat type as strongest predictor of the body size distribution of *Chydorus*

- sphaericus (O. F. Müller) in small water bodies. *International Review of Hydrobiology* **99**, 382–392.
- Bayley S.E. & Prather C.M. (2003) Do wetland lakes exhibit alternative stable states? Submersed aquatic vegetation and chlorophyll in western boreal shallow lakes. *Limnology and Oceanography* **48**, 2335–2345.
- Bendell-Young L.I., Bennett K.E., Crowe A., Kennedy C.J., Kermode A. R., Moore M.M., *et al.* (2000) Ecological characteristics of wetlands receiving an industrial effluent. *Ecological Applications* **10**, 310–322.
- BGC Engineering Inc. (2010) Review of Reclamation Options for Oil Sands Tailings Substrates. University of Alberta, School of Energy and the Environment, Edmonton, Alberta. OSRIN Report No. TR-2., 59 pp.
- BGC Engineering Inc. (2010) *Oil Sands Tailings Technology Review*. University of Alberta, School of Energy and the Environment, Edmonton, Alberta. OSRIN Report No. TR-1. 136 pp.
- Borrely S.I., Sampa M.H.O., Pedroso C.B., Oikawa H., Silveira C.G., Cherbakian E.H., *et al.* (2000) Radiation processing of wastewater evaluated by toxicity assays. *Radiation Physics and Chemistry* **57**, 507–511.
- Bortolotti L.E., St. Louis V.L., Vinebrooke R.D. & Wolfe A.P. (2016) Net ecosystem production and carbon greenhouse gas fluxes in three prairie wetlands. *Ecosystems* **19**, 411–425.
- Bottrell H.H., Duncan A., Gliwicz Z.M., Grygierek E., Herzig A., Hillbricht-Ilkowska A., *et al.* (1976) A review of some problems in zooplankton production studies. *Norwegian Journal of Zoology* **24**, 419–456.
- Boudens R., Reid T., VanMensel D., Sabari Prakasan M.R., Ciborowski J.J.H. & Weisener C.G. (2016) Bio-physicochemical effects of gamma irradiation treatment for naphthenic acids in oil sands fluid fine tailings. *Science of the Total Environment* **539**, 114–124.
- Bownik A. (2017) Daphnia swimming behaviour as a biomarker in toxicity assessment: A review. *Science of the Total Environment* **601–602**, 194–205.
- Brett M.T., Muller-Navarra D.C. & Persson J. (2009) *Lipids in aquatic ecosystems*. (Eds M.T. Arts, M.T. Brett & M.J. Kainz), Springer Science+ Business Media, New York, NY.

- Brock M.A., Nielsen D.L. & Crosslé K. (2005) Changes in biotic communities developing from freshwater wetland sediments under experimental salinity and water regimes. *Freshwater Biology* **50**, 1376–1390.
- Brown L.D. & Ulrich A.C. (2015) Oil sands naphthenic acids: A review of properties, measurement, and treatment. *Chemosphere* **127**, 276–290.
- Bunch A.J., Allen M.S. & Gwinn D.C. (2010) Spatial and temporal hypoxia dynamics in dense emergent macrophytes in a Florida lake. *Wetlands* **30**, 429–435.
- Cairns J. (1983) Are single species toxicity tests alone adequate for estimating environmental hazard? *Environmental Monitoring and Assessment* **4**, 259–273.
- Carpenter S.R. & Lodge D.M. (1986) Effects of submersed macrophytes on ecosystem processes. *Aquatic Botany* **26**, 341–370.
- Chapin F.S., Woodwell G.M., Randerson J.T., Rastetter E.B., Lovett G.M., Baldocchi D.D., *et al.* (2006) Reconciling carbon-cycle concepts, terminology, and methods. *Ecosystems* **9**, 1041–1050.
- Chaychian M., Al-Sheikhly M., Silverman J. & McLaughlin W.L. (1998) The mechanisms of removal of heavy metals from water by ionizing radiation. *Radiation Physics and Chemistry* **53**, 145–150.
- Chen H.H. (2011) *The Effects of Nutrient and Peat Amendments on Oil Sands Reclamation Wetlands: A Microcosm Study*. M.Sc. University of Waterloo.
- Chen M., Walshe G., Chi Fru E., Ciborowski J.J.H. & Weisener C.G. (2013) Microcosm assessment of the biogeochemical development of sulfur and oxygen in oil sands fluid fine tailings. *Applied Geochemistry* **37**, 1–11.
- Chi C., Brownlee B.G. & Bunce N.J. (2006) Mass spectrometric and toxicological assays of Athabasca oil sands naphthenic acids. *Water Research* **40**, 655–664.
- Chimney M.J., Wenkert L. & Pietro K.C. (2006) Patterns of vertical stratification in a subtropical constructed wetland in south Florida (USA). *Ecological Engineering* **27**, 322–330.
- Chu L. & Wang J. (2016) Degradation of 3-chloro-4-hydroxybenzoic acid in biological treated effluent by gamma irradiation. *Radiation Physics and Chemistry* **119**, 194–199.
- Clemente J.S. & Fedorak P.M. (2005) A review of the occurrence, analyses, toxicity, and biodegradation of naphthenic acids. *Chemosphere* **60**, 585–600.

- Cobbaert D., Wong A.S. & Bayley S.E. (2015) Resistance to drought affects persistence of alternative regimes in shallow lakes of the Boreal Plains (Alberta, Canada). *Freshwater Biology* **60**, 2084–2099.
- Cole J.J., Pace M.L., Carpenter S.R. & Kitchell J.F. (2000) Persistence of net heterotrophy in lakes during nutrient addition and food web manipulations. *Limnology and Oceanography* **45**, 1718–1730.
- Coloso J.J., Cole J.J., Hanson P.C. & Pace M.L. (2008) Depth-integrated, continuous estimates of metabolism in a clear-water lake. *Canadian Journal of Fisheries and Aquatic Sciences* **65**, 712–722.
- Cooper N.J. (2004) *Vegetation community development of reclaimed oil sands wetlands*. University of Alberta.
- Cottenie K., Nuytten N., Michels E. & Meester L. De (2001) Zooplankton community structure and environmental conditions in a set of interconnected ponds. *Hydrobiologia* **442**, 339–350.
- Crowe A.U., Plant A.L. & Kermode A.R. (2002) Effects of an industrial effluent on plant colonization and on the germination and post-germination.pdf. *Environmental Pollution* **117**, 179–189.
- Daly C. (2007) *Carbon sources, microbial community production, and respiration in constructed wetlands of the Alberta, Canada oil sands mining area*. M.Sc.
- Dumont H.J., Van de Velde I. & Dumont S. (1975) The dry weight estimate of biomass in a selection of Cladocera, Copepoda and Rotifera from the plankton, periphyton and benthos of continental waters. *Oecologia* **19**, 75–97.
- Dwyer F.J., Burch S. a, Ingersoll C.G. & Hunn J.B. (1992) Toxicity of trace-element and salinity mixtures to striped bass (*Morone saxatilis*) and *Daphnia magna*. *Environmental Toxicology and Chemistry* **11**, 513–520.
- Edmondson W.T. (1959) *Fresh-water biology*. Wiley, New York.
- Español C., Gallardo B., Pino M.R., Martín A. & Comín F.A. (2013) Is net ecosystem production higher in natural relative to constructed wetlands? *Aquatic Sciences* **75**, 385–397.
- Ferone J.M. & Devito K.J. (2004) Shallow groundwater – surface water interactions in pond – peatland complexes along a Boreal Plains topographic gradient. *Journal of Hydrology* **292**, 75–95.

- Foot L. & Krogman N. (2006) Wetlands in Canada's western boreal forest: agents of change. *The Forestry Chronicle* **82**, 825–833.
- Frank R.A., Milestone C.B., Rowland S.J., Headley J. V., Kavanagh R.J., Lengger S.K., *et al.* (2016) Assessing spatial and temporal variability of acid-extractable organics in oil sands process-affected waters. *Chemosphere* **160**, 303–313.
- Frank R.A., Kavanagh R., Kent Burnison B., Arsenault G., Headley J. V., Peru K.M., *et al.* (2008) Toxicity assessment of collected fractions from an extracted naphthenic acid mixture. *Chemosphere* **72**, 1309–1314.
- Frederick K.R. (2011) *Productivity and carbon accumulation potential of transferred biofilms in reclaimed oil sands-affected wetlands* Master of Science Land Reclamation and Remediation Renewable Resources. M.Sc. University of Alberta.
- Frodge J.D., Thomas G.L. & Pauley G.B. (1990) Effects of canopy formation by floating and submergent aquatic macrophytes on the water quality of two shallow Pacific Northwest lakes. *Aquatic Botany* **38**, 231–248.
- Fryer B.Y.G. (1968) Evolution and adaptive radiation in the Chydoridae (Crustacea: Cladocera): A study in comparative functional morphology and ecology. *Philosophical Transactions of the Royal Society B: Biological Sciences* **254**, 221–385.
- FTFC (Fine Tailings Fundamentals Consortium) (1995) *Advances in oil sands tailings research*. Edmonton, Alberta.
- Gardner Costa J.M. (2010) *Spatial and temporal variation in sediment-associated microbial respiration in oil sands mine-affected wetlands of north-eastern Alberta, Canada*. M.Sc. University of Windsor.
- Getoff N. (1996) Radiation-induced degradation of water pollutant - state of the art. *Radiation Physics and Chemistry* **47**, 581–593.
- Golby S., Ceri H., Gieg L.M., Chatterjee I., Marques L.L.R. & Turner R.J. (2012) Evaluation of microbial biofilm communities from an Alberta oil sands tailings pond. *FEMS Microbiology Ecology* **79**, 240–250.
- Graf M. & Rochefort L. (2009) Examining the peat-accumulating potential of fen vegetation in the context of fen restoration of harvested peatlands. *Écoscience* **16**, 158–166.

- Grewer D.M., Young R.F., Whittal R.M. & Fedorak P.M. (2010) Naphthenic acids and other acid-extractables in water samples from Alberta: What is being measured? *Science of the Total Environment*.
- Gulley J.R. & Klym D.J. (1992). Wetland treatment of oil sands operation waste waters. pages 1431-1438 in R.K. Singhal, A. K. Mehrotra, K. Fytas and J-L. Collins (Editors), *Environmetnal Issues and Management of Waste in Energy and Mineral Production. Vol.2*. Balkema, Rotterdam.
- Guo F. & Shen H. (2014) Study of gamma irradiation-induced effects on organic pollutants and suspended solids in coking wastewater. *Desalination and Water Treatment* **52**, 1850–1854.
- Han X., MacKinnon M.D. & Martin J.W. (2009) Estimating the in situ biodegradation of naphthenic acids in oil sands process waters by HPLC/HRMS. *Chemosphere* **76**, 63–70.
- Hanazato T. (2001) Pesticide effects on freshwater zooplankton: an ecological perspective. *Environmental Pollution* **112**, 1–10.
- Harris M. (2007) *Guideline for wetland establishment on reclaimed oil sands leases (revised second edition)*. Prepared by Lorax Environmental for CEMA Wetlands and Aquatics Subgroup of the Reclamation Working Group, Fort McMurray, AB.
- He Y., Patterson S., Wang N., Hecker M., Martin J.W., Gamal El-din M., *et al.* (2012) Toxicity of untreated and ozone-treated oil sands process-affected water (OSPW) to early life stages of the fathead minnow (*Pimephales promelas*). *Water Research* **46**, 6359–6368.
- Headley J. V., Peru K.M., Fahlman B., Colodey A. & McMartin D.W. (2013) Selective solvent extraction and characterization of the acid extractable fraction of Athabasca oils sands process waters by Orbitrap mass spectrometry. *International Journal of Mass Spectrometry* **345–347**, 104–108.
- Headley J. V., Peru K.M. & Barrow M.P. (2016) Advances in mass spectrometric characterization of naphthenic acids fraction compounds in oil sands environmental samples and crude oil - A review. *Mass Spectrometry Reviews* **35**, 311–328.
- Herman D.C., Fedorak P.M., Mackinnon M.D. & Costerton J.W. (1994) Biodegradation of naphthenic acids by microbial populations indigenous to oil sands tailings. *Canadian Journal of Microbiology* **40**, 467–477.

- Hersikorn B.D. & Smits J.E.G. (2011) Compromised metamorphosis and thyroid hormone changes in wood frogs (*Lithobates sylvaticus*) raised on reclaimed wetlands on the Athabasca oil sands. *Environmental Pollution* **159**, 596–601.
- Holowenko F.M., MacKinnon M.D. & Fedorak P.M. (2002) Characterization of naphthenic acids in oil sands wastewaters by gas chromatography-mass spectrometry. *Water Research* **36**, 2843–2855.
- Hornung J.P. & Foote A.L. (2006) Aquatic invertebrate responses to fish presence and vegetation complexity in western boreal wetlands, with implications for waterbird productivity. *Wetlands* **26**, 1–12.
- Huang R., Chen Y., Meshref M.N.A., Chelme-Ayala P., Dong S., Ibrahim M.D., *et al.* (2018) Characterization and determination of naphthenic acids species in oil sands process-affected water and groundwater from oil sands development area of Alberta, Canada. *Water Research* **128**, 129–137.
- Hunt R.J. & Swift M. (2010) Predation by larval damselflies on cladocerans. *Journal of Freshwater Ecology* **25**, 345–351.
- Jeppesen E., Jensen J.P., Søndergaard M. & Lauridsen T. (1999) Trophic dynamics in turbid and clearwater lakes with special emphasis on the role of zooplankton for water clarity. *Hydrobiologia* **408/409**, 217–231.
- Jeziorski A., Tanentzap A., Yan N.D., Paterson A.M., Palmer M.E., Korosi J.B., *et al.* (2015) The jellification of north temperate lakes. *Proceedings of the Royal Society B* **282**, 20142449.
- Jia W., He Y., Ling Y., Hei D., Shan Q., Zhang Y., *et al.* (2015) Radiation-induced degradation of cyclohexane butyric acid in aqueous solutions by gamma ray irradiation. *Radiation Physics and Chemistry* **109**, 17–22.
- Johnson E.A. & Miyanishi K. (2008) Creating new landscapes and ecosystems: The Alberta Oil Sands. *Annals of the New York Academy of Sciences* **1134**, 120–145.
- Kannel P.R. & Gan T.Y. (2012) Naphthenic acids degradation and toxicity mitigation in tailings wastewater systems and aquatic environments: a review. *Journal of Environmental Science and Health* **47**, 1–21.
- Karakaya N. (2011) Does different versus equal daytime and night-time respiration matter for quantification of lake metabolism using diel dissolved oxygen cycles? *International Journal of Limnology* **47**, 251–257.

- Kasperski K.L. & Mikula R.J. (2011) Waste streams of mined oil sands: Characteristics and remediation. *Elements* **7**, 387–392.
- Kavanagh R.J., Frank R.A., Burnison B.K., Young R.F., Fedorak P.M., Solomon K.R., *et al.* (2012) Fathead minnow (*Pimephales promelas*) reproduction is impaired when exposed to a naphthenic acid extract. *Aquatic Toxicology* **116–117**, 34–42.
- Kennedy K.D. (2012) *Growth, survival, and community composition of Chironomidae (Diptera) larvae in selected Athabasca oil sands process-affected wetland waters of northeastern Alberta*. M.Sc. University of Windsor.
- Kessler S., Barbour S.L., van Rees K.C.J. & Dobchuk B.S. (2010) Salinization of soil over saline-sodic overburden from the oil sands in Alberta. *Canadian Journal of Soil Science* **90**, 637–647.
- Ketcheson S.J., Price J.S., Carey S.K., Petrone R.M., Mendoza C.A. & Devito K.J. (2016) Constructing fen peatlands in post-mining oil sands landscapes : Challenges and opportunities from a hydrological perspective. *Earth Science Reviews* **161**, 130–139.
- Kovalenko K.E., Ciborowski J.J.H., Daly C., Dixon D.G., Farwell A.J., Foote A.L., *et al.* (2013) Food web structure in oil sands reclaimed wetlands. *Ecological Applications* **23**, 1048–1060.
- Kurek J., Kirk J.L., Muir D.C.G., Wang X., Evans M.S. & Smol J.P. (2013) Legacy of a half century of Athabasca oil sands development recorded by lake ecosystems. *Proceedings of the National Academy of Sciences* **110**, 1761–1766.
- Laas A., Noges P., Koiv T. & Noges T. (2012) High-frequency metabolism study in a large and shallow temperate lake reveals seasonal switching between net autotrophy and net heterotrophy. *Hydrobiologia*, 57–74.
- Lari E., Wiseman S., Mohaddes E., Morandi G., Alharbi H. & Pyle G.G. (2016) Determining the effect of oil sands process-affected water on grazing behaviour of *Daphnia magna*, long-term consequences, and mechanism. *Chemosphere* **146**, 362–370.
- Lauster G.H., Hanson P.C. & Kratz T.K. (2006) Gross primary production and respiration differences among littoral and pelagic habitats in northern Wisconsin lakes. *Canadian Journal of Fisheries and Aquatic Sciences* **63**, 1130–1141.
- Leppänen J.J. (2018) An overview of Cladoceran studies conducted in mine water impacted lakes. *International Aquatic Resources* **10**, 207–221.

- Leshuk T., Wong T., Linley S., Peru K.M., Headley J. V. & Gu F. (2016) Solar photocatalytic degradation of naphthenic acids in oil sands process-affected water. *Chemosphere* **144**, 1854–1861.
- Leung S., MacKinnon M.D. & Smith R. (2001) Aquatic reclamation in the Athabasca, Canada, oil sands: Naphthenate and salt effects on phytoplankton communities. *Environmental Toxicology and Chemistry* **20**, 1532–1543.
- Leung S., MacKinnon M.D. & Smith R.E. (2001) Aquatic reclamation in the Athabasca, Canada, oil sands: Naphthenate and salt effects on phytoplankton communities. *Environmental toxicology and chemistry / SETAC* **20**, 1532–1543.
- Leung S., MacKinnon M. & Smith R. (2003) The ecological effects of naphthenic acids and salts on phytoplankton from the Athabasca oil sands region. *Aquatic Toxicology* **62**, 11–26.
- Li C., Fu L., Stafford J., Belosevic M. & Gamal El-din M. (2017) The toxicity of oil sands process-affected water (OSPW): A critical review. *Science of the Total Environment* **601–602**, 1785–1802.
- Liss P.S. (1973) Processes of gas exchange across an air-water interface. *Deep-Sea Research and Oceanographic Abstracts* **20**, 221–238.
- Littell R.C., Pendergast J. & Natarajan R. (2000) Modelling covariance structure in the analysis of repeated measures data. *Statistics in Medicine* **19**, 1793–1819.
- Loreau M., Naeem S., Inchausti P., Bengtsson J., Grime J.P., Hector A., *et al.* (2001) Biodiversity and ecosystem functioning: current knowledge and future challenges. *Science* **294**, 804–808.
- Lougheed V.L. & Chow-Fraser P. (1998) Factors that regulate the zooplankton community structure of a turbid, hypereutrophic Great Lakes wetland. *Canadian Journal of Fisheries and Aquatic Sciences* **55**, 150–161.
- Lynch M. (1978) Complex Interactions between Natural Coexploiters--*Daphnia* and *Ceriodaphnia*. *Ecology* **59**, 552–564.
- MacKinnon M.D., Matthews J.G., Shaw W.H. & Cuddy R.G. (2001) Water quality issues associated with implementation of composite tailings (CT) technology for managing oil sands tailings. *International Journal of Surface Mining, Reclamation and Environment* **15**, 235–256.

- MacLennan M., Dings-Avery C. & Vinebrooke R.D. (2015) Invasive trout increase the climatic sensitivity of zooplankton communities in naturally fishless lakes. *Freshwater Biology* **60**.
- Marentette J.R., Frank R.A., Bartlett A.J., Gillis P.L., Hewitt L.M., Peru K.M., *et al.* (2015) Toxicity of naphthenic acid fraction components extracted from fresh and aged oil sands process-affected waters, and commercial naphthenic acid mixtures, to fathead minnow (*Pimephales promelas*) embryos. *Aquatic Toxicology* **164**, 108–117.
- Martin J.W., Barri T., Han X., Fedorak P.M., El-din M.G., Perez L., *et al.* (2010) Ozonation of oil sands process-affected water accelerates microbial bioremediation. *Environmental Science and Technology* **44**, 8350–8356.
- Matthews J.G., Shaw W.H., MacKinnon M.D. & Cuddy R.G. (2002) Development of composite tailings technology at Syncrude. *International Journal of Surface Mining, Reclamation and Environment* **16**, 24–39.
- McCormick J.K. *The effects of oil sands tailings on zooplankton communities in Northern Alberta*. University of Waterloo, Waterloo, Ontario.
- McMartin D.W., Headley J. V., Friesen D.A., Peru K.M. & Gillies J.A. (2004) Photolysis of naphthenic acids in natural surface water. *Journal of Environmental Science and Health* **39**, 1361–1383.
- McQueen A.D., Hendrikse M., Gaspari D.P., Kinley C.M., Rodgers J.H. & Castle J.W. (2017) Performance of a hybrid pilot-scale constructed wetland system for treating oil sands process-affected water from the Athabasca oil sands. *Ecological Engineering* **102**, 152–165.
- McQueen A.D., Kinley C.M., Hendrikse M., Gaspari D.P., Calomeni A.J., Iwinski K.J., *et al.* (2017) A risk-based approach for identifying constituents of concern in oil sands process-affected water from the Athabasca Oil Sands region. *Chemosphere* **173**, 340–350.
- Meli P., Benayas J.M.R., Balvanera P. & Ramos M.M. (2014) Restoration enhances wetland biodiversity and ecosystem service supply, but results are context-dependent: A meta-analysis. *PLoS ONE* **9**, e93507.
- Menard K. (2017) *Community Development of terrestrial and semi-terrestrial invertebrates along environmental gradients in a reclaimed watershed*. M.Sc. University of Windsor.
- Mitsch W.J. & Gosselink J.G. (2015) *Wetlands*, 5th edn. John Wiley & Sons, Inc., Hoboken, New Jersey.

- Mollard F.P.O., Roy M.C. & Foote A.L. (2013) *Typha latifolia* plant performance and stand biomass in wetlands affected by surface oil sands mining. *Ecological Engineering* **58**, 26–34.
- Mollard F.P.O., Roy M., Frederick K. & Foote L. (2012) Growth of the dominant macrophyte *Carex aquatilis* is inhibited in oil sands affected wetlands in Northern Alberta, Canada. *Ecological Engineering* **38**, 11–19.
- Moore M. & Folt C. (1993) Zooplankton body size and community structure: Effects of thermal and toxicant Stress. *Trends in Ecology & Evolution* **8**, 178–183.
- Moreno-Mateos D., Power M.E., Comín F. A. & Yockteng R. (2012) Structural and functional loss in restored wetland ecosystems. *PLoS Biology* **10**.
- Nevalainen L., Luoto T.P., Levine S. & Manca M. (2011) Paleolimnological evidence for increased sexual reproduction in chydorids (Chydoridae, Cladocera) under environmental stress. *Journal of Limnology* **70**, 255–262.
- Norlin J.I., Bayley S.E. & Ross L.C.M. (2006) Zooplankton composition and ecology in western boreal shallow-water wetlands. *Hydrobiologia* **560**, 197–215.
- Odum H.T. (1956) Primary production in flowing waters. *Limnology and Oceanography* **1**, 102–117.
- Odum H.T. & Odum E.P. (1955) Trophic structure and productivity of a windward coral reef community on Eniwetok Atoll. *Ecological Monographs* **25**, 291–320.
- O’Gorman E.J. & Emmerson M.C. (2009) Perturbations to trophic interactions and the stability of complex food webs. *Proceedings of the National Academy of Sciences of the United States of America* **106**, 13393–13398.
- Pennak R.W. (1966) Structure of zooplankton populations in the littoral macrophyte zone of some Colorado lakes. *Transactions of the American Microscopical Society* **85**, 329–349.
- Price J.S., McLaren R.G. & Rudolph D.L. (2010) Landscape restoration after oil sands mining: conceptual design and hydrological modelling for fen reconstruction. *International Journal of Mining, Reclamation and Environment* **24**, 109–123.
- Puttaswamy N. & Liber K. (2012) Influence of inorganic anions on metals release from oil sands coke and on toxicity of nickel and vanadium to *Ceriodaphnia dubia*. *Chemosphere* **86**, 521–529.

- Quagraine E.K., Peterson H.G. & Headley J. V (2005) In situ bioremediation of naphthenic acids contaminated tailing pond waters in the Athabasca oil sands region--demonstrated field studies and plausible options: a review. *Journal of Environmental Science and Health* **40**, 685–722.
- Quinlan P.J. & Tam K.C. (2015) Water treatment technologies for the remediation of naphthenic acids in oil sands process-affected water. *Chemical Engineering Journal* **279**, 696–714.
- Raab D. & Bayley S.E. (2012) A vegetation-based Index of Biotic Integrity to assess marsh reclamation success in the Alberta oil sands, Canada. *Ecological Indicators* **15**, 43–51.
- Reeder B.C. (2011) Assessing constructed wetland functional success using diel changes in dissolved oxygen, pH, and temperature in submerged, emergent, and open-water habitats in the Beaver Creek Wetlands Complex, Kentucky (USA). *Ecological Engineering* **37**, 1772–1778.
- Reeder B.C. & Binion B.M. (2001) Comparison of methods to assess water column primary production in wetlands. *Ecological Engineering* **17**, 445–449.
- Reid T., Boudens R., Ciborowski J.J.H. & Weisener C.G. (2016) Physicochemical gradients, diffusive flux, and sediment oxygen demand within oil sands tailings materials from Alberta, Canada. *Applied Geochemistry* **75**, 90–99.
- Rejmánková E. (2011) The role of macrophytes in wetland ecosystems. *Journal of Ecology and Field Biology* **34**, 333–345.
- Rey Benayas J.M., Newton A.C., Diaz A. & Bullock J.M. (2009) Enhancement of biodiversity and ecosystem services by ecological restoration: a meta-analysis. *Science* **325**, 1121–1124.
- Rooney R.C. & Bayley S.E. (2011) Setting reclamation targets and evaluating progress: submersed aquatic vegetation in natural and post-oil sands mining wetlands in Alberta, Canada. *Ecological Engineering* **37**, 569–579.
- Rooney R.C., Bayley S.E. & Schindler D.W. (2012) Oil sands mining and reclamation cause massive loss of peatland and stored carbon. *Proceedings of the National Academy of Sciences* **109**, 4933–4937.
- Rosen R.A. (1981) Length-dry weight relationships of some freshwater zooplankton. *Journal of Freshwater Ecology* **1**, 225–229.

- Roy M.C., Foote L. & Ciborowski J.J.H. (2016) Vegetation community composition in wetlands created following oil sand mining in Alberta, Canada. *Journal of Environmental Management* **172**, 18–28.
- Roy M., Mollard F.P.O. & Foote A.L. (2014) Do peat amendments to oil sands wet sediments affect *Carex aquatilis* biomass for reclamation success? *Journal of Environmental Management* **139**, 154–163.
- Sánchez-Bayo F. (2006) Comparative acute toxicity of organic pollutants and reference values for crustaceans. I. Branchiopoda, Copepoda and Ostracoda. *Environmental Pollution* **139**, 385–420.
- Sargent J.R., Bell J.G., Bell M. V., Henderson R.J. & Tocher D.R. (1995) Requirement criteria for essential fatty acids. *Journal of Applied Ichthyology* **11**, 183–198.
- Scheffer M., Hosper S.H., Meijer M., Moss B. & Jeppesen E. (1993) Alternative equilibria in shallow lakes. *Trends in Ecology & Evolution* **8**, 275–279.
- Schiffer S. & Liber K. (2017) Toxicity of aqueous vanadium to zooplankton and phytoplankton species of relevance to the Athabasca oil sands region. *Ecotoxicology and Environmental Safety* **137**, 1–11.
- Scott A.C., Zubot W., MacKinnon M.D., Smith D.W. & Fedorak P.M. (2008) Ozonation of oil sands process water removes naphthenic acids and toxicity. *Chemosphere* **71**, 156–160.
- Scott A.C., Young R.F. & Fedorak P.M. (2008) Comparison of GC – MS and FTIR methods for quantifying naphthenic acids in water samples. *Chemosphere* **73**, 1258–1264.
- Scher O., McNutt K.E. & Thiéry A. (2010) Designing a standardised sampling method for invertebrate monitoring: A pilot experiment in a motorway retention pond. *Limnetica* **29**, 121–132.
- Seltman H. (2015) Mixed Models. In *Experimental Design and Analysis*. p.357 - 358 Department of Statistics at Carnegie Mellon.
- Shaw J.L. & Kennedy J.H. (1996) the Use of aquatic field mesocosm studies in risk assessment. *Environmental Toxicology and Chemistry* **15**, 605–607.
- Slama C.A. (2010) *Sediment oxygen demand and sediment nutrient content of reclaimed wetlands in the oil sands region of northeastern Alberta*. M.Sc. University of Windsor.

- Šorf M., Davidson T.A., Brucet S., Menezes R.F., Søndergaard M., Lauridsen T.L., *et al.* (2015) Zooplankton response to climate warming: a mesocosm experiment at contrasting temperatures and nutrient levels. *Hydrobiologia* **742**, 185–203.
- Staeher P.A., Testa J.M., Kemp W.M., Cole J.J., Sand-Jensen K. & Smith S. V. (2012) The metabolism of aquatic ecosystems: History, applications, and future challenges. *Aquatic Sciences* **74**, 15–29.
- Staeher P.A., Bade D., Koch G.R., Williamson C., Hanson P., Cole J.J., *et al.* (2010) Lake metabolism and the diel oxygen technique: State of the science. *Limnology and Oceanography: Methods* **8**, 628–644.
- Stansfield J.H., Perrow M.R., Tench L.D., Jowitt A.J.D. & Taylor A.A.L. (1997) Submerged macrophytes as refuges for grazing Cladocera against fish predation: observations on seasonal changes in relation to macrophyte cover and predation pressure. *Hydrobiologia* **342/343**, 229–240.
- Steiner C.F. (2004) Daphnia dominance and zooplankton community structure in fishless ponds. *Journal of Plankton Research* **26**, 799–810.
- Swadling K.M., Pienitz R. & Nogrady T. (2000) Zooplankton community composition of lakes in the Yukon and Northwest Territories (Canada): Relationship to physical and chemical limnology. *Hydrobiologia* **431**, 211–224.
- Thormann M.N., Szumigalski A.R. & Bayley S.E. (1999) Aboveground peat and carbon accumulation potentials along a bog-fen-marsh wetland gradient in southern boreal Alberta, Canada. *Wetlands* **19**, 305–317.
- Tonn W.M., Langlois P.W., Prepas E.E., Danylchuk A.J. & Boss S.M. (2004) Winterkill cascade: Indirect effects of a natural disturbance on littoral macroinvertebrates in boreal lakes. *Journal of the North American Benthological Society* **23**, 237–250.
- Toor N.S., Franz E.D., Fedorak P.M., MacKinnon M.D. & Liber K. (2013) Degradation and aquatic toxicity of naphthenic acids in oil sands process-affected waters using simulated wetlands. *Chemosphere* **90**, 449–458.
- Trites M. & Bayley S.E. (2009) Vegetation communities in continental boreal wetlands along a salinity gradient: Implications for oil sands mining reclamation. *Aquatic Botany* **91**, 27–39.
- Turney D.E., Smith W.C. & Banerjee S. (2005) A measure of near-surface fluid motions that predicts air-water gas transfer in a wide range of conditions. *Geophysical Research Letters* **32**, 1–4.

- Vadeboncoeur Y., Kalff J., Christoffersen K. & Jeppesen E. (2006) Substratum as a driver of variation in periphyton chlorophyll and productivity in lakes. *Journal of the North American Benthological Society* **25**, 379–392.
- Vanderstukken M., Declerck S.A.J., Pals A., Meester L. De & Muylaert K. (2010) The influence of plant-associated filter feeders on phytoplankton biomass : a mesocosm study. *Hydrobiologia* **646**, 199–208.
- VanMensel D., Chaganti S.R., Boudens R., Reid T., Ciborowski J.J.H. & Weisener C.G. (2017) Investigating the Microbial Degradation Potential in Oil Sands Fluid Fine Tailings Using Gamma Irradiation: A Metagenomic Perspective. *Microbial Ecology* **74**, 362–372.
- Vanni M.J. (2002) Nutrient cycling by animals in freshwater ecosystems. *Annals of the New York Academy of Sciences* **33**, 341–370.
- Vinebrooke R.D., Schindler D.W., Findlay D.L., Turner M. A., Paterson M. & Mills K.H. (2003) Trophic dependence of ecosystem resistance and species compensation in experimentally acidified Lake 302s (Canada). *Ecosystems* **6**, 101–113.
- Vitt D.H., Halsey L.A., Campbell C., Bayley S.E. & Thormann M.N. (2001) Spatial patterning of net primary production in wetlands of continental western Canada. *Écoscience* **8**, 499–505.
- Wade H.W. (1969) Cladoceran faunas associated with aquatic macrophytes in some lakes in Northwestern Minnesota. *Ecology* **50**, 170–179.
- Wærvågen S., Rukke N. & Hessen D. (2002) Calcium content of crustacean zooplankton and its potential role in species distribution. *Freshwater Biology* **47**, 1866–1878.
- Wang J. & Wang J. (2007) Application of radiation technology to sewage sludge processing: A review. *Journal of Hazardous Materials* **143**, 2–7.
- Warner B.G. & Asada T. (2006) Biological diversity of peatlands in Canada. *Aquatic Sciences* **68**, 240–253.
- Wetzel R.G. (2001) *Limnology Lake and River Ecosystems*, 3rd edn. Academic Press, Orlando, Florida.
- White K.B. (2017) *Characterizing annual changes in the chemistry and toxicity of surface water from Base Mine Lake, an Alberta oil sands end pit lake*. M.Sc. University of Saskatchewan.

- Xue J., Huang C., Zhang Y., Liu Y. & Gamal El-din M. (2018) Bioreactors for oil sands process-affected water (OSPW) treatment : A critical review. *Science of the Total Environment* **627**, 916–933.
- Zedler J.B. (2000) Progress in wetland restoration ecology. *Trends in Ecology & Evolution* **15**, 402–407.
- Zedler J.B. & Callaway J.C. (1999) Tracking wetland restoration: Do mitigation sites follow desired trajectories? *Restoration Ecology* **7**, 69–73.
- Zedler J.B. & Kercher S. (2005) Wetland resources: status, trends, ecosystem services, and restorability. *Annual Review of Environment and Resources* **30**, 39–74.
- Zhang L., Zhang Y. & Mohamed El-din G. (2018) Degradation of recalcitrant naphthenic acids from raw and ozonated oil sands process-affected waters by a semi-passive bio filtration process. *Water Research* **133**, 310–318.
- Zubot W., Mackinnon M.D., Chelme-Ayala P., Smith D.W. & Gamal El-Din M. (2012) Petroleum coke adsorption as a water management option for oil sands process-affected water. *Science of the Total Environment* **427–428**, 364–372.

Appendix 1 – Summary of wetlands and tailings ponds used in the construction of mesocosms

Table A1-1: Selected characteristics of wetland materials collected for the construction of reference mesocosms

Relative salinity							
Freshwater reference wetlands FW	Crescent	2004	C	Sand, PMM	47.26	4	253
	Muskeg	1978	O	Natural	12.14	1	457
	Shallow	1989	C	Clay overburden	9.5	2	473
Hyposaline reference wetlands HSW	Golden	2000	C	Overburden, marsh mud	34.6	2	1961
	High	1985	O	Lean oil sand, PMM	43.32	8	2063
	Sulphate	1991	O	Clay overburden	13.73	5	1256
	Saline						

^a Origin indicates whether wetlands were C- Constructed by oil sands companies or O – formed opportunistically as a result of mining activity

^b Substrate indicates the type of material the wetland was constructed from or formed on according to CFRAW classifications. PMM – peat mineral mix

^c Average particle size as measured using by laser diffraction spectroscopy to determine particle size distribution from a subsample of the material collected to construct mesocosms

^d Naphthenic acid fraction compounds measured in a subsample of the material collected for the construction of mesocosms using the Fourier-transform infrared spectroscopy (FTIR) method by Syncrude Canada Limited

^e Specific conductance measured as temperature compensated conductivity to 25°C by a handheld YSI 85 in synoptic surveys of the wetlands conducted during the summer of 2014

Table A1-2: Selected characteristics of tailings pond materials collected for the construction of mesocosms

Relative salinity	Company and tailings pond name	Year of construction	Median particle size (μm) ^a	NAFCs OSPW (mg/L) ^b	NAFCs FFT (mg/L) ^b	EC (μS) ^c
Tailings Ponds OSPM	Suncor STP	2006	7.3	69	26	2297
	Suncor P1A	1968	2.2	64	71	2013
	Syncrude MLSB	1978 ^d	5.7	57	68	2200
	Shell MRM	2003	6.9	59	15	1790

STP – South Tailings Pond, P1A – Pond 1A, MLSB – Mildred Lake Settling Basin, MRM – Muskeg River Mine

^a Average particle size as measured using by laser diffraction spectroscopy to determine particle size distribution from a subsample of the material collected to construct mesocosms.

^b Naphthenic acid fraction compounds measured in a subsample of the material collected for the construction of mesocosms using the Fourier-transform infrared spectroscopy (FTIR) method by Syncrude Canada Limited.

^c Specific conductance measured as temperature compensated conductivity to 25°C by a handheld YSI 85 in synoptic surveys of the wetlands conducted during the summer of 2014.

^d Construction of MLSB began in 1978, however the FFT and OSPW were collected directly from the inflow pipe

Appendix 2 – Proportion of relative abundance of all zooplankton taxa including rotifers identified in all mesocosm for all sampling dates and total crustacean zooplankton biomass

Table A2-1: Proportion of crustacean zooplankton and rotifer relative abundance identified in all G- and G+ reference and OSPM mesocosms for all sampling dates and the total crustacean zooplankton biomass. Bold values indicate when an individual taxa made up greater than 0.05 of the sample.

	July 2015									
	G-									
	Cr	Mu	Sh	Go	Hi	Sa	P1A	STP	MLSB	MRM
Total density (individuals/L)	3	46	4	5	994	1	3	226	3	N/A
Crustacean zooplankton density (µg/L)	20.7	48	4.6	53.1	1269	0.6	0	0	0	N/A
Taxon										
CLADOCERA										
Chydoridae										
<i>Acroperus harpae</i>	0.00	0.01	0.00	0.00	0.00	0.00	0.00	0.00	0.00	0.00
<i>Alona rectangula</i>	0.20	0.02	0.63	0.00	0.04	1.00	0.00	0.00	0.00	0.00
<i>Chydorus sphaericus</i>	0.40	0.81	0.25	0.00	0.16	0.00	0.00	0.00	0.00	0.00
<i>Grapteloberis testudinaria</i>	0.00	0.00	0.00	0.00	0.00	0.00	0.00	0.00	0.00	0.00
<i>Leydigia quadrangularis</i>	0.00	0.00	0.00	0.00	0.00	0.00	0.00	0.00	0.00	0.00
<i>Pleuroxus denticulatus</i>	0.00	0.00	0.00	0.00	0.00	0.00	0.00	0.00	0.00	0.00
Daphniidae										
<i>Ceriodaphnia</i>	0.00	0.02	0.00	0.00	0.78	0.00	0.00	0.00	0.00	0.00
<i>Daphnia pulex</i>	0.00	0.00	0.00	0.00	0.00	0.00	0.00	0.00	0.00	0.00
<i>Daphnia rosea</i>	0.00	0.00	0.00	0.00	<0.01	0.00	0.00	0.00	0.00	0.00
<i>Daphnia sp.</i>	0.00	0.00	0.00	0.00	0.00	0.00	0.00	0.00	0.00	0.00
<i>Scapheloberis kingi</i>	0.00	0.00	0.00	0.00	0.00	0.00	0.00	0.00	0.00	0.00

<i>Simocephalus</i>	0.00	0.03	0.00	0.00	0.00	0.00	0.00	0.00	0.00
Macrothricidae									
<i>Streblocercus</i>	0.00	0.00	0.00	0.00	0.00	0.00	0.00	0.00	0.00
Sididae									
<i>Diaphanosoma brachyurum</i>	0.00	0.00	0.00	0.00	0.00	0.00	0.00	0.00	0.00
OSTRACODA	0.40	0.01	0.00	1.00	0.01	0.00	0.00	0.00	0.00
ARTHROPODA									
Chaoboridae									
<i>Chaoborus</i>	0.00	0.00	0.00	0.00	0.00	0.00	0.00	0.00	1.00
ROTIFERA									
Bdelloidea	0.00	0.03	0.00	0.00	0.00	0.00	0.00	0.00	0.00
<i>Brachionus</i>	0.00	0.00	0.00	0.00	0.00	0.00	1.00	1.00	0.00
<i>Euchlanis</i>	0.00	0.00	0.00	0.00	0.00	0.00	0.00	0.00	0.00
<i>Lecane</i>	0.00	0.05	0.00	0.00	<0.01	0.00	0.00	0.00	0.00
<i>Lepadella</i>	0.00	0.00	0.13	0.00	0.00	0.00	0.00	0.00	0.00
<i>Trichocerca</i>	0.00	0.00	0.00	0.00	0.00	0.00	0.00	0.00	0.00

July 2015

G+

	Cr	Mu	Sh	Go	Hi	Sa	P1A	STP	MLSB	MRM
Total density (individuals/L)	25	19	1	49	146	4	69	13	8	N/A
Crustacean zooplankton density (µg/L)	17.1	15.6	1	30.5	21330	248.9	0	28.9	1.9	N/A

CLADOCERA

Chydoridae

<i>Acroperus harpae</i>	0.000	0.000	0.000	0.000	0.000	0.000	0.000	0.000	0.000
<i>Alona rectangula</i>	0.061	0.000	1.000	0.673	0.000	0.000	0.000	0.000	0.000
<i>Chydorus sphaericus</i>	0.286	0.162	0.000	0.122	0.007	0.000	0.000	0.000	0.375
<i>Grapteloberis testudinaria</i>	0.000	0.000	0.000	0.000	0.000	0.000	0.000	0.000	0.000

<i>Leydigia quadrangularis</i>	0.000	0.000	0.000	0.000	0.000	0.000	0.000	0.000	0.000
<i>Pleuroxus denticulatus</i>	0.000	0.000	0.000	0.000	0.000	0.000	0.000	0.000	0.000
Daphniidae									
<i>Ceriodaphnia</i>	0.000	0.000	0.000	0.000	0.000	0.000	0.000	0.615	0.000
<i>Daphnia pulex</i>	0.000	0.000	0.000	0.041	0.000	0.000	0.000	0.000	0.000
<i>Daphnia rosea</i>	0.000	0.000	0.000	0.000	0.000	0.000	0.000	0.000	0.000
<i>Daphnia sp.</i>	0.000	0.000	0.000	0.020	0.000	0.000	0.000	0.000	0.000
<i>Scapheloberis kingi</i>	0.000	0.000	0.000	0.000	0.000	0.000	0.000	0.000	0.000
<i>Simocephalus</i>	0.000	0.000	0.000	0.000	0.000	0.000	0.000	0.000	0.000
Macrothricidae									
<i>Streblocercus</i>	0.000	0.000	0.000	0.000	0.000	0.000	0.000	0.000	0.000
Sididae									
<i>Diaphanosoma brachyurum</i>	0.592	0.811	0.000	0.000	0.000	0.000	0.000	0.000	0.000
OSTRACODA	0.020	0.027	0.000	0.020	0.747	0.750	0.000	0.000	0.000
ARTHROPODA									
Chaoboridae									
<i>Chaoborus</i>	0.000	0.000	0.000	0.000	0.000	0.000	0.000	0.000	0.000
ROTIFERA									
Bdelloidea	0.000	0.000	0.000	0.000	0.000	0.000	0.000	0.000	0.000
<i>Brachionus</i>	0.000	0.000	0.000	0.000	0.233	0.000	1.000	0.154	0.625
<i>Euchlanis</i>	0.000	0.000	0.000	0.000	0.000	0.000	0.000	0.000	0.000
<i>Lecane</i>	0.020	0.000	0.000	0.122	0.014	0.250	0.000	0.231	0.000
<i>Lepadella</i>	0.000	0.000	0.000	0.000	0.000	0.000	0.000	0.000	0.000
<i>Trichocerca</i>	0.020	0.000	0.000	0.000	0.000	0.000	0.000	0.000	0.000

August 2015

G-

	Cr	Mu	Sh	Go	Hi	Sa	P1A	STP	MLSB	MRM
Total density (individuals/L)	199	563	115	407	372	25	3	26	1	N/A

CZB (µg/L)	664	626	394	3999	977	129	1.62	1525	5.85	N/A
Taxon										
CLADOCERA										
Chydoridae										
<i>Acroperus harpae</i>	0.000	0.000	0.000	0.000	0.000	0.000	0.000	0.000	0.000	0.000
<i>Alona rectangula</i>	0.020	0.091	0.031	0.291	0.094	0.020	0.000	0.000	0.000	0.000
<i>Chydorus sphaericus</i>	0.776	0.752	0.668	0.249	0.487	0.220	0.000	0.000	0.000	0.000
<i>Grapteloberis testudinaria</i>	0.000	0.124	0.000	0.012	0.000	0.000	0.000	0.000	0.000	0.000
<i>Leydigia quadrangularis</i>	0.000	0.000	0.000	<0.01	0.000	0.000	0.000	0.000	0.000	0.000
<i>Pleuroxus denticulatus</i>	0.025	0.000	0.000	<0.01	0.000	0.000	0.000	0.000	0.000	0.000
Daphniidae										
<i>Ceriodaphnia</i>	0.010	0.012	0.188	0.016	0.309	0.540	0.167	0.000	1.000	
<i>Daphnia pulex</i>	0.000	0.000	0.000	0.004	0.000	0.000	0.000	0.000	0.000	0.000
<i>Daphnia rosea</i>	0.000	0.000	0.000	0.000	0.000	0.000	0.000	0.000	0.000	0.000
<i>Daphnia sp.</i>	0.000	0.000	0.000	0.059	0.000	0.000	0.000	0.000	0.000	0.000
<i>Scapheloberis kingi</i>	0.000	0.000	0.000	0.000	0.000	0.000	0.000	0.000	0.000	0.000
<i>Simocephalus</i>	0.015	<0.01	<0.01	<0.01	0.000	0.100	0.000	0.000	0.000	0.000
Macrothricidae										
<i>Streblocercus</i>	0.000	0.000	0.000	<0.01	0.000	0.000	0.000	0.000	0.000	0.000
Sididae										
<i>Diaphanosoma brachyurum</i>	0.000	0.000	0.000	0.000	0.000	0.000	0.000	0.000	0.000	0.000
OSTRACODA	0.154	0.000	0.110	0.348	0.110	0.120	0.000	0.941	0.000	0.000
ARTHROPODA										
Chaoboridae										
<i>Chaoborus</i>	0.000	0.000	0.000	0.000	0.000	0.000	0.000	0.000	0.000	0.000
ROTIFERA										
Bdelloidea	0.000	0.000	0.000	0.000	0.000	0.000	0.000	0.000	0.000	0.000
<i>Brachionus</i>	0.000	0.000	0.000	0.000	0.000	0.000	0.833	0.059	0.000	0.000

<i>Euchlanis</i>	0.000	0.000	0.000	<0.01	0.000	0.000	0.000	0.000	0.000	
<i>Lecane</i>	0.000	0.000	0.000	0.000	0.000	0.000	0.000	0.000	0.000	
<i>Lepadella</i>	0.000	0.000	0.000	0.000	0.000	0.000	0.000	0.000	0.000	
<i>Trichocerca</i>	0.000	0.000	0.000	0.000	0.000	0.000	0.000	0.000	0.000	
August 2015										
G+										
	Cr	Mu	Sh	Go	Hi	Sa	P1A	STP	MLSB	MRM
Total density (individuals/L)	341	232	133	2360	351	92	167	4	38	N/A
CZB (µg/L)	1488	1435	2231	9867	2124	1634	69.2	20.6	152	N/A
Taxon										
CLADOCERA										
Chydoridae										
<i>Acroperus harpae</i>	0.000	0.000	0.000	0.000	0.000	0.000	0.000	0.000	0.000	0.000
<i>Alona rectangula</i>	0.037	0.052	<0.01	<0.01	0.010	0.033	0.000	0.000	0.000	0.000
<i>Chydorus sphaericus</i>	0.199	0.644	0.517	0.800	0.365	0.536	0.000	0.143	0.027	0.000
<i>Grapteloberis testudinaria</i>	0.000	0.000	0.000	0.000	0.000	0.000	0.000	0.000	0.000	0.000
<i>Leydigia quadrangularis</i>	0.000	0.000	0.000	0.000	0.000	0.000	0.000	0.000	0.000	0.000
<i>Pleuroxus denticulatus</i>	0.000	0.000	0.000	0.000	0.000	0.000	0.000	0.000	0.000	0.000
Daphniidae										
<i>Ceriodaphnia</i>	0.680	0.194	0.098	0.000	0.526	0.000	0.042	0.286	0.973	0.000
<i>Daphnia pulex</i>	0.000	0.000	0.000	0.011	0.000	0.000	0.000	0.000	0.000	0.000
<i>Daphnia rosea</i>	0.000	0.000	0.000	0.000	0.000	<0.01	0.000	0.000	0.000	0.000
<i>Daphnia sp.</i>	0.000	0.000	0.000	>0.01	0.000	0.000	0.000	0.000	0.000	0.000
<i>Scapheloberis kingi</i>	0.000	0.000	0.000	0.000	0.000	0.000	0.000	0.000	0.000	0.000
<i>Simocephalus</i>	<0.01	0.000	0.000	0.061	0.000	0.049	0.000	0.000	0.000	0.000
Macrothricidae										
<i>Streblocercus</i>	0.000	0.000	0.000	0.000	0.000	0.000	0.000	0.000	0.000	0.000
Sididae										

<i>Diaphanosoma brachyurum</i>	<0.01	0.000	0.000	0.000	0.000	0.000	0.000	<0.01	0.000	0.000
OSTRACODA	0.062	0.108	0.377	0.122	0.098	0.377	0.000	0.429	0.000	0.000
ARTHROPODA										
Chaoboridae										
<i>Chaoborus</i>	0.000	0.000	0.000	0.000	0.000	0.000	0.000	0.000	0.000	0.000
ROTIFERA										
Bdelloidea	0.000	0.000	0.000	0.000	0.000	0.000	0.000	0.000	0.000	0.000
<i>Brachionus</i>	0.000	0.000	0.000	0.000	0.000	0.000	0.952	0.143	0.000	0.000
<i>Euchlanis</i>	0.000	0.000	0.000	0.000	0.000	0.000	0.000	0.000	0.000	0.000
<i>Lecane</i>	0.000	0.000	0.000	0.000	0.000	0.000	0.000	0.000	0.000	0.000
<i>Lepadella</i>	0.000	0.000	0.000	0.000	0.000	0.000	0.000	0.000	0.000	0.000
<i>Trichocerca</i>	0.013	0.000	0.000	0.000	0.000	0.000	0.000	0.000	0.000	0.000

July 2016

G-

	Cr	Mu	Sh	Go	Hi	Sa	P1A	STP	MLSB	MRM
Total density (individuals/L)	723	1198	107	226	826	107	2	50	20	1
CZB (µg/L)	4658	7861	1436	6002	3697	433.4	1.75	413	528	0
Taxon										
CLADOCERA										
Chydoridae										
<i>Acroperus harpae</i>	0.000	0.000	0.000	0.000	0.000	0.000	0.000	0.000	0.000	0.000
<i>Alona rectangula</i>	0.223	0.046	0.099	0.262	0.070	0.296	0.330	0.000	0.000	0.000
<i>Chydorus sphaericus</i>	0.443	0.657	0.174	0.164	0.075	0.164	0.660	0.000	0.000	0.000
<i>Grapteloberis testudinaria</i>	0.000	0.000	0.000	0.000	0.000	0.000	0.000	0.000	0.000	0.000
<i>Leydigia quadrangularis</i>	0.000	0.000	0.000	0.000	0.000	0.000	0.000	0.000	0.000	0.000
<i>Pleuroxus denticulatus</i>	0.044	0.000	0.000	0.197	0.000	0.000	0.000	0.000	0.000	0.000
Daphniidae										
<i>Ceriodaphnia</i>	0.033	0.000	0.000	0.000	0.806	0.000	0.000	0.000	0.000	0.000

<i>Daphnia pulex</i>	0.000	0.000	0.000	0.000	0.000	0.000	0.000	0.000	0.000	0.000
<i>Daphnia rosea</i>	0.000	0.000	0.000	0.000	0.000	0.000	0.000	0.000	0.000	0.000
<i>Daphnia sp.</i>	0.000	0.000	0.000	0.000	0.000	0.000	0.000	0.000	0.000	0.000
<i>Scapheloberis kingi</i>	0.000	0.000	0.000	0.000	0.000	0.000	0.000	0.000	0.000	0.000
<i>Simocephalus</i>	0.122	0.039	0.498	0.000	0.000	0.066	0.000	0.000	0.000	0.000
Macrothricidae										
<i>Streblocercus</i>	0.000	0.000	0.000	0.000	0.000	0.000	0.000	0.000	0.000	0.000
Sididae										
<i>Diaphanosoma brachyurum</i>	0.000	0.000	0.000	0.000	0.000	0.000	0.000	0.000	0.000	0.000
OSTRACODA	0.119	0.122	0.230	0.355	0.050	0.188	0.000	0.170	0.487	0.000
ARTHROPODA										
Chaoboridae										
<i>Chaoborus</i>	0.000	0.000	0.000	0.018	0.000	0.000	0.000	0.000	0.000	0.000
ROTIFERA										
Bdelloidea	0.000	0.078	0.000	0.000	0.000	0.000	0.000	0.000	0.000	1.000
<i>Brachionus</i>	0.000	0.000	0.000	0.000	0.000	0.000	0.000	0.830	0.513	0.000
<i>Euchlanis</i>	0.000	0.000	0.000	<0.01	0.000	0.000	0.000	0.000	0.000	0.000
<i>Lecane</i>	0.017	0.058	0.000	0.000	0.000	0.146	0.000	0.000	0.000	0.000
<i>Lepadella</i>	0.000	0.000	0.000	0.000	0.000	0.000	0.000	0.000	0.000	0.000
<i>Trichocerca</i>	0.000	0.000	0.000	0.000	0.000	0.000	0.000	0.000	0.000	0.000

July 2016

G+

	Cr	Mu	Sh	Go	Hi	Sa	PIA	STP	MLSB	MRM
Total density (individuals/L)	542	335	139	153	2358	154	5	3	11	30
CZB (µg/L)	15045	3158	434	10883	31107	501.4	83.3	84.9	1108	143

Taxon

CLADOCERA

Chydoridae

<i>Acroperus harpae</i>	0.000	0.000	0.000	0.000	0.000	0.000	0.000	0.000	0.000	0.000
<i>Alona rectangularis</i>	0.028	0.042	0.076	<0.01	0.003	0.026	0.000	0.167	0.048	0.167
<i>Chydorus sphaericus</i>	0.479	0.830	0.307	<0.01	0.329	0.929	0.333	0.167	0.000	0.000
<i>Grapteloberis testudinaria</i>	0.000	0.000	0.000	0.000	0.000	0.000	0.000	0.000	0.000	0.000
<i>Leydigia quadrangularis</i>	0.000	0.000	0.000	0.000	0.000	0.000	0.000	0.000	0.000	0.000
<i>Pleuroxus denticulatus</i>	0.000	0.000	0.000	0.000	0.000	0.000	0.111	0.000	0.000	0.000
Daphniidae										
<i>Ceriodaphnia</i>	0.000	0.000	0.058	0.000	0.345	0.000	0.000	0.333	0.048	0.000
<i>Daphnia pulex</i>	0.000	0.000	0.000	0.000	0.000	0.000	0.000	0.000	0.000	0.833
<i>Daphnia rosea</i>	0.000	0.000	0.000	0.000	0.000	0.000	0.000	0.000	0.000	0.000
<i>Daphnia sp.</i>	0.000	0.000	0.000	0.000	0.000	0.000	0.000	0.000	0.000	0.000
<i>Scapheloberis kingi</i>	0.000	0.000	0.000	0.000	0.000	0.000	0.000	0.000	0.000	0.000
<i>Simocephalus</i>	0.000	0.000	0.000	0.000	0.000	0.000	0.000	0.000	0.000	0.000
Macrothricidae										
<i>Streblocercus</i>	0.000	0.000	0.000	0.000	0.000	0.000	0.000	0.000	0.000	0.000
Sididae										
<i>Diaphanosoma brachyurum</i>	0.000	0.000	0.000	0.000	0.000	0.000	0.000	0.000	0.000	0.000
OSTRACODA	0.456	0.128	0.220	0.990	0.323	0.042	0.556	0.167	0.905	0.000
ARTHROPODA										
Chaoboridae										
<i>Chaoborus</i>	0.000	0.000	0.000	0.000	0.000	<0.01	0.000	0.000	0.000	0.000
ROTIFERA										
Bdelloidea	0.037	0.000	0.000	0.000	0.000	0.000	0.000	0.000	0.000	0.000
<i>Brachionus</i>	0.000	0.000	0.000	<0.01	0.000	0.000	0.000	0.000	0.000	0.000
<i>Euchlanis</i>	0.000	0.000	0.014	0.000	0.000	0.000	0.000	0.000	0.000	0.000
<i>Lecane</i>	0.000	0.000	0.321	0.000	0.000	0.000	0.000	0.167	0.000	0.000
<i>Lepadella</i>	0.000	0.000	0.000	0.000	0.000	0.000	0.000	0.000	0.000	0.000
<i>Trichocerca</i>	0.000	0.000	0.000	0.000	0.000	0.000	0.000	0.000	0.000	0.000

	August 2016									
	G-									
Taxon	Cr	Mu	Sh	Go	Hi	Sa	PIA	STP	MLSB	MRM
Total density (individuals/L)	163	552	79	339	92	32	18	21	1	2
CZB (µg/L)	581	2059	1191	1104	1543	149.8	63.1	927	0.92	0.81
CLADOCERA										
Chydoridae										
<i>Acroperus harpae</i>	0.000	0.000	0.000	0.000	0.000	0.000	0.000	0.000	0.000	0.000
<i>Alona rectangula</i>	0.108	0.139	<0.01	0.044	0.429	0.016	0.028	0.098	0.000	0.666
<i>Chydorus sphaericus</i>	0.191	0.604	0.611	0.377	0.027	0.730	0.444	0.000	1.000	0.000
<i>Grapteloberis testudinaria</i>	0.000	0.000	0.000	0.000	0.000	0.000	0.000	0.024	0.000	0.000
<i>Leydigia quadrangularis</i>	0.000	0.000	0.000	0.000	0.000	0.000	0.000	0.000	0.000	0.000
<i>Pleuroxus denticulatus</i>	0.000	0.000	0.000	0.561	0.000	0.000	0.000	0.000	0.000	0.000
Daphniidae										
<i>Ceriodaphnia</i>	0.597	0.053	0.000	<0.01	0.060	0.000	0.333	0.000	0.000	0.000
<i>Daphnia pulex</i>	0.000	0.000	0.000	0.000	0.000	0.000	0.000	0.000	0.000	0.000
<i>Daphnia rosea</i>	0.000	0.000	0.000	0.000	0.000	0.000	0.000	0.000	0.000	0.000
<i>Daphnia sp.</i>	0.000	0.000	0.000	0.000	0.000	0.000	0.000	0.000	0.000	0.000
<i>Scapheloberis kingi</i>	0.000	0.000	0.000	0.000	0.000	0.000	0.000	0.000	0.000	0.000
<i>Simocephalus</i>	0.034	0.181	0.115	0.000	0.000	0.175	0.000	0.000	0.000	0.000
Macrothricidae										
<i>Streblocercus</i>	0.000	0.000	0.000	0.000	0.000	0.000	0.000	0.000	0.000	0.000
Sididae										
<i>Diaphanosoma brachyurum</i>	0.000	0.000	0.000	0.000	0.000	0.000	0.000	0.000	0.000	0.000
OSTRACODA	0.043	0.015	0.268	0.012	0.478	0.143	0.139	0.878	0.000	0.333
ARTHROPODA										
Chaoboridae										

<i>Chaoborus</i>	0.000	<0.01	0.000	<0.01	0.000	0.000	0.000	0.000	0.000	0.000
ROTIFERA										
Bdelloidea	0.000	0.000	0.000	0.000	0.000	0.000	0.000	0.000	0.000	0.000
<i>Brachionus</i>	<0.01	0.000	0.000	0.003	0.000	0.000	0.056	0.000	0.000	0.000
<i>Euchlanis</i>	0.000	0.000	0.000	0.000	<0.01	0.000	0.000	0.000	0.000	0.000
<i>Lecane</i>	0.016	0.000	0.000	0.000	0.000	0.000	0.000	0.000	0.000	0.000
<i>Lepadella</i>	0.000	0.000	0.000	0.000	0.000	0.000	0.000	0.000	0.000	0.000
<i>Trichocerca</i>	0.000	0.000	0.000	0.000	0.000	0.000	0.000	0.000	0.000	0.000

August 2016

G+

	Cr	Mu	Sh	Go	Hi	Sa	P1A	STP	MLSB	MRM
Total density (individuals/L)	370	67	272	1069	6036	678	51	80	39	29
CZB (µg/L)	1178	1128	8410	1437	39318	6976	3024	752	79	321

Taxon

CLADOCERA

Chydoridae

<i>Acroperus harpae</i>	0.000	0.000	0.000	0.000	0.000	0.000	0.000	0.000	0.000	0.000
<i>Alona rectangula</i>	0.116	0.000	0.035	0.655	0.095	0.021	0.020	0.031	0.000	0.105
<i>Chydorus sphaericus</i>	0.769	0.526	0.424	0.319	0.497	0.776	0.108	<0.01	0.026	0.000
<i>Grapteloberis testudinaria</i>	0.000	0.000	0.000	0.000	0.000	0.000	0.000	0.000	0.000	0.000
<i>Leydigia quadrangularis</i>	0.000	0.000	0.000	0.000	0.000	0.000	0.000	0.000	0.000	0.000
<i>Pleuroxus denticulatus</i>	<0.01	0.000	0.000	0.000	0.000	0.000	0.000	0.000	0.000	0.035

Daphniidae

<i>Ceriodaphnia</i>	0.000	0.015	0.164	0.000	0.228	0.000	0.000	0.000	0.935	0.018
<i>Daphnia pulex</i>	0.000	0.000	0.000	0.000	0.000	0.000	0.000	0.000	0.000	0.123
<i>Daphnia rosea</i>	0.000	0.000	0.000	0.000	0.000	0.000	0.000	0.000	0.000	0.000
<i>Daphnia sp.</i>	0.000	0.000	0.000	0.000	0.000	0.000	0.000	0.000	0.000	0.158
<i>Scapheloberis kingi</i>	0.014	0.000	0.000	0.000	0.000	0.000	0.000	0.000	0.000	0.000

<i>Simocephalus</i>	0.060	0.000	0.000	0.023	0.000	<0.01	0.000	0.000	0.000	0.000
Macrothricidae										
<i>Streblocercus</i>	0.000	0.000	0.000	0.000	0.000	0.000	0.000	0.000	0.000	0.000
Sididae										
<i>Diaphanosoma brachyurum</i>	0.000	0.000	0.000	0.000	0.000	0.000	0.000	0.000	0.000	0.000
OSTRACODA	0.038	0.451	0.378	<0.01	0.180	0.198	0.873	0.175	0.026	0.088
ARTHROPODA										
Chaoboridae										
<i>Chaoborus</i>	<0.01	<0.01	0.000	0.000	0.000	<0.01	0.000	0.000	0.000	0.000
ROTIFERA										
Bdelloidea	0.000	0.000	0.000	0.000	0.000	0.000	0.000	0.000	0.000	0.000
<i>Brachionus</i>	0.000	0.000	0.000	0.000	0.000	0.000	0.000	0.788	0.013	0.000
<i>Euchlanis</i>	0.000	0.000	0.000	0.000	0.000	0.000	0.000	0.000	0.000	0.000
<i>Lecane</i>	0.000	0.000	0.000	0.000	0.000	0.000	0.000	0.000	0.000	0.000
<i>Lepadella</i>	0.000	0.000	0.000	0.000	0.000	0.000	0.000	0.000	0.000	0.000
<i>Trichocerca</i>	0.000	0.000	0.000	0.000	0.000	0.000	0.000	0.000	0.000	0.000

Table A2-2: Proportion of relative abundance of all zooplankton taxa including rotifers identified in Blank mesocosms for all sampling dates and the total crustacean zooplankton biomass. Bold values indicate when an individual taxa made up greater than 0.05 of the sample.

Date	July 2015			August 2015			July 2016			August 2016		
	B1	B2	B3	B1	B2	B3	B1	B2	B3	B1	B2	B3
Mesocosm												
Total density (individuals/L)				1	13	2	32	9.5	2.5	31.5	81.5	92.5
CZB ($\mu\text{g/L}$)	N/A	N/A	N/A	1.08	83.1	19.3	193	149	5.15	189	5.15	483
Taxon												
CLADOCERA												
Chydoridae												
<i>Acroperus harpae</i>				0.000	0.000	0.000	0.000	0.000	0.000	0.000	0.000	0.000
<i>Alona rectangularis</i>				0.500	0.000	0.250	0.250	0.263	0.400	0.603	0.018	0.059
<i>Chydorus sphaericus</i>				0.500	0.120	0.250	0.000	0.000	0.000	0.222	0.110	0.054
<i>Grabteloiberis testudinaria</i>				0.000	0.000	0.000	0.000	0.000	0.000	0.000	0.000	0.000
<i>Leydigia quadrangularis</i>				0.000	0.000	0.000	0.000	0.000	0.000	0.000	0.000	0.000
<i>Pleuroxus denticulatus</i>				0.000	0.000	0.000	0.000	0.000	0.000	0.000	0.000	0.000
Daphniidae												
<i>Ceriodaphnia</i>				0.000	0.000	0.000	0.000	0.000	0.000	0.032	0.000	0.843
<i>Daphnia pulex</i>				0.000	0.200	0.000	0.000	0.000	0.000	0.000	0.012	0.000
<i>Daphnia rosea</i>				0.000	0.000	0.000	0.000	0.000	0.000	0.000	0.000	0.000
<i>Daphnia spp</i>				0.000	0.680	0.000	0.000	0.000	0.000	0.000	0.859	0.000
<i>Scapheloberis kingi</i>				0.000	0.000	0.000	0.000	0.000	0.000	0.000	0.000	0.000
<i>Simocephalus</i>				0.000	0.000	0.000	0.000	0.000	0.000	0.000	0.000	0.000
Macrothricidae												
<i>Streblocerus</i>				0.000	0.000	0.000	0.000	0.000	0.000	0.000	0.000	0.000

<i>Sididae</i>									
<i>Diaphanosoma brachyurum</i>	0.000	0.000	0.000	0.000	0.000	0.000	0.000	0.000	0.000
OSTRACODA	0.000	0.000	0.500	0.094	0.632	0.400	0.143	0.000	0.022
ARTHROPODA									
Chaoboridae									
<i>Chaoborus</i>	0.000	0.000	0.000	0.000	0.000	0.000	0.000	0.000	0.000
ROTIFERA									
Bdelloidea	0.000	0.000	0.000	0.000	0.000	0.000	0.000	0.000	0.000
<i>Brachionus</i>	0.000	0.000	0.000	0.656	0.000	0.000	0.000	0.000	0.027
<i>Euchlanis</i>	0.000	0.000	0.000	0.000	0.000	0.000	0.000	0.000	0.000
<i>Lecane</i>	0.000	0.000	0.000	0.000	0.105	0.200	0.000	0.000	0.000
<i>Lepadella</i>	0.000	0.000	0.000	0.000	0.000	0.000	0.000	0.000	0.000
<i>Trichocera</i>	0.000	0.000	0.000	0.000	0.000	0.000	0.000	0.000	0.000

Appendix 3 – Macrophyte percent cover and biomass

Table A3-1: Estimated mean % cover SAV, and the minimum and maximum estimated % cover of SAV in untreated mesocosms, n is the number of replicates in each treatment. Early measurements refer to estimates collected between the 1st and 15th of the month while late measurements refer to estimates collected from the 16th to the last day of the month. * n = 3 OSPM replicates in 2015 and n = 4 OSPM replicates in 2016 and 2017.

Year	Month	G-								
		FW			HSW			OSPM		
		% SAV	Min	Max	% SAV	Min	Max	% SAV	Min	Max
2015	Early July	62	50	80	54	20	85	0	0	0
	Late July	72	60	80	64	30	90	0	0	0
	Early August	80	70	90	70	30	90	0	0	0
	Late August	83	55	90	75	30	100	0	0	0
	August									
2016	Early July	28	5	55	47.5	1	90	0	0	0
	Late July	34	10	70	32	1	100	<0.1	0	0.1
	Early August	25	25	40	35	1	100	<0.5	0	0.5
	Late August	50	1	100	36	0	100	0.3	0	1
	August									
2017	Early May	7	0	15	42	0	100	0	0	0
	Late May	46	10	100	64	0	100	0	0	0

Table A3-2: Estimated mean % cover SAV, and the minimum and maximum estimated % cover of SAV in gamma irradiated mesocosms, n is the number of replicates within the treatment. Early measurements refer to estimates collected between the 1st and 15th of the month while late measurements refer to estimates collected from the 16th to the last day of the month. * n = 3 OSPM replicates in 2015 and n = 4 OSPM replicates in 2016 and 2017.

Year	Month	G+								
		FW n = 3			HSW n = 3			OSPM n = 3*		
		% SAV	Min	Max	% SAV	Min	Max	% SAV	Min	Max
2015	Early July	45	30	70	41	20	70	0	0	0
	Late July	63	35	80	51	30	75	0	0	0
	Early August	88	85	100	75	65	85	0	0	0
	Late August	90	85	100	77	65	85	0	0	0
	Early July	1.5	0	5	49	2	85	>0.1	0	0.1
2016	Late July	31	0	60	61	2	100	1.5	0	5
	Early August	39	0	87	58.4	2	100	3	0	10
	Late August	48	0	95	63	5	95	3	0	10
	Early May	35	0	100	62	10	100	1.5	0	5
2017	Late May	58	10	100	48	0	100	1.5	0	5

Table A3-3: Dry weight (g) of different macrophyte components and the biofilm collected from destructive sampling of mesocosms on the final day of the study. SAV – submerged aquatic vegetation; EM – Emergent macrophytes; EM (C) – Carbon weight of emergent macrophytes calculated from ash free dry weight; Roots – Emergent macrophyte roots

GI	Salinity	Descriptive statistics	Dry weight (g)				
			SAV	EM	EM (C)	Roots	Biofilm
G-	FW	Mean±SE	6.86±0.78	17.67±5.26	14.64±3.01	74.74±44.57	1.81±0.61
		Min	5.54	10.94	8.62	17.68	0.97
		Max	8.23	28.04	17.90	144.89	2.99
	HSW	Mean±SE	3.10±1.77	11.18±7.19	8.09±5.32	91.86±53.16	4.50±3.53
		Min	0	0	0	0	0.6
		Max	6.13	24.61	18.13	184.15	11.54
	OSPM	Mean±SE	0.27±0.27	0	0	0	6.32±2.29
		Min	0	0	0	0	0
		Max	1.09	0	0	0	10.6
G+	FW	Mean±SE	9.60±3.91	12.85±9.50	9.01±6.90	77.09±28.26	1.86±0.52
		Min	3.58	0	0	47.17	1.32
		Max	16.94	31.41	22.57	133.57	2.9
	HSW	Mean±SE	18.88±4.33	5.3±4.01	3.64±2.75	36.10±28.04	1.6±0.95
		Min	11.13	0	0	0	0.5
		Max	26.1	13.17	9.02	91.31	3.5
	OSPM	Mean±SE	0.27±0.27	0.49±0.43	0.36±0.36	1.97±1.97	2.29±0.86
		Min	0	0	0	0	0.28
		Max	1.09	1.79	0.72	7.89	4.38

Appendix 4 – Supplementary information for Chapter 3

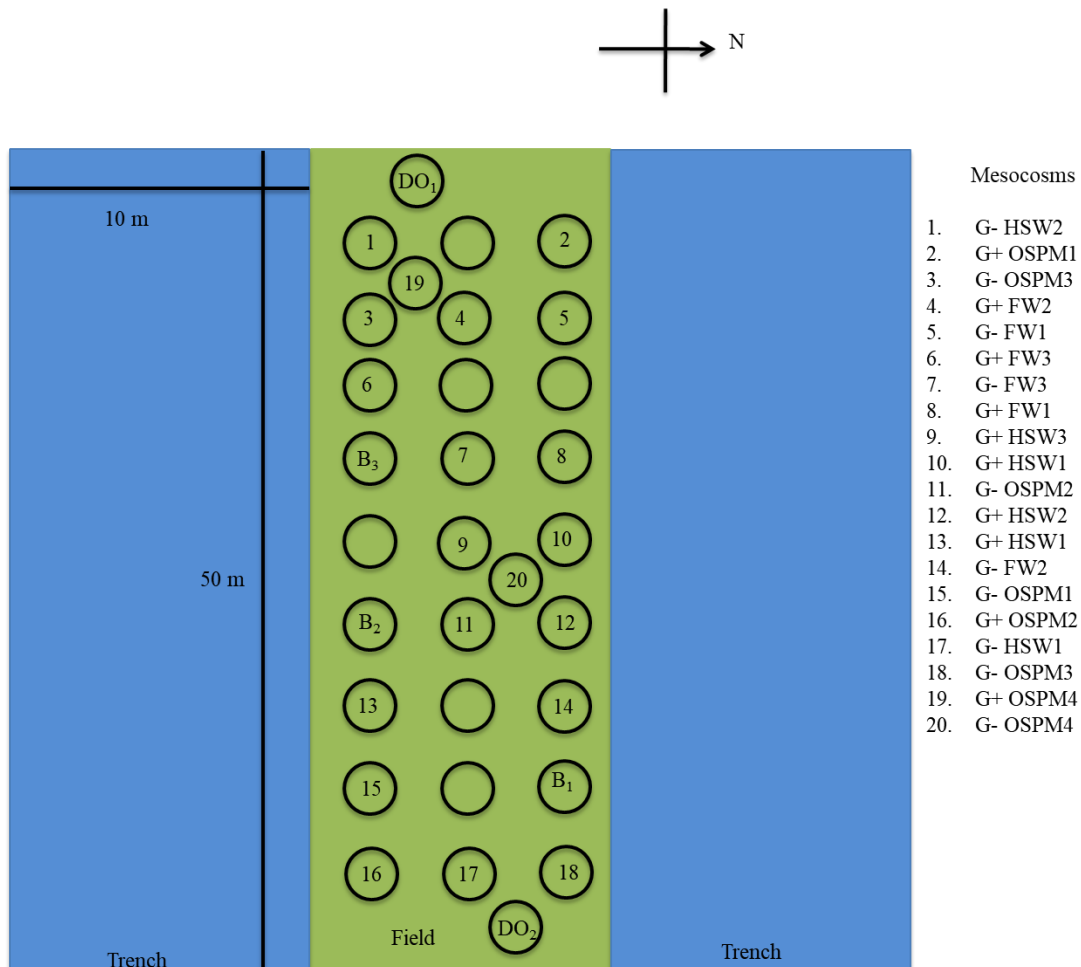


Fig A4-1: Schematic diagram of the the mesocosms (black circles) set up at the Experimental Trench Complex. Mesocosms w – 18 were sampled in 2015, 2016 and 2017. Mesocosms 19 and 20 were not added until September 2015 and were sampled in 2016 and 2017. Unlabelled mesocosms are mesocosms that were set up to parallel a microcosm lab study conducted by Boudens et al. (2016) for P1A, STP, and MLSB and were not sampled as part of this thesis. B₁₋₃ are experimental blank mesocosms filled with 25 cm of water to observe the passive accrual of organic matter from the environment. DO₁₋₂ are experimental blanks that were filled weekly with 25 cm of water and used in Chapter 3 to determine the atmospheric flux of dissolved oxygen. In the legend to the left, G- indicates untreated replicates and G+ indicates replicates which have been gamma irradiated.

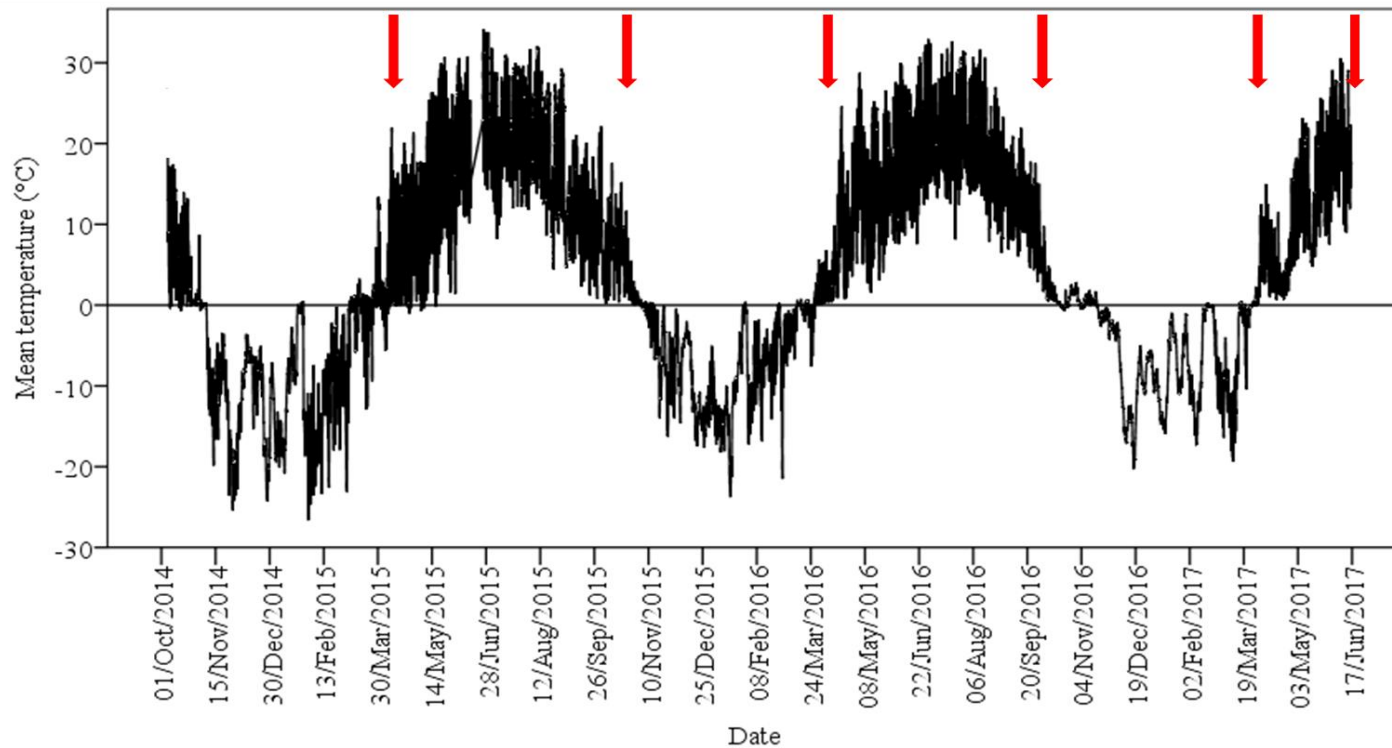


Fig. A4 – 2: Continuous record of mean mesocosm water temperature in °C (y-axis) over the length of the study (x-axis). Red arrows mark the start and end of the estimated growing season. Gray bars represent when onsite sampling of mesocosms occurred. Temperature was logged every 15 mins during the active sampling periods, and reduced to 1 hour during non-active sampling periods to preserve battery life.

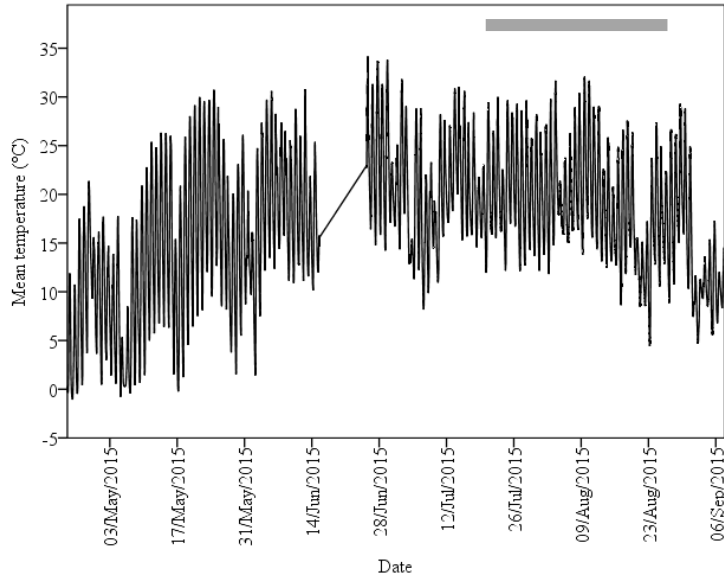


Fig. A4-3: Mean mesocosm water temperature (°C) recorded at a 15 min logging frequency from May 1 – September 7, 2015. The gray bar represents when DO loggers were deployed in mesocosms from July 11 – August 31.

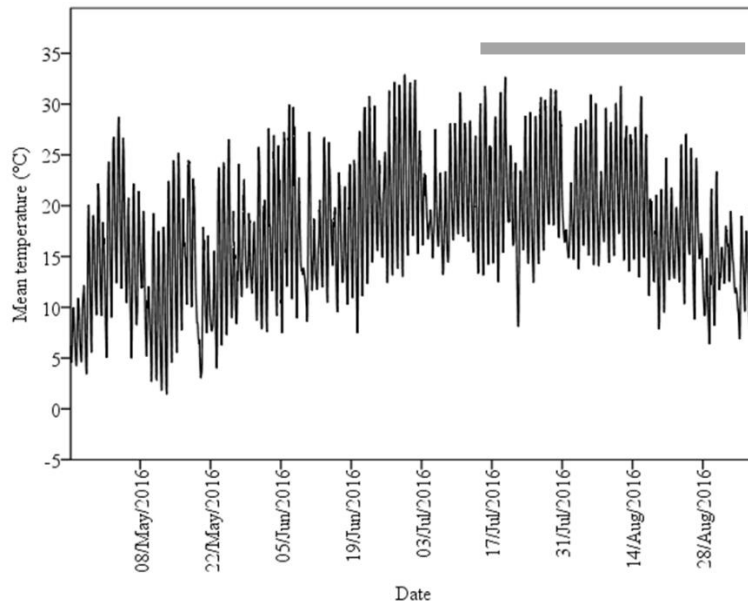


Fig. A4-4: Mean mesocosm water temperature (°C) recorded at a 15 min logging frequency from May 1 – September 7 2016. The gray bar represents when DO loggers were deployed in mesocosms from July 13 – September 7.

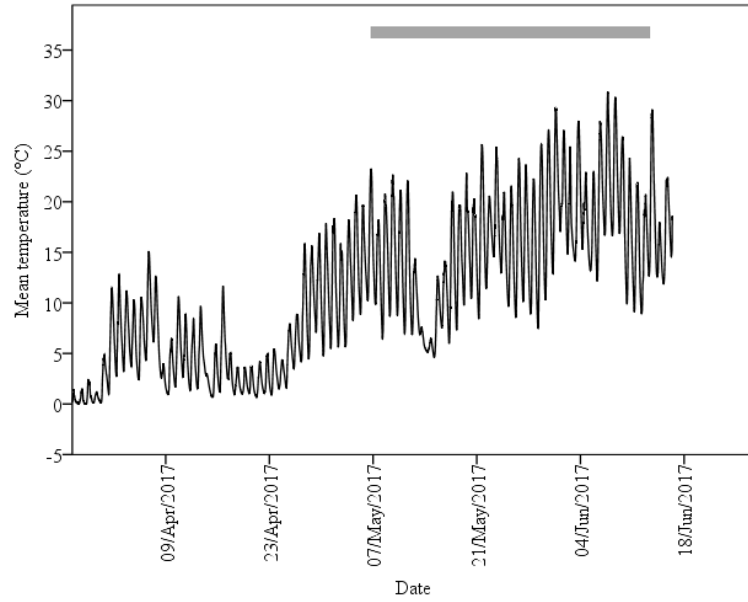


Fig. A4-5: Mean mesocosm water temperature (°C) recorded at a 15 min logging frequency from April 1 – June 16 2017. The gray bar represents when DO loggers were deployed in mesocosms from May 8 – June 13.

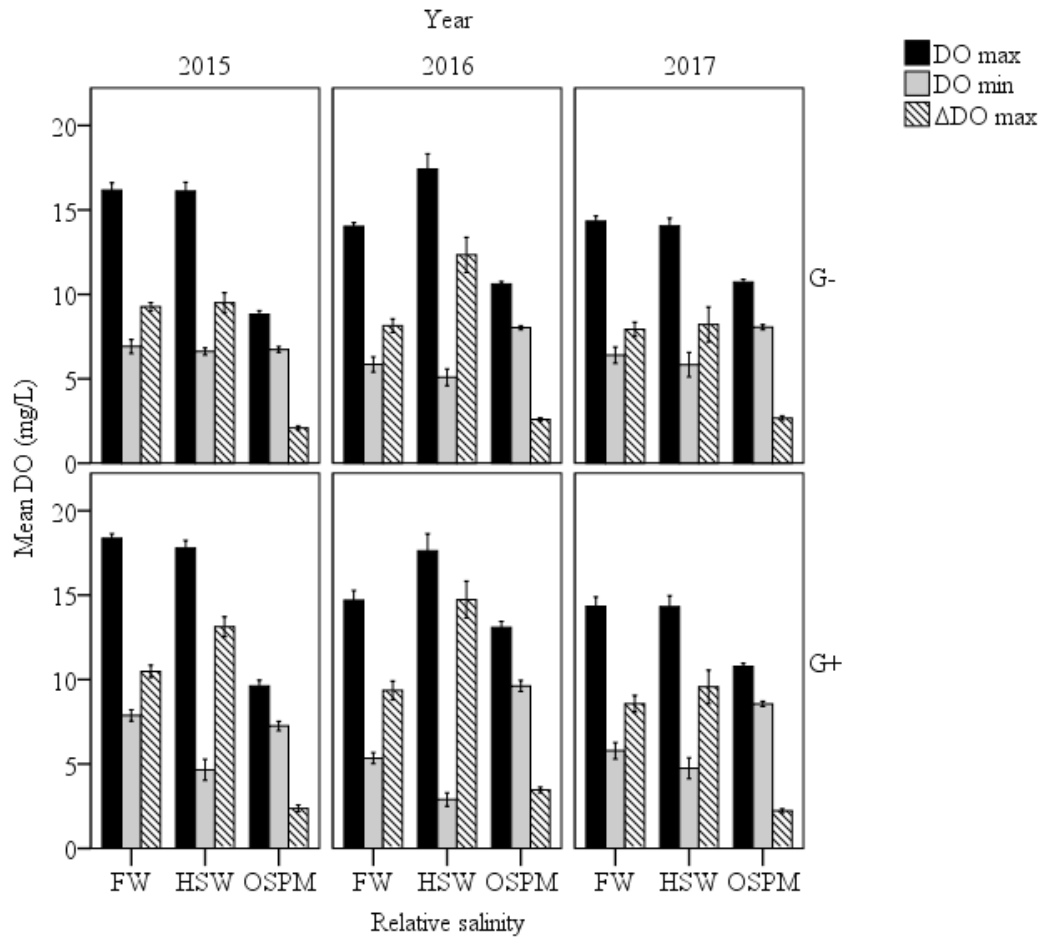


Fig. A4-6: Mean differences in minimum DO, maximum DO, and the maximum diel change in DO among all treatments, across all three sampling years. FW- freshwater mesocosms, HSW – hyposaline water mesocosms, OSPM – tailings pond mesocosms

Table A4-1: Mean volume and standard error in litres of distilled water added throughout active sampling period from 2015 – 2017, days on site are the number of days between the first and last visit to the experimental trenches, n is the number of mesocosms in each treatment.

Year	2015		2016		2017	
	105		70		48	
Days on site	G-	G+	G-	G+	G-	G+
Treatment						
FW						
Mean	37.7	35.4	48.5	51.3	12	13.7
SE	7.2	1.6	4.8	4.1	2.5	3.5
n	3	3	3	3	3	3
HSW						
Mean	32	39.3	44.2	41	12	8.3
SE	6.1	6.4	6.4	6.8	3.6	1.9
n	3	3	3	3	3	3
OSPM						
Mean	23.7	26.7	31.75	28.75	7.75	5.25
SE	1.3	2.0	2.1	3.9	1.4	1.0
n	3	3	4	4	4	4

Vita Auctoris

NAME	Chantal V. Dings-Avery
PLACE OF BIRTH	Fort McMurray, Alberta
YEAR OF BIRTH	1990
EDUCATION	Father Patrick Mercredi High School, Fort McMurray, Alberta, 2004 – 2008 University of Alberta, B.Sc. in Biology specializing in Freshwater Ecology, Edmonton, Alberta, 2008 – 2012 University of Windsor, M.Sc. in Biology Windsor, Ontario, 2014 - 2019